Stony Brook University

The anaphase promoting complex targeting subunit Ama1links meiotic exit to cytokinesis during sporulation in *Saccharomyces cerevisiae*

A Dissertation Presented

by

Aviva Elyse Diamond

to

The Graduate School

in Partial Fulfillment of the

Requirements

for the Degree of

Doctor of Philosophy

in

Molecular Genetics and Microbiology

Stony Brook University

December 2008

Stony Brook University

The Graduate School

Aviva Elyse Diamond

We, the dissertation committee for the above candidate for the

Doctor of Philosophy degree, hereby recommend

acceptance of this dissertation.

Aaron M. Neiman, Thesis Advisor
Associate Professor, Department of Biochemistry and Cell Biology

James B. Konopka, Chairperson of Defense
Professor, Department of Molecular Genetics and Microbiology

Bruce Futcher
Professor, Department of Molecular Genetics and Microbiology

Nancy M. Hollingsworth
Professor, Department of Biochemistry and Cell Biology

William P. Tansey
Professor, Cold Spring Harbor Laboratory

This dissertation is accepted by the Graduate School

Lawrence Martin
Dean of the Graduate School

The anaphase promoting complex targeting subunit Ama1 links meiotic exit to cytokinesis during sporulation in *Saccharomyces cerevisiae*

by
Aviva Elyse Diamond
Doctor of Philosophy
in
Molecular Genetics and Microbiology
Stony Brook University
2008

During Meiosis II, four individual prospore membranes encapsulate four haploid nuclei resulting from the meiotic divisions. Closure of each individual prospore membrane is a cytokinetic event that gives rise to a unique daughter cell (prospore). The leading edge complex, found at the lip of the growing prospore membrane, consists of three proteins: Ady3, Don1, and Ssp1. *AMA1* is a meiosis-specific activator of the anaphase promoting complex and is required for spore formation in *Saccharomyces cerevisiae*. *ama1Δ* cells complete the second meiotic division but fail to form visible spores. Video microscopy of sporulating wild-type cells containing Don1-GFP reveals a post-meiotic disappearance of the leading edge complex corresponding at the time of prospore membrane closure. In contrast, video microscopy of sporulating *ama1Δ* cells reveals a stabilization of the leading edge complex. Inactivation of a conditional allele of the leading edge complex component *SSP1* partially suppresses the *ama1Δ* sporulation defect. Western blot analysis reveals that during sporulation Ssp1 accumulates and then rapidly disappears at around the time of prospore membrane closure. In contrast, Ssp1 is stabilized in *ama1Δ* cells. Taken together, these results indicate that cytokinesis at the end of meiosis is controlled by APC^{Ama1} – dependent turnover of Ssp1.

Table of Contents

Acknowledgments

Members of the Neiman Laboratory and my advisor, Aaron Neiman, provided a stimulating and supportive working environment in which to pursue science. My committee members, James Konopka, Bruce Futcher, Nancy Hollingsworth, and William Tansey provided excellent advice throughout my graduate career at Stony Brook University. My mother, Naomi Diamond, encouraged me to continue when it might have been easier to stop working towards my degree. Most of all, my husband, Peter Radunzel, who willingly became a Long Island Refugee in order that I complete my academic goal. Thank you.

Chapter 1: Introduction

The budding yeast, *Saccharomyces cerevisiae*, proliferates in either haploid or diploid states. Under rich nutrient conditions, when a haploid *MAT**a*** cell encounters a haploid *MATα* cell, the cells fuse to form a single diploid cell. When a diploid *MAT**a*** */MATα* budding yeast cell encounters poor nutrient conditions, specifically, the absence of nitrogen in the presence of a non-fermentable carbon source (for example, acetate), growth ceases and the diploid cell undergoes a program of meiosis and forms four haploid spores encased in an ascus (Esposito and Klapholz, 1981). When nutrient conditions improve, the ascus degrades, the haploid spores germinate and the budding yeast life cycle begins anew (Figure 1-1).

Meiosis and Prospore Membrane Formation

The decision to enter meiosis occurs in G1 and affects the way the G1 to S transition is controlled. Culturing diploid *MAT**a*** */MATα* budding yeast cells in poor nutrient conditions induces cells to initiate a premeiotic S phase. In contrast to mitotic S phase, premeiotic S phase is longer and utilizes additional meiosis-specific factors (Petronczki *et al.,* 2003; Marston and Amon, 2004). The major cytological events that prepare the cell for the first meiotic division are outlined below. During DNA replication, cohesin, a ring-like protein complex containing a meiosis-specific protein, Rec8, assembles linking sister chromatids (Michaelis *et al*., 1997; Uhlmann *et al.*, 1998). As homologous chromosomes align at the metaphase plate, the synaptonemal complex forms resulting in cohesion of homologous chromosomes (Sym *et al.*, 1993; Uhlmann *et*

al., 1998). Meiotic recombination between the homologous chromosomes forms chiasmata, physical links between the homologs **(**Klein *et al.,* 1999; Marston and Amon, 2004**)**. Following spindle pole body duplication, a meiotic spindle assembles connecting the kinetochore, a protein complex located at the centromere region of the linked sister chromatids, to the spindle pole body (Adams and Kilmartin, 2000; Byers, 1981; Toth *et al.*, 2000**)**. Tension, necessary for chromosome segregation, occurs because sister chromatids of homologous chromosomes, attach to opposite spindle poles by a single microtubule (monopolar attachment) and pull in an opposite direction against the chiasmata formed during meiotic recombination (Pinsky and Biggins, 2005). During the metaphase I to anaphase I transition, the anaphase promoting complex (APC), activated by Cdc20 (discussed below), targets securin for degradation liberating separase, a protease, free to cleave cohesin subunits that tether sister chromatids together **(**Buonomo *et al.*, 2000; Cohen-Fix *et al.*, 1996; Shirayama *et al.*, 1999). Activated separase cleaves only along the sister homolog arms and not at the centromere region because meiosis-specific kinetochore proteins protect cohesin subunits from premature degradation **(**Katis *et al*., 2004; Kitajima *et al*., 2004; Shonn *et al*., 2002; Toth *et al.*, 2000**)**. At the completion of anaphase I, securin rapidly accumulates inhibiting further cleavage of cohesin subunits by separase (Salah and Nasmyth, 2000).

At the end of the first meiotic division and during prophase II, the spindle pole bodies are duplicated again (Moens, 1971; Moens and Rapport, 1971; Neiman, 2005). The outer plaque, a proteinacious structure located at on the cytoplasmic side of the spindle pole body, is modified to form a meiotic outer plaque (Moens, 1971; Moens and Rapport, 1971). In mitotic cells, the outer plaque consists of three proteins, Cnm67, Nud1

and Spc72, and serves as an anchor for cytoplasmic (astral) microtubules **(**Knop and Schiebel, 1998; Wigge *et al*., 1998**)**. In meiotic cells, Spc72 is lost from the outer plaque and several meiosis-specific proteins (Spo74, Mpc54, Spo21 and Ady4) assemble onto the spindle pole body altering the mitotic outer plaque from a microtubule organizing center into a membrane nucleation center (Bajgier *et al*., 2001; Davidow *et al*., 1980; Guth *et al*., 1972; Knop and Strasser, 2000; Nickas *et al*., 2003**)**. Thus, the Meiosis II spindle pole body consists of a multilaminar structure containing three distinct layers: 1) an inner plaque, from which spindle microtubules are nucleated, 2) a central plaque containing proteins that span the nuclear envelope, and 3) and an outer layer that serves as a membrane nucleation center rather than an organizing center for cytoplasmic microtubules.

During metaphase II, the meiotic outer plaque of the spindle pole body serves as a site for vesicle fusion and formation of the prospore membrane (Figure 1-2) (Neiman, 1998). Once an initial cap has been established by the fusion of post-Golgi vesicles on each meiotic outer plaque, four prospore membranes lengthen to engulf each daughter nucleus (Neiman, 1998). Prospore membrane extension occurs with the fusion of cytoplasmic vesicles that carry v-SNAREs (Snc1/2) and t-SNAREs (Sso1/2) that include a meiosis-specific SNAP-25 homolog, Spo20 located on the growing prospore membrane (Neiman, 1998; Neiman *et al*., 2000). Expansion of the prospore membrane is controlled by two protein complexes: the septins and the leading edge complex (Neiman, 2005). The septins are a conserved family of filament forming proteins (Gladfelter *et al*., 2001; Longtine and Bi, 2003). In vegetative cells, septin proteins, located at the plasma membrane, form rings and are necessary for cytokinesis (Gladfelter *et al*., 2001; Longtine

and Bi, 2003). During sporulation, septin rings disassemble and are relocalized to the forming prospore membranes (Fares *et al.*, 1996; Tachikawa *et al*., 2000). Deletion of septin genes produces no obvious sporulation phenotypes, though a strain that lacks all septin genes has not been constructed (Tachikawa *et al*., 2000).

Prospore Membrane Closure and Spore Wall Formation

The lips of the growing prospore membrane contain a coat termed the leading edge complex (Byers, 1981; Knop and Strasser, 2000; Moreno-Borchart *et al*., 2001). The leading edge complex consists of three proteins: Don1 (**don**uts), Ady3 (**a**ccumulation of **dy**ads) and Ssp1 (**s**porulation **sp**ecific) (Knop and Strasser, 2000; Moreno-Borchart *et al*., 2001; Nag *et al*., 1997; Nickas and Neiman, 2002). *DON1* was originally identified on the basis of its sporulation-specific expression (Chu *et al*., 1997; Moreno-Bochart *et al*., 2001). The function of Don1 is unknown, and a *don1* deletion mutant has no discernable phenotype (Moreno-Borchart *et al.*, 2001). Immunofluorescence studies show localization of Don1-GFP to the leading edge complex and its localization requires both Ady3 and Ssp1 (discussed below) (Moreno-Borchart *et al*., 2001; Nickas and Neiman, 2002). Ady3 was identified by its ability to bind to meiotic spindle pole body components in both two hybrid and co-purification studies (Ito *et al*., 2001; Moreno-Borchart *et al*., 2001; Uetz *et al*., 2001). *ady3Δ* mutants have a subtle phenotype in that asci containing fewer than four spores accumulate during sporulation (Moreno-Borchart *et al*., 2001; Nickas and Neiman, 2002). The localization of Ady3 and Don1 to the leading edge of the prospore membrane depends on the presence of Ssp1 (Maier *et al*., 2007; Moreno-Borchart *et al*., 2001; Nickas and Neiman, 2002).

SSP1 was originally identified in a screen for mutants defective in meiosis and sporulation (Esposito and Esposito, 1969). Later, expression studies demonstrated *SSP1* to be meiotically induced (Chu *et al*., 1998; Nag *et al.*, 1997). Deletion of *SSP1* causes a dramatic phenotype in sporulating cells: while the meiotic divisions progress as in wild type, all three leading edge complex components (Ssp1, Don1 and Ady3) are mislocalized (Maier *et al*., 2007; Moreno-Borchart *et al*., 2001). Thus, Ssp1 may anchor the other two proteins to the leading edge complex during prospore membrane expansion (Moreno-Borchart *et al*., 2001). Prospore membranes are still formed, but they are grossly abnormal and appear to be adherent to the nuclear envelope (Moreno-Borchart *et al*., 2001). Additionally, the prospore membranes occasionally grow in the wrong direction, resulting in a failure to capture daughter nuclei (Moreno-Borchart *et al*., 2001). The *ssp1Δ* phenotype demonstrates the necessity for the leading edge complex for proper membrane growth. Ssp1 also has an anti-fusion function: ectopic over-expression of *SSP1* in vegetative cells blocks mitotic growth by interfering with the fusion of secretory vesicles to the plasma membrane (Maier *et al*., 2007). These results have led to the proposal that removal of Ssp1 from the leading edge regulates the timing of cytokinesis during sporulation (Maier *et al.,* 2007).

At the end of Meiosis II, the ends of the double membrane fuse, capturing four daughter nuclei. This cytokinetic event forms four immature prospores, each containing distinct cytoplasm and organelles from the mother cell (Figure 1-2) (Suda *et al*., 2007). Though cytokinesis in vegetative cells requires cytoskeletal elements including actin, septins and microtubules, prospore membrane closure does not seem to be dependent on these structural proteins (Figure 1-3) (Tachikawa *et al*., 2000; Taxis *et al*., 2006).

Following closure of the prospore membrane, spore wall formation begins in between the two membranes derived from the prospore membrane (Lynn and Magee, 1970). The spore wall is a more extensive structure than the vegetative cell wall (Smits *et al*., 2001). The vegetative cell wall consists of two major layers, an inner layer containing some chitin and mainly β-glucan (chains of beta-1,3-linked glucose) and an outer mannan layer consisting of proteins that have been heavily N and O glycosylated with primarily mannose side chains (Orlean, 1997; Klis *et al*., 2002). In contrast, the spore wall consists of four layers (Smits *et al*., 2001). Specific layers of the spore wall are deposited in a particular temporal order in between the lumen of the prospore membrane (Tachikawa *et al*., 2001). The inner two layers consist of primarily mannan and β-glucan though their order is reversed compared to vegetative cell walls (Kreger-Van, 1978). The third layer of the spore wall consists of the polymer of chitosan (Briza *et al*., 1988). Spore wall completion occurs with the deposition of the final layer, dityrosine (Briza *et al*., 1986). Spore walls provide resistance to environmental stress and spores can exist in a quiescent state until environmental conditions improve and permit germination and proliferation to proceed (Figure 1-4) (Briza *et al.*, 1990).

Meiosis is coupled to the process of sporulation in budding yeast. In order to define meiosis and sporulation genetically, transcriptional studies of sporulating budding yeast cells sought to identify genes whose transcription was upregulated during sporulation (Holloway *et al*., 1985; Percival-Smith and Segall, 1984). Subsequently, microarray studies examined genome-wide expression during sporulation (Chu *et al*., 1998; Enyenihi and Saunders, 2003; Primig *et al.*, 2000). Gene expression during sporulation in budding yeast can be divided into three temporal classes: early, middle,

and late meiotic genes (Mitchell, 1994). Early genes are expressed at the onset of transfer to nutrient-limited media. *IME1*, an early gene, is a key transcription factor necessary for the transcription of genes critical to early meiotic events such as DNA synthesis, synapsis of homologous chromosomes and meiotic recombination (Chu *et al*., 1998; Kassir *et al*., 1988; Primig *et al.*, 2000). The middle gene category has been subdivided into early-middle and middle late genes (Briza *et al*., 1990; Pak and Segall, 2002). *NDT80*, an early middle expressed at the onset of the first meiotic division, is a transcription factor required for the transcription of middle and late middle meiotic genes (Chu *et al*., 1998; Enyenihi and Saunders, 2003; Primig *et al.*, 2000). Middle and late genes encode proteins that control nuclear division, components of the anaphase promoting complex and spore formation (Chu *et al*., 1998; Chu and Herskowitz, 1998; Enyenihi and Saunders, 2003; Primig *et al.*, 2000). Spore maturation depends on the expression of late genes. For example, *DIT1* and *DIT2*, middle-late meiotic genes, encode proteins involved in assembly of the final spore wall layer, dityrosine (Briza *et al*., 1990; Briza *et al.*, 1994; Felder *et al*., 2002). Biochemical and genetic characterization of strains that contain deletions in genes whose expression is upregulated during meiosis have identified discrete steps in a morphogenetic pathway governing spore wall assembly (Rabitsch *et al*., 2001; Coluccio *et al*., 2004).

Anaphase Promoting Complex

Passage through critical cell cycle transitions in vegetative cells strictly depends on the successful completion of the previous phase. Forward movement through the cell cycle is forced by an irreversible switch: regulated cyclical proteolysis (Glotzer *et al.*,

1991; Harper *et al*., 2002; Peters, 2006; Thornton and Toczyski, 2006). The ubiquitin-proteasome pathway, a common strategy all eukaryotic cells utilize to rapidly degrade critical proteins necessary for cell cycle advancement, involves three well-defined enzymes: E1, E2 and E3 (Ciechanover *et al*., 1984; Finley *et al.*, 1984; Harper *et al*., 2002; Hershko and Ciechanover, 1998; Peters, 2006). The first enzyme, E1, uses ATP to form a high energy thiol ester with the C-terminal glycine of ubiquitin. Subsequently the ubiquitin subunit is transferred to a cysteine residue on one of several E2s, ubiquitin conjugating enzymes. An E2 enzyme along with an E3 enzyme, or ubiquitin ligase, transfers the ubiquitin tag from the E2 to a lysine residue on a substrate protein. The processive attachment of ubiquitin moieties produces a polyubiquitylated protein that is rapidly recruited to the 26S proteasome, a large multisubunit protease complex that selectively degrades proteins. The anaphase promoting complex (APC), initially identified as an ubiquitin ligase involved in cyclin B ubiquitylation as a result of a simultaneous genetic screen in budding yeast and two different biochemical studies in clam and Xenopus egg extracts, is a tightly regulated multi-subunit E3 ubiquitin ligase whose function is essential during the eukaryotic cell cycle (Figure 1-5) (Harper *et al*., 2002; Irniger *et al*., 1995; King *et al*., 1995; Peters, 2006; Sudakin *et al*., 1995, Thornton and Toczyski, 2006; Zachariae *et al*., 1998).

The APC core complex in budding yeast contains thirteen subunits, eight of which are required for viability (Peters *et al*., 1996; Peters, 2006; Thornton and Toczyski, 2006; Yoon *et al*., 2002; Yu *et al.*, 1998; Zachariae *et al*., 1996, 1998). Structural studies of the APC have produced the construction of an architectural map of the protein complex and suggest the APC may be fully active only as a dimer (Dube *et al*., 2005;

Gieffers *et al*., 2001; Herzog *et al*., 2005; Passmore *et al*., 2005; Thornton *et al*., 2006; Vodermaier *et al*., 2003). The catalytic core, composed of two subunits, Apc2 and Apc11, can transfer ubiquitin to a substrate protein but with poor specificity and processivity (Gmachl *et al*., 2000; Leverson *et al*., 2000; Tang *et al*., 2001; Passmore *et al*., 2004). Three subunits of the APC, Cdc27, Cdc16 and Cdc23, contain TPR (Tetratricopeptide) domains, protein regions that function in promoting protein-protein interactions (Tang *et al*., 2001; Vodermaier *et al*., 2003). Most phosphorylation sites located in the APC are present in the TPR subunits (Kraft *et al*., 2003). Two subunits, Apc4 and Apc5, might serve as structural elements connecting the enzymatic core to the TPR subunits **(**Harper *et al*., 2002; Peters, 2006**)**. Studies suggest Doc1 (Apc10) may be involved in substrate recognition and promote processivity of the ubiquitin reaction (Carrol1 and Morgan, 2002; Carroll *et al*., 2005; Grossberger *et al*., 1999; Hwang and Murray, 1997; Kominami *et al*., 1998; Kurasawa and Todokoro, 1999; Passmore *et al*., 2003). Two APC subunits display meiosis-specific phenotypes: Swm1 (Apc13) and Mnd2 (Apc15) (Hall *et al*., 2003; Oelschlaegel, *et al*., 2005; Passmore *et al*, 2005; Penkner *et al*., 2005; Ufano *et al*., 1999). Both Swm1 and Mnd2 interact with core subunits suggesting a role in core stability (Hall *et al*., 2003; Yoon *et al*., 2002). Swm1 and Mnd2 could provide an essential function for the APC during meiosis that is not required during mitosis (Hall *et al*., 2003).

The APC is only fully active as an E3 ubiquitin ligase when bound to a co-activator **(**Fang *et al*., 1998; Kramer *et al*., 1998; Jasperson *et al*., 1999; Harper *et al*., 2002; Peters, 2006). Activators are not stable components of the APC but instead interact with the APC core at specific times to promote E3 ubiquitin ligase activity (Fang *et al*.,

1998; Kallio *et al*., 1998; Zachariae *et al.*, 1998). In mitotic cells, the APC ubiquitylation pathway is initiated by the accumulation of two activators conserved in all eukaryotic genomes, Cdc20 (Fizzy) and Cdh1 (Hct1p or Fzr1) (Harper *et al.*, 2002; Peters, 2002; Schwab *et al*., 1997; Visintin *et al*., 1997). The active form of the APC is designated by the activator in superscript, e.g. APC^{Cdc20}.

One target of the mitotic APC^{Cdc20} is securin. Securin binds to separase, a cysteine protease, rendering the protease inactive. When released from securin, separase degrades cohesin subunits that maintain cohesion between the sister chromatids (Ciosk *et al*., 1998; Hauf *et al*., 2001; Tanaka *et al*., 1999; Uhlmann *et al*., 1999, 2000; Yanagida, 2000). Securin destruction is necessary for the progression from metaphase to anaphase (Cohen-Fix *et al.*, 1996; Funabiki *et al*., 1996; Lim *et al*., 1998; Morgan, 1999; Schott and Hoyt, 1998; Tinker-Kulberg *et al.*, 1999; Visintin *et al.*, 1997; Yamamoto *et al*., 1996; Zou *et al*., 1999). APC^{Cdc20} has been shown to mediate the degradation of securin in meiosis during the metaphase I to anaphase I transition and the metaphase II to anaphase II transition (Salah and Nasmyth, 2000). APC^{Cdh1} regulates mitotic exit by targeting Clb2 for degradation during the G2 phase of the mitotic cell cycle (Schwab *et al*., 1997; Visintin *et al.*, 1997). While both Cdc20 and Cdh1 direct the degradation of multiple, overlapping targets, each controls the degradation of a specific target essential for cell division: mitotic cyclins for Cdh1 and securin for Cdc20 (Thornton and Toczyski, 2003).

All APC activators share several conserved features in their primary amino acid sequence. Two separate sequence elements found in all APC activators contribute to the binding of the activator to core subunits of the APC. A C-box, sequence element

(consensus DRF/YIPXR), is located in the N-terminal region of APC activator proteins (Schwab *et al*., 2001). An IR tail, sequence element (consensus IR), is located at the extreme C-terminus of APC activators and the APC subunit, Doc1 (Apc10) (Oelschlaegel *et al.*, 2005; Passmore *et al.*, 2003; Thorton *et al*., 2006; Vodemaier *et al.*, 2003; Wendt *et al.*, 2001). Another feature characteristic of all APC activators is the presence of multiple WD40 repeats, a protein binding motif predicted to fold into a beta-propeller structure (Kraft *et al*., 2005). The WD40 domain region of APC activators is believed to recognize APC substrates by interacting with specific recognition elements in a target substrate (Kraft *et al*., 2005; Pfleger *et al*., 2000).

Two well-characterized degradation motifs present in many target proteins recognized by an APC activator are the D box (consensus RxxLxxxN), first discovered in the N terminus of mitotic cyclins, and the KEN box (consensus KENxxxxN/D/E), a sequence element first identified by Pfleger and Kirschner (2001) (Glotzer *et al.*, 1991; Harper *et al.*, 2002; King *et al.*, 1996; Passmore and Barford, 2004; Peters, 2006; Pfleger and Kirschner, 2001). As more APC target substrates are identified, novel degradation sequences continue to be characterized. Other degradation motifs include a GxEN box, an A box, a CRY box and the sequence LxExxxN (Castro *et al*., 2003; Littlepage and Ruderman, 2002; Reis *et al*., 2006; Sullivan *et al*., 2007). Additionally, the APC subunit Doc1 contributes to substrate recognition (Carroll and Morgan, 2002; Carroll *et al.*, 2005; Passmore *et al*., 2003). Several labs have demonstrated that APC activators bind directly to target substrates for degradation but the molecular mechanisms of substrate recognition and subsequent ubiquitylation of targets remain uncertain (Burton and Solomon, 2001; Burton *et al.*, 2005; Hayes *et al.*, 2006; Hilioti *et al.*, 2001; Oelschlaegel

et al., 2005; Ohtoshi *et al*., 2000; Passmore *et al.*, 2005; Pfleger *et al.*, 2001; Schwab *et al*., 1997, 2001; Sorensen *et al*., 2001; Visintin *et al*., 1997; Wan and Kirschner, 2001; Yamano *et al*., 2004).

Though the functions of Cdc20 and Cdh1 are best understood during the mitotic cell cycle, several groups have identified functions of the APC in post-mitotic cells. APC^{Cdh1} activity, abundant in post-mitotic differentiated neurons, is involved in the regulation of axonal growth and patterning as well as learning and memory in the developing brain (Almeida *et al.*, 2005; Gieffers *et al*., 1999; Juo and Kaplan, 2004; Kaplow *et al.*, 2007; Konishi *et al*., 2004; Lasorella *et al*., 2006; Li *et al.*, 2008; Maestro *et al*., 2008; Stegmuller *et al*., 2005, 2006, 2008; Teng and Tang, 2005; van Roessel *et al*., 2004). Accumulating evidence demonstrates the APC regulates cell cycle events indirectly through specific signal transduction pathways. For example, the APC regulates transforming growth factor-beta signaling, a signal transduction pathway involved in cell growth and differentiation (Liu *et al*., 2007; Strochein *et al*., 2001; Wan *et al*., 2001).

During meiosis in *Saccharomyces cerevisiae*, virtually all subunits of the APC are upregulated (Chu *et al*., 1998; Enyenihi and Saunders, 2003; Primig *et al.*, 2000). Two subunits of the budding yeast APC are associated with meiosis-specific phenotypes, *SWM1* and *MND2* (Hall *et al*., 2003; Ufano *et al*., 1999). Within the last decade, several meiosis-specific APC activators have been identified in budding yeast, fission yeast and Drosophila (Asakawa *et al*., 2001; Blanco *et al*., 2001; Chu *et al*., 2001; Cooper *et al.*, 2000; Pesin and Orr-Weaver, 2007; Swan and Shupbach, 2007). The existence of these activators suggests a unique role and set of substrates for the APC in meiosis that are outside of the functions of APC^{Cdc20} and APC^{Cdh1}. Though no meiosis-specific APC

activators have yet been identified in vertebrates, the presence of meiotic APC activators in organisms as diverse as yeast and fly suggests meiotic APC activators may be present in vertebrates as well.

AMA1 (Activator of Meiotic Anaphase Promoting Complex)

Spore formation requires the APC activator *AMA1* in budding yeast (Cooper *et al*., 2000). Electron micrograph studies demonstrate prospore membranes are formed in an *ama1*Δ homozygous mutant sporulating cell. However, in contrast to the thick spore walls seen in wild-type cells, there is no evidence of spore wall material between the lumen of the prospore membrane (Figure 1-6) (Coluccio *et al*., 2004). Consequently, an *ama1*Δ homozygous mutant was identified in a screen for genes essential for sporulation in budding yeast (Rabitsch *et al*., 2001). *AMA1* is necessary for expression of mid-late meiotic genes, such as *SPS100,* and late genes, such as *DIT1* (Cooper *et al*., 2000; Collucio *et al*., 2004). Because proteolysis is an irreversible process, APC^{Ama1} activity is tightly regulated. *AMA1* is under transcriptional control and is highly induced during sporulation (Chu *et al*., 1998; Cooper *et al*., 2000). The *AMA1* open reading frame contains an intron that is removed by the regulated splicing factor, Mer1, ensuring Ama1 protein is present only in meiotic cells (Chu *et al*., 1998; Cooper *et al.*, 2000). Although Ama1 protein is present early in meiosis, genetic and biochemical experiments demonstrate Ama1 is not fully active as an APC activator until metaphase II because Mnd2, a subunit of the APC, specifically restrains APC^{Ama1} and not APC^{Cdc20} function (Oelschlaegel *et al*., 2005; Penkner *et al.*, 2005). Genetic studies in budding yeast suggest that in *mnd2Δ* homozygous mutant cells, APC^{Ama1} can target Pds1, Sgo1 and Clb5 for

degradation during meiotic prophase (Oelschlaegel *et al*., 2005; Penkner *et al*., 2005). Importantly, Oelschlaegel and co-workers (2005) demonstrated APC^{Cdc20} is responsible for the bulk of securin degradation during the meiotic divisions and securin turnover is unaffected in *ama1*Δ mutants (Oelschlaegel *et al*., 2005). Cyclin-dependent kinase activity may also regulate APC^{Ama1} function, possibly by the phosphorylation of Ama1 (Carlile and Amon, 2008; Dahmann and Futcher, 1995; Oelschlaegel *et al*., 2005).

In this dissertation, I report that Ama1 is a pivotal protein coordinating meiotic exit with cytokinesis and the onset of spore wall formation. We propose that, during sporulation, Ama1 activates the APC to target an inhibitor(s) of spore wall formation whose degradation is required for the initiation of spore wall construction (Figure 1-7). Therefore, the identification of targets of APC^{Ama1} will likely contribute to greater understanding of molecular events that link meiotic exit and cytokinesis during sporulation in budding yeast.

Figures Chapter 1: Introduction

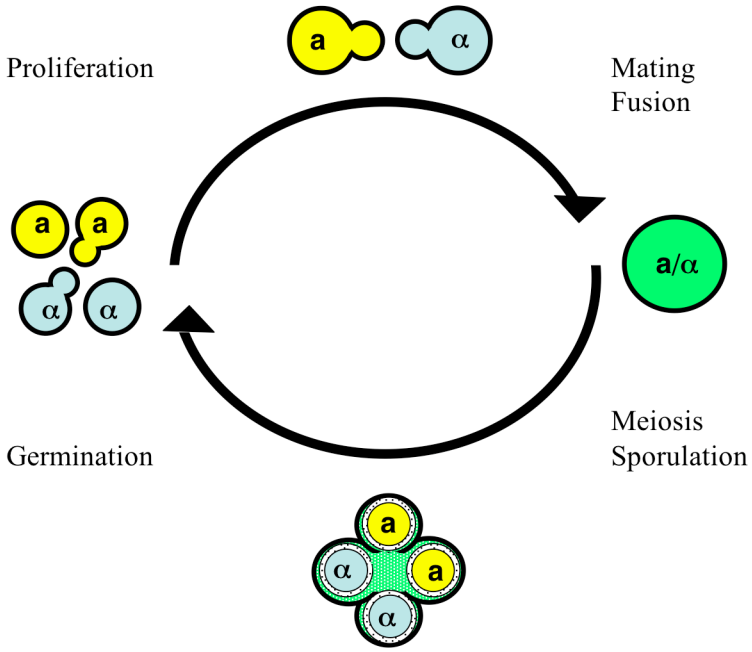

Figure 1-1. *Saccharomyces cerevisiae* life cycle

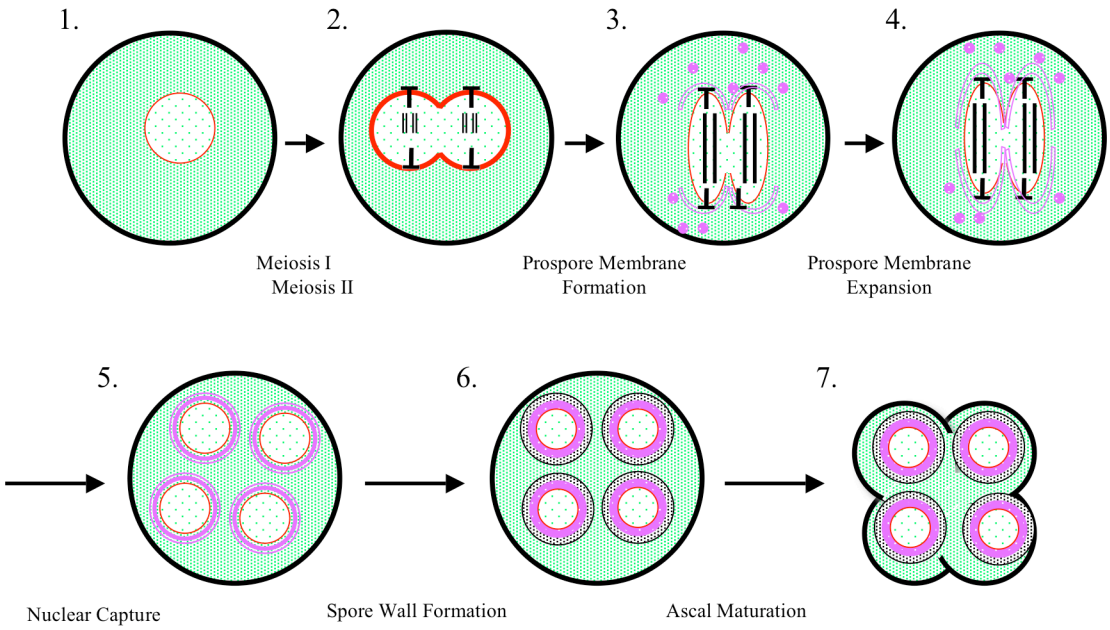

Figure 1-2. Overview of the stages of spore formation
(1) and (2) The beginning stages of the meiotic program are omitted. This cartoon concentrates on the second meiotic division when prospore membrane formation begins. (3) and (4) During Meiosis II, the prospore membrane is formed and continues to lengthen until four haploid daughter nuclei are captured in four individual membrane structures. (5) Cytokinesis occurs when the ends of the prospore membrane fuse to form four immature prospores. (6) Construction of the outer spore wall occurs within the lumen of the prospore membrane. (7) After spore wall synthesis is complete, the mother cell collapses to form the ascus. The spindle pole bodies (indicated as a "T") are embedded in the nuclear envelope (red). The double lines represent microtubules.

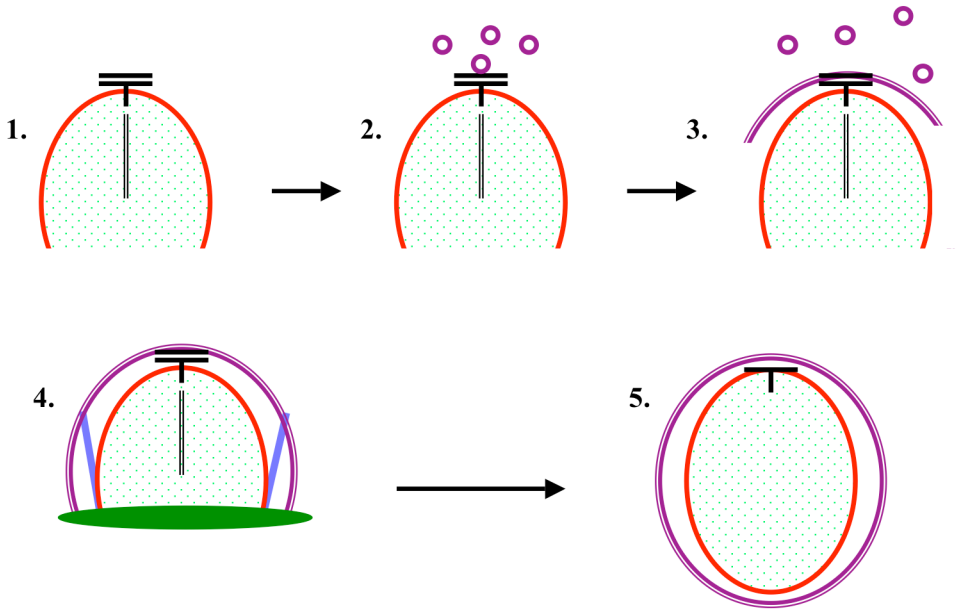

Figure 1-3. Stages of prospore membrane growth
(1) During Meiosis II, the spindle pole body is modified and a meiotic outer plaque is assembled. (2) and (3) The meiotic outer plaque serves as a nucleation site for recruited vesicles to form the nascent prospore membrane. (4) As the prospore membrane expands to engulf a daughter nucleus, two membrane-associated complexes control its growth: the septins (blue) and the leading edge complex (green ring). The leading edge complex is located at the lip of each growing prospore membrane and is composed of three proteins: Ssp1, Ady3, and Don1. (5) At the time of prospore membrane closure, prospore membrane-associated complexes (meiotic outer plaque components, the septins and the leading edge complex proteins) disassemble.

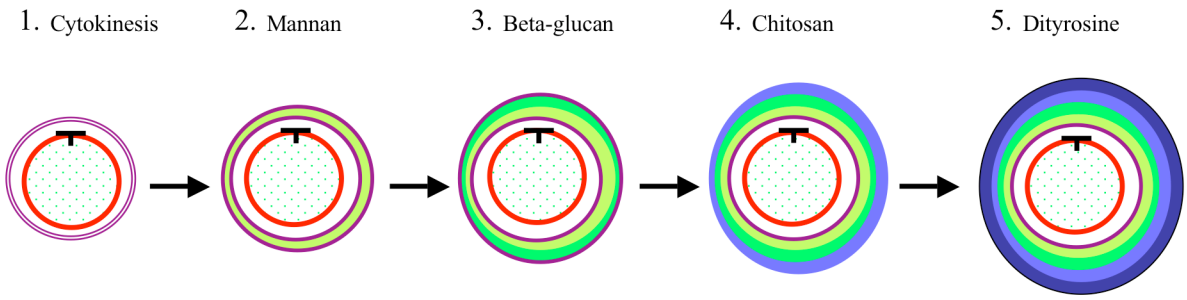

Figure 1-4. Pathway of spore wall assembly
(1)-(5) After closure of the prospore membrane, specific layers of the spore wall are deposited in between the lumen of the double membrane. First, a mannan layer is deposited followed by a β-glucan layer followed by a chitosan layer. Finally, a dityrosine layer is deposited. Spore walls provide resistance to environmental stress and spores can exist in a quiescent state until environmental conditions improve and permit germination and proliferation.

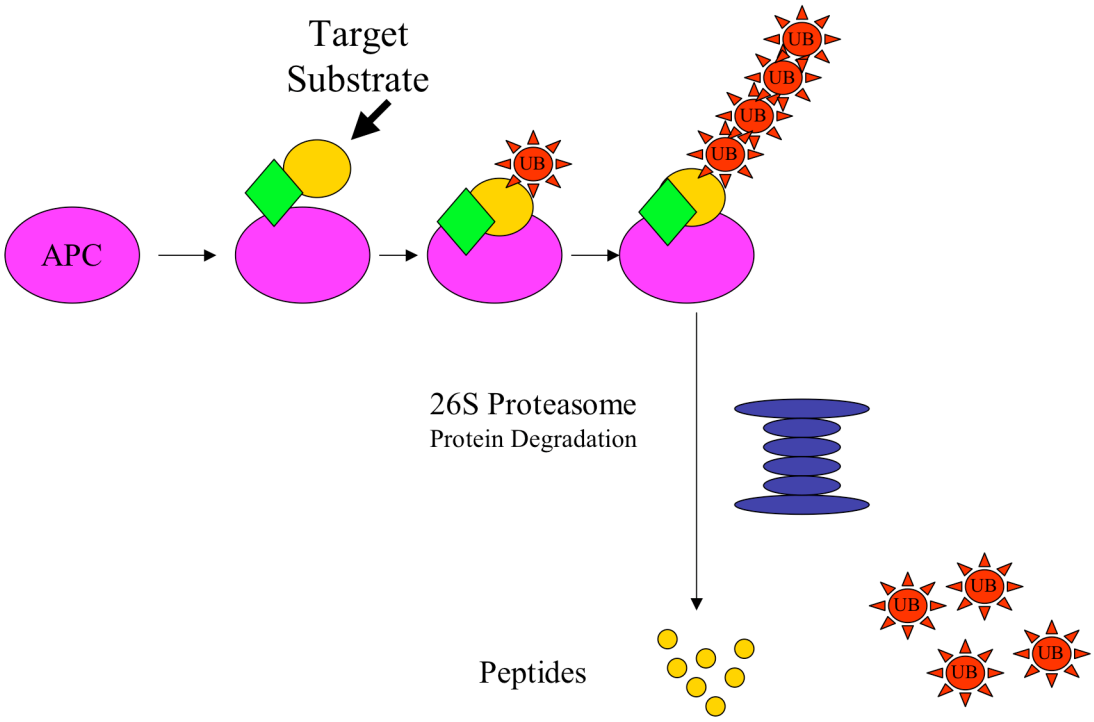

Figure 1-5. The anaphase promoting complex (APC) is an E3 ubiqitin ligase
The APC is a tightly regulated multi-subunit ubiquitin ligase whose function is essential during the eukaryotic cell cycle. For simplicity, the APC is depicted as a single entity although in fact, the APC core consists of 13 subunits, eight of which are required for viability. The APC is only fully active as an ubiquitin ligase when bound to an activator (green diamond). Activators are not stable components of the APC but instead interact with it at specific times to promote its activity. The APC along with its bound activator is an E3 ubiquitin ligases, a well-defined enzyme involved in the ubiquitin-proteasome pathway. The APC activator is thought to provide specificity by recognizing and binding to specific sequences on a target substrate (yellow oval). Multiple rounds of ubiquitylation ensue to ensure that several ubiquitin tags are transferred onto a target substrate protein. Poly-ubiquitylated proteins are recruited to the 26S proteasome and destroyed while the ubiquitin tag is recycled for future use.

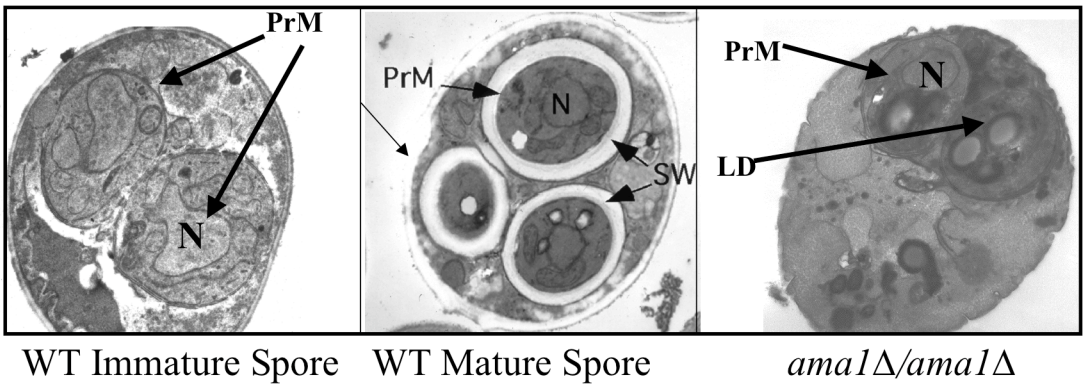

Figure 1-6. Electron micrographs of wild type and *ama1Δ/ ama1Δ* sporulating cells
Wild-type immature spores complete closure of the prospore membrane and mature wild-type spores display thick spore walls. *ama1Δ* homozygous diploid mutants complete Meiosis II. There is no evidence of any of the spore wall material in between the lumen of the prospore membrane. PrM, prospore membrane; N, nucleus; SW, spore wall; LD, lipid droplet.

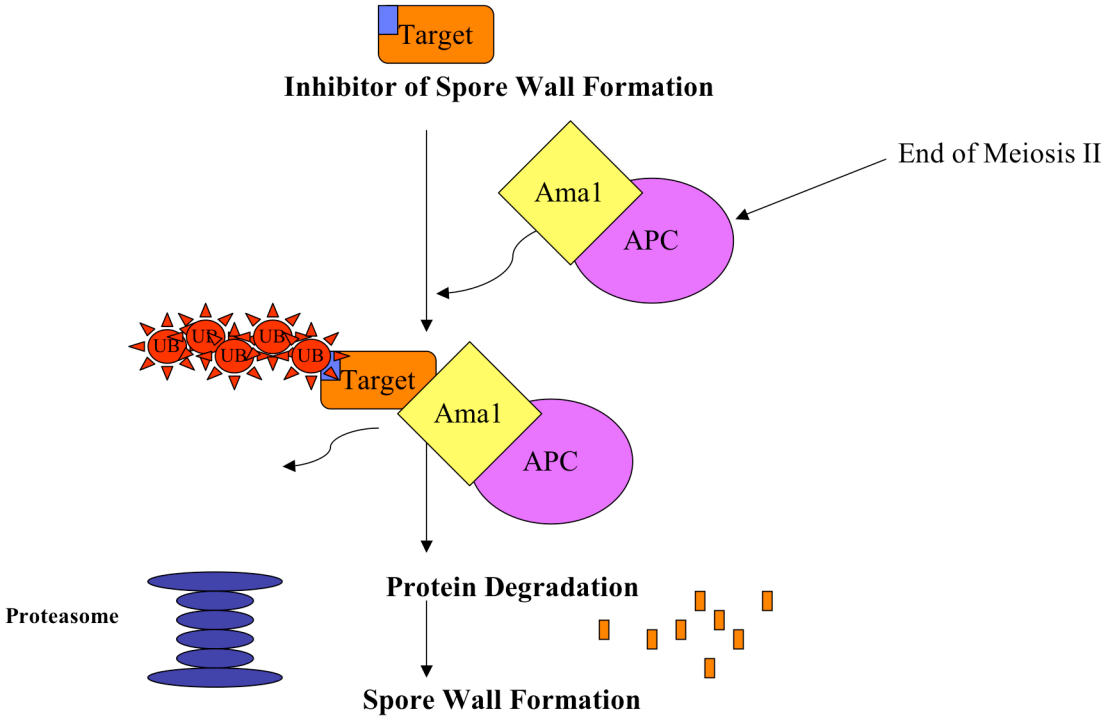

Figure 1-7. Model of APC^{Ama1} function
At the end of Meiosis II, there exists an inhibitor(s) of spore wall formation whose degradation is necessary to allow spore wall formation to occur. During sporulation, Ama1 binds to the APC rendering the multi-subunit E3 ubiquitin ligase competent to target a protein to the 26S proteasome. The proteasome then degrades this putative inhibitor of spore wall formation and allows spore wall synthesis to occur.

Chapter 2: Genetic Analyses of *AMA1*

Introduction

A variety of genetic approaches were used to attempt to identify possible targets of APC^{Ama1}-mediated degradation. A yeast two-hybrid screen was performed for Ama1-intereacting proteins. For all non-essential interacting proteins uncovered in the screen, double homozygous deletion mutants were generated between *ama1Δ* and the putative target protein, *orfxΔ*. The constructed double mutant strains, *ama1Δ orfxΔ*, were examined for suppression of the *ama1Δ* phenotype by inspecting for spores by light microscopy.

CDC20 family members share conserved regions known to interact with core subunits of the APC. The corresponding conserved residues were mutated in Ama1 and the phenotypes of these mutants were examined. Structure-function analyses of *AMA1* determined the C-terminal IR (isoleucine and arginine) residues are critical for Ama1-dependent activation of the APC and spore wall formation. To determine the smallest critical region of Ama1 that suppresses the spore wall phenotype, chimeric fusion proteins between Ama1 and Cdc20 were constructed and examined for suppression phenotypes in the *cdc20ts* or *ama1Δ* homozygous mutant strains.

Genetic screens sought to identify genetic interactions with *AMA1*. A high copy suppressor screen aimed to identify a gene that when over-expressed in *ama1Δ* homozygous sporulating cells, could suppress the *ama1Δ* failure to sporulate. A second-site suppressor screen intended to identify a mutation in the open reading frame of a putative substrate target of APC^{Ama1} whose inactivation would suppress the *ama1Δ*

phenotype and form spores. Further, the *ama1Δ* phenotype could be suppressed by dosage-dependent expression of $AMA1^{IR\Delta}$ demonstrating $AMA1^{IR\Delta}$ represents a hypomorphic allele of *AMA1*. A second-site suppressor screen was pursued that utilized a transposon mutagenesis strategy in a strain containing two copies $AMA1^{IR\Delta}$. The mutants were examined for suppression of the *ama1Δ* phenotype by examination for spores.

Ama1 had previously been suggested to direct the ubiquitylation of Clb1 (Cooper *et al*., 2000), though more recent work casts doubt on this result (Oelschlaegel *et al*., 2005; Penkner *et al*., 2005). Several homozygous diploid mutant strains were constructed to determine if (specific) *CLB* deletions in a homozygous *ama1Δ* strain suppresses the *ama1Δ* phenotype allowing spore formation to proceed.

Materials and Methods

Strains and Growth Medium

Unless otherwise noted, standard media and genetic techniques were used (Rose and Fink, 1990). The strains used in this study are listed in Table 2-1. All strains are in the SK-1 background except when noted. ADY12 and ADY13 were constructed by PCR-mediated knockout of *AMA1* in AN117-4B and AN117-16D, respectively, using pFA6a CgTRP1 as a template for PCR and oligonucleotides (oligos) F1AMA1 and R1AMA1 in both AN117-4B and AN117-16D (Longtine *et al.*, 1998). ADY64 and ADY65 were constructed in the same manner except pFA6a HisMX6 was the PCR template. ADY15 and ADY16 were constructed by PCR-mediated knockout of *CLB1* using pFA6a KlURA3 as a template for PCR and oligos F1-CLB1 and R1-CLB1. ADY18 and ADY19 were constructed by PCR-mediated knockout of *CLB4* using pFA6a HisMX6 as template and oligos F1-CLB4 and R1-CLB4. All PCR-mediated integrations were confirmed by genomic PCR with appropriate primers. Strains ADY21 and ADY22 (*ama1Δ*::*TRP1 clb1Δ*::*URA3*) were constructed by crossing ADY13 with ADY15 followed by identification of the appropriate segregant. Strains ADY24 and ADY25 (*ama1Δ*::*TRP1 clb4Δ*::*HIS3*) were constructed by crossing ADY13 with ADY18 followed by identification of the appropriate segregant. Strains ADY27 and ADY28 (*clb1Δ*::*URA3 clb4Δ*::*HIS3*) were constructed by crossing ADY15 with ADY19 and followed by identification of the appropriate segregant. Strains ADY30 and ADY31 were constructed by crossing ADY15 with ADY28 and followed by identification of the appropriate segregant. Strains 603 and 604 were a gift from N. M. Hollingsworth (by way of S. Keeney) and each haploid contains an analog sensitive allele of *CDC28*,

cdc28as-1, for inhibition with 1-NM-PP1 (gift of N. M. Hollingsworth). Strains ADY91 and ADY96 were constructed by crossing ADY64 with ADY88 and followed by identification of the appropriate segregant. Strains EW1202 and EW1204 were a gift from E. Winter and contain a temperature sensitive allele of *CDC28*, *cdc28-4*. Strains ADY126 and ADY127 (*cdc28-4*) were created by mating AN117-4B with ADY111 and followed by identification of the appropriate segregant. Strains ADY130 and ADY132 were created by mating ADY64 with ADY127. The temperature sensitive *CDC20*, *cdc20ts*, was a gift from R. Sternglanz. Strain 1xΔIR was created by linearizing pRS306AMA1prAMA1ΔIR with EcoRV and transforming the integrating plasmid into strain ADY66 (*MATα/ MAT**a*** *ama1Δ::HIS3/ama1Δ::HIS3*). Strain 2xΔIR was created by linearizing pRS306AMA1pr-AMA1ΔIR with EcoRV and transforming the integrating plasmid into both ADY64 (*MATα ama1Δ::HIS3*) and ADY65 (*MAT**a*** *ama1Δ::HIS3*) creating ADY64ΔIR and ADY65ΔIR. The transformed haploids were subsequently mated to each other yielding strain ADY66-2xΔIR. Strains ADY66-3xΔIR and ADY66-4xΔIR were created as follows: plasmid pRS304AMA1pr-AMA1ΔIR was linearized with EcoRV and transformed separately into ADY64ΔIR and ADY65ΔIR yielding ADY64-2xΔIR and ADY65-2xΔIR, respectively. ADY66-3xΔIR was created by mating strain ADY64-2xΔIR withADY65-1xΔIR. Strain ADY66-4xΔIR was created by mating ADY64-2xΔIR with ADY65-2xΔIR. Strain L40 was a gift from R. Sternglanz. Strain NKY895 was a gift from N.M. Hollingsworth (by way of N. Kleckner).

Plasmids

Plasmids used in this study are listed in Table 2-2. pBTM116AMA1 was constructed as follows. To remove the sporulation-specific intron (base pairs 1184-1276), a 5' fragment of *AMA1* ORF was amplified with primers FAMA1EcoRI (ADO60) (+631) and RAMA1NdeI (ADO58) and blunt-end ligated into pBluescript at the EcoRV restriction enzyme site to create pBluescriptAma1A. This was followed by amplification of a 3' *AMA1* ORF fragment with primers FAMA1Nde1 (ADO59) and RAMA1Pst1stop (ADO61). This fragment was digested with NdeI and PstI and ligated to similarly digested pBluescriptAma1A. The removal of the intron sequence yielded an amino acid change at position 236 from a cysteine to a serine. This intronless segment sequence of *AMA1* was digested with EcoRI and PstI and ligated into similarly digested pBTM116 (gift from R. Sternglanz). The pACTII library was a gift from N. M. Hollingsworth. The pUV1 library was a gift from N. M. Hollingsworth. The mTN library was a gift from H. Nakanishi by way of M. Snyder. Constructions of the various chimeras are described as follows (Table 2-3). Expression vectors were constructed by cloning 500 base pairs of the upstream regions of the *AMA1* gene or the *CDC20* gene into the polylinker of plasmid pRS306 (Sikorski and Heiter, 1989). The *AMA1* upstream region was amplified using oligonucleotides PAMA1F (ADO1) and PAMA1R (ADO2). The PCR fragment was digested with KpnI and XhoI and then cloned into similarly digested pRS306 to create pRS306-AMA1pr. The *CDC20* promoter was similarly amplified and subcloned using oligonucleotides PCDC20F (ADO6) and PCDC20R (ADO7) to create pRS306-CDC20pr. The full-length intronless *AMA1* sequence was amplified utilizing overlap PCR. A 5' fragment of *AMA1* was amplified using primers AMA1PfXhoI (ADO5) and

AMA1USR (ADO10) using yeast genomic DNA as a template. This PCR product was mixed with a vector carrying the intronless *AMA1* 3' sequence, pBTM116AMA1, and amplified with primers Ama1pFXhoI (ADO5) and Ama1StopSpeI (ADO3) yielding a ~2Kb DNA fragment. The PCR fragment was digested with XhoI and SpeI and then cloned into similarly digested pRS306 to create pRS306AMA1. To place the intronless *AMA1* ORF under the control of its own promoter, the *AMA1* intronless insert was digested with XhoI and SpeI and inserted into similarly digested pRS306AMA1pr to yield pRS306AMA1pr-AMA1. The *AMA1* in this plasmid was shown to be functional based on its ability to complement the *ama1Δ* phenotype (Table 2-4). Oligos CDC20pF (ADO9) and CDC20STOP (ADO8) were used to amplify the ORF of *CDC20* using genomic DNA as template (AN117-4B) and ligated into pRS306CDC20pr digested with XhoI and SpeI to create pRS306CDC20prCDC20. The *CDC20* in this plasmid was shown to be functional based on its ability to complement the *cdc20ts* phenotype **(**Table 2-4**)**. To create pRS306AMA1prCDC20, the vector, pRS306AMA1pr, was digested with XhoI and SpeI and the *CDC20* ORF insert was obtained from digesting pRS306CDC20 with XhoI and SpeI. To create pRS306CDC20pr-AMA1, the vector, pRS306CDC20pr was digested with XhoI and SpeI and the *AMA1* cDNA was obtained from digesting pRS306AMA1 with XhoI and SpeI. Chimeric molecules were constructed by overlapping PCR (Hornton *et al.,* 1989; Yon and Fried, 1989). As an example, chimera AMA1-A1, encoding a fusion of the Ama1 protein N terminus to the Cdc20 protein WD40 repeat C-terminal region, was constructed by amplification of the 5' end of the *AMA1* gene using primers AMA1pFXhoI (ADO5) and N1AMA1CCdc20 (ADO11) (see Appendix 2 for primer sequences used in this study). The ADO11 primer has homology

to the *AMA1* N-terminal region at its 3' end and *CDC20* WD40 region 1 at its 5' end. The product of this amplification was included in a second PCR reaction using *CDC20* as a template obtained in pRS306CDC20pr-CDC20 along with the primers Ama1pFXhoI (ADO5) and CDC20Stop (ADO8) primers. These outside primers introduce a XhoI site upstream of the start codon and a SpeI site downstream of the stop codon of the chimeric gene. The PCR product was digested with XhoI and SpeI and cloned into similarly digested pRS306AMA1pr or pRS306-CDC20pr to create pRS306AMA1prA1 or pRS306CDC20prA1, respectively. All of the chimeras were constructed in a similar manner, varying the primers and the templates used (Table 2-3). The junctions in the chimera fusion constructs were verified by DNA sequencing. Plasmids pRS306AMA1pr-AMA1-IA and pRS306AMA1pr-AMA1-ΔIR were constructed by reamplifying the intronless *AMA1* ORF using the oligo pairs Ama1pFXhoI (ADO5) and Ama1StopIA (ADO17), or Ama1pFXhoI (ADO5) and Ama1StopΔIR (ADO151), respectively. The Ama1StopIA (ADO17) and Ama1StopΔIR (ADO151) oligos incorporate mutations at the extreme C-terminus of the coding region. The PCR fragments carrying the mutant alleles were then cloned into pRS306AMA1pr as XhoI-SpeI fragments. pRS316AMA1prAMA1-ΔIR and pRS426AMA1pr-AMA1-ΔIR were created by moving a KpnI-SpeI fragment carrying the gene from pRS306-AMA1pr-AMA1-ΔIR into pRS316 and pRS426, respectively (Christianson *et al.*, 1992). pRS316AMA1pr-AMA1-IA and pRS426AMA1pr-AMA1-IA were created by moving a KpnI-SpeI fragment carrying the gene from pRS306AMA1pr-AMA1-IA into pRS316

and pRS426, respectively. All DNA sequencing analysis was performed at the Stony Brook DNA sequencing facility.

Sporulation assays

Cells were sporulated in liquid medium (2% potassium acetate) as described previously (Neiman, 1998). Briefly, strains were grown at 30°C overnight in YPD or in selective medium if they contained plasmids. The cultures were then diluted to a cell density of 0.2 at OD_{660} in YP media containing 2% potassium acetate and incubated at 30˚ C overnight. Cells were then washed once in distilled water and then resuspended in sporulation medium (2% potassium acetate) at a cell density of 1.2 at OD_{660} and these cultures were incubated at 30˚C.

Ether test

Cells were sporulated on agar plates at 30˚C and replica-plated onto two duplicate YPD plates (Rockmill *et al*., 1991). One plate was exposed to ether vapor for 5 minutes by inversion over an ether soaked paper filter. Plates were analyzed after incubation at 30°C for one day for growth.

Results

Identification of Ama1-Interacting Proteins

BLAST (Basic Local Alignment Search Tool) studies reveal the Ama1 protein contains the strongest homology to APC activators Cdc20 and Cdh1 in the C-terminal WD40 repeat region (Chu *et al*., 1998). Further, the Ama1 protein sequence from amino acids 417 to 464 (contains the fourth WD40 repeat region) displays the highest conserved homology to Cdc20 and Cdh1 showing 46% identity and 67% similarity and 55% identity and 70% similarity, respectively (Figure 2-1). Analysis of sequenced genomes of closely related fungi identified likely Ama1 orthologs in *Candida glabrata*, *Kluyveromyces lactis*, *Ashbya gossypii*, *Debaryomyces hansenii* and *Yarrowia lipolytica*. Ama1 has more homology, particularly in the WD40 repeat binding region, to these Ama1 orthologs than to budding yeast Cdc20 and Cdh1. If WD40 repeats are important for substrate binding, these highly conserved regions may be substrate binding sites.

The yeast two-hybrid system, commonly employed to identify proteins that interact with each other, is a reasonable approach to identify substrate targets of APC^{Ama1} (Fields and Song, 1989). All APC activator proteins contain seven WD40 repeats located in their C-termini, a protein interaction domain that forms beta-propellers and is involved in protein binding (Vodermaier *et al*., 2001). Utilization of the yeast two-hybrid system identified Hsl1 as a target of APC^{Cdh1} (Burton and Solomon, 2000). Additionally, Pds1 was shown to bind to the C-terminal region of Cdc20 while another study narrowed the binding region of p55/Cdc20 to the seventh beta-propeller as sufficient to bind cyclin A (Hilioti *et al*., 2001; Ohtoshi *et al*., 2000).

Previous high throughput genomic screens implemented in vegetative cells were unsuccessful in identifying protein-binding partners of Ama1. Because *AMA1* is only spliced in sporulating cells, these screens utilized a truncated form of Ama1 that lacked the entire WD40 repeat region important in protein-protein interactions (Kraft *et al*., 2005). A specially designed "bait" was used to "fish for prey," or interacting proteins, from a *S. cerevisiae* genomic library consisting of fragments fused to a transactivation domain. A host strain containing a DNA binding region that regulates the expression of two reporter genes, a nutritional marker, *HIS3*, and *LacZ*, which encodes a colorimetric marker, was used to look at a phenotypic readout to measure interaction, or binding, between bait and prey proteins. Instead of using full-length Ama1 protein as bait, the C-terminal two thirds containing the entire WD40 repeat region, (beginning at amino acid 231 to the stop codon at position 593) was fused to the LexA DNA binding domain. DNA sequencing verified Ama1 is in frame with the LexA protein. Western blot analysis showed the fusion protein was at the expected length (blot performed by A. Sutton).

pBTM116-AMA1$^{231\text{-}593}$ was co-transformed with a pACTII library and the transformation mixture was plated onto agar plates lacking tryptophan, leucine and histidine and in the presence of the drug 3-AT (3-Amino-1,2,4-triazole), a His3 competitive inhibitor, at 20mM. Colonies growing more quickly compared to background transformants were selected. To compensate for auto-activation of reporter gene expression, positive interactions between the bait and prey fusion proteins were identified by the ability of individual yeast colonies to grow on histidine-deficient agar plates that contain 3-AT. Colonies expressing LexA-Ama1$^{231\text{-}593}$ fusion protein that interacts with a putative target protein will activate expression of the reporter gene, *HIS3*,

and grow above background levels. A candidate was considered to be positive based on two criteria: there was no interaction between the library fragment and human lamin protein (gift of R. Sternglanz) and by ability to grow on medium containing of 50mM 3AT. Plasmids coding for putative interacting target proteins were retrieved using standard protocols and sent for DNA sequencing analysis.

The yeast two-hybrid screen identified 45 candidates (see Table 2-6 for a complete list of genes recovered in the screen). Six candidates were isolated more than once (*YFL034W*, *GYP5*, *ISW1*, *HSL1*, *SAC7* and *SWE1*). Eight essential genes (*SEN1*, *UTP14*, *NUP159*, *MGE1*, *BRN1*, *RSC3*, *YTM1* and *SWC4*), three uncharacterized open reading frames (*YFL034W*, *YKL050C* and *YNR047W*), and several genes involved in chromatin remodeling (*CHD1*, *ISW1*, *RSC2*, *RSC3*, *BRN1*, and *SWC4*) were found. When the two-hybrid screen was initiated, all identified APC substrates had been shown to contain either a KEN box degradation motif or D box degradation motif (Peters, 2002; Harper *et al*., 2002). Eight candidates contain KEN box motifs, approximately a five-fold enrichment over what would be expected by chance (*UTP14*, *LTE1*, *ENA2*, *UBP9*, *ISW1*, *HSL1*, *NUP159* and *YKL050C*) and eighteen candidates contain a D box motif, approximately a two-fold enrichment over what would be expected randomly (*ISW1*, *HSL1*, *BRN1*, *CLB1*, *SEN1*, *HIR3*, *RDH54*, *YFL034W*, *YTM1*, *NEW1*, *SWC4*, *LTE1*, *NUP159*, *RGA2*, *RSC3*, *SEY1*, *SPT10* and *UTP14*).

For all 37 non-essential open reading frames identified in the yeast two-hybrid screen, homozygous diploid double mutants between *MAT**a** orfxΔ::kanMX6* (Research Genetics collection, S288c strain background) and *MATα ama1Δ::HIS3* were constructed. Both light microscope inspection and ether test analysis showed that none of

the homozygous double mutant strains are capable of spore formation. This suggests that the yeast two-hybrid screen failed to identify a single essential target of APC^{Ama1} whose degradation is both necessary and sufficient for spore formation (data not shown). Perhaps a more sensitive readout other than complete spore formation would indicate if any of the homozygous double deletion mutants are capable of proceeding further in the pathway of spore formation than diploid *ama1Δ* mutants alone. Additionally, it is possible APC^{Ama1} must degrade more than one target before spore formation can progress.

A Structure-Function Analysis Determines Critical Portions of Ama1 Required for Spore Wall Formation.

It is known that *CDC20* family members share conserved regions known to interact with core subunits of the APC as well as a region in the C-terminus important for substrate recognition (Figure 2-3) (Oelschlaegel *et al.*, 2005; Passmore *et al.*, 2003; Schwab *et al*., 2001; Thorton *et al*., 2006; Vodemaier *et al.*, 2003; Wendt *et al.*, 2001). Although the APC activators Cdc20 and Cdh1 have a high degree of homology (30% Identity and 51% similarity, SGD), Cdh1 cannot substitute for Cdc20, an essential gene. I sought to determine if Ama1 could substitute for Cdc20 and conversely, if Cdc20 could substitute for Ama1. Previous investigations indicated APC^{Ama1} is capable of targeting substrates of APC^{Cdc20} such as securin for degradation (Oelschlaegel *et al*., 2005). Plasmids containing 500 base pairs upstream of the ORF in the promoter region and the entire coding sequence were constructed. Upon complementation analysis, integration with a plasmid containing *CDC20pr-CDC20* rescued the *cdc20ts* mutant phenotype as

determined by ability to grow at restrictive temperature (Table 2-4). Similarly, an integrating plasmid containing *AMA1pr-AMA1* rescued the *ama1Δ* mutant phenotype as determined by the ability to form spores (Table 2-4). To determine if *AMA1* can substitute for *CDC20*, the *AMA1* coding region was placed under the control of the *CDC20* promoter and *CDC20* coding region under the control of the *AMA1* promoter. Both *AMA1pr-AMA1* and *CDC20pr-AMA1* rescued the *ama1Δ* phenotype while *CDC20pr-CDC20* and *AMA1pr-CDC20* failed to rescue sporulation when transformed into an *ama1Δ* strain. Similarly, both *CDC20pr-CDC20* and *AMA1pr-CDC20* rescues growth at restrictive temperature in a *cdc20ts* strain (Table 2-4). The results obtained in these genetic tests demonstrate the specificity of function of both Ama1 and Cdc20.

Several chimeric fusion proteins between Ama1 and Cdc20 were constructed to reveal the smallest region of Ama1 necessary for sporulation, The C-terminal WD40 repeat region is believed to be important for activator-target interaction (Kraft *et al*., 2005; Pfleger *et al*., 2000). Chimeric fusion proteins between Ama1 and Cdc20 were generated with junctions at the beginning of the entire WD40 repeat region (blades 1-7), and at the third (blade 3) and fifth (blade 5) WD40 repeats (Figure 2-2**)**. All APC activators contain a conserved C-box domain, DRY/FIP, in their N-terminal region which is essential in budding yeast Cdh1 and Cdc20 for both binding to APC subunits and *in vivo* function (Schwab *et al*., 2001). Chimeric fusion proteins between Ama1 and Cdc20 with junctions at the C-box region were also constructed. All chimeras were constructed by overlap PCR (Table 2-3) and placed under the control of both the *AMA1* and *CDC20* promoters. The chimera constructs were transformed into *ama1Δ* and *cdc20ts* strains and the transformants were examined for suppression phenotypes: vegetative growth in a

temperature-sensitive strain, *cdc20ts* at restrictive termperature, 37˚C, and spore formation in an *ama1Δ* homozygous mutant strain (Table 2-4). Full-length *AMA1pr-AMA1* and *CDC20pr-CDC20* were used as positive controls. None of the Ama1-Cdc20 or Cdc20-Ama1 chimeric constructs rescued the *ama1Δ* phenotype or *cdc20ts* phenotype. One explanation for failure to suppress the mutant phenotypes is that the three-dimensional structure produced by the native protein (and not the chimeric protein) is necessary for protein binding. Another possibility is more than one region of Cdc20 is required to rescue temperature-sensitive growth and more than one region of Ama1 is necessary to target an inhibitor of spore wall formation.

APC activator proteins Cdh1 and Cdc20 contain a conserved isoleucine-arginine (IR) C-terminal tail essential for *in vivo* function (Oelschlaegel *et al.*, 2005; Passmore *et al.*, 2003; Thornton *et al.*, 2006; Vodemaier *et al.*, 2003; Wendt *et al.*, 2001). Mutation of the C-terminal arginine to alanine obliterates *in vitro* ability of the APC activators Cdc20, Cdh1, and Ama1 to bind to and activate the APC to target securin for ubiquitylation (Oelschlaegel *et al.*, 2005). Two different alleles of *AMA1* were constructed to examine the importance of the C-terminal IR tail in Ama1 function. One *AMA1* allele, $AMA1^{R593A}$, contains a substitution of the C-terminal arginine to an alanine while a second *AMA1* allele, $AMA1^{IR\Delta}$, contains a deletion of the C-terminal isoleucine arginine pair (Table 2-3). $AMA1^{R593A}$ and $AMA1^{IR\Delta}$ were transformed into an *ama1Δ* strain and the cells were examined for spore formation (Table 2-5**)**. Transformed vector alone does not restore sporulation and full-length Ama1 complements the *ama1Δ* phenotype. *AMA1pr-*$AMA1^{R593A}$ complements the *ama1Δ* phenotype *in vivo* though $APC^{Ama1R593A}$ fails to activate the APC to support ubiquitylation of securin *in vitro*

(Oelschlaegel *et al.,* 2005). Another possible explanation is that Ama1 does not act as an APC activator *in vivo*. However, $AMA1^{IR\Delta}$ does not suppress the *ama1Δ* sporulation phenotype suggesting the C-terminal IR in Ama1 is required for APC^{Ama1} activity (Table 2-5).

$AMA1^{IR\Delta}$ may bind to the APC poorly and an increased expression of this allele may compensate for low binding ability and promote APC activity. High copy plasmids containing $AMA1^{IR\Delta}$ or $AMA1^{R593A}$ were transformed into an *ama1Δ* diploid strain (Table 2-5). Over-expression of both $AMA1^{R593A}$ and $AMA1^{IR\Delta}$ partially complements the *ama1Δ* sporulation defect. Since one integrated copy of $AMA1^{IR\Delta}$ as the only allele of *AMA1* in sporultating cells was not sufficient to suppress the *ama1Δ* phenotype and over-expression of $AMA1^{IR\Delta}$ on a 2μ plasmid suppresses the *ama1Δ* phenotype, a dosage analysis was conducted to determine how many copies of $AMA1^{IR\Delta}$ are necessary to suppress the *ama1Δ* phenotype (Table 2-5). One, two, three and four copies of $AMA1^{IR\Delta}$ were systematically introduced into an *ama1Δ* diploid strain and the transformants were examined for spores. Increasing the dosage of $AMA1^{IR\Delta}$ from two to three copies leads to the appearance of spores. Apparently, $Ama1^{IR\Delta}$ reduces, but does not eliminate, the interaction with the APC because spores are produced with increased dosage of $Ama1^{IR\Delta}$. Thus, $AMA1^{IR\Delta}$ represents a hypomorphic allele of *AMA1*. To examine if $AMA1^{IR\Delta}$ has a dominant negative effect (i.e., has the ability to bind substrate at the same time as an inability to bind to the APC core), $AMA1^{IR\Delta}$ was over-expressed in a wild-type strain. All transformants behaved similarly to the untransformed diploid and produced viable spores. Therefore, ectopic over-expression of $AMA1^{IR\Delta}$ in sporulating wild-type cells does not inhibit spore formation.

Genomic Screen Approaches Sought to Identify Genetic Interactions with *AMA1*

A high copy suppressor screen sought to identify a gene, which when over-expressed, could suppress the *ama1Δ* sporulation defect. A pUV1 2μ plasmid library (gift from N. M. Hollingsworth) containing *URA3* was transformed into diploid *ama1Δ* cells. Approximately 14,000 independent transformants were patched (100 transformants per plate with a total of 140 plates) onto plates lacking uracil to maintain the high copy plasmid. To induce sporulation, the plates were replica-plated onto sporulation medium (SpoAc). After incubation at 30˚C for 48 hours, each SpoAc plate was replica-plated onto two YPD plates, one of which was exposed to ether vapor. Spores are resistant to ether and therefore growth on the ether treated plates may be indicative of that spore formation was successful **(**Coluccio *et al*., 2004; Rockmill *et al*., 1991**)**. Ether test analysis identified ten ether-resistant candidates. Plasmids from each transformant were recovered and transformed into a naive *ama1Δ* diploid strain. Subsequent ether test analysis showed no difference between transformants containing the transformed library fragment and vector alone. Some explanations for the failure of this suppressor screen include utilizing an unsaturated library as evidenced by the failure to recover a plasmid containing the *AMA1* ORF (or part of the *AMA1* ORF) at least one time. Another reason may be that the premise of the screen is faulty in that there is no protein that, when over-expressed, suppresses the *ama1Δ* phenotype.

If APC^{Ama1} is involved in targeting an inhibitor of spore wall formation, then a mutation in the target of APC^{Ama1} in an *ama1Δ* strain might recover sporulation. This possibility is predicated on at least two assumptions. The first assumption is that the target itself does not possess a sporulation phenotype when the gene encoding the protein

is mutated. A strain homozygous for *ama1Δ* that also contains a mutation in a putative critical target of APC^{Ama1} in the genome, *supx*, may be unable to form spores because *SUPX* itself is required for sporulation. The second assumption is that there is only one critical target substrate protein of APC^{Ama1} whose degradation is both necessary and sufficient to suppress the *ama1Δ* phenotype. Both APC^{Cdc20} and APC^{Cdh1} have multiple, overlapping targets, but both APC activators direct the ubiquitylation of one critical target: APC^{Cdc20} specifically targets securin and APC^{Cdh1} specifically targets Clb2 for degradation (Thornton and Toczyski, 2003). Thus, it is a reasonable prediction APC^{Ama1} also contains one critical target whose degradation is necessary and sufficient for sporulation.

A diploid strain homozygous for *HO* (NKY895, gift of N. Hollingsworth) and heterozygous for *ama1Δ::kanMX6* was constructed. Following sporulation, haploid spores were isolated by enzymatic digestion of the ascal wall. From initial pilot experiments, a kill curve determined a 20 second exposure to UV irradiation kills approximately 90% of haploid spores. Haploid spores were exposed to short wave UV, randomly mutagenizing the genomic DNA and the irradiated cells were spread onto plates containing G418, thereby selecting for haploid spores containing the *ama1Δ::kanMX6* deletion. Because the strain contains *HO*, an endonuclease responsible for mating-type switching, any mutation in a haploid cell will become homozygous upon self-mating to form a diploid. After incubation at 30˚C for two days, individual colonies were patched onto YPD containing G418 plates followed by replica-plating onto SpoAc plates. Cells were examined for sporulation by ether test analysis. The ether test has two possible outcomes: 1) *ama1Δ::kanMX6* homozygous deletion mutants will not sporulate

and fail to survive ether treatment, and 2) *ama1Δ::kanMX6* homozygous deletion mutants containing a homozygous mutation in a critical APC^{Ama1} target, *supx*, may suppress the *ama1Δ* phenotype, sporulate and survive ether treatment. After two retests, 125 putative homozygous *ama1Δ::kanMX6 supx* candidates remained out of 30,000 individual transformants. Survivor candidates were purified producing approximately ten colonies and retested by exposure to ether vapor. After the fourth pass, 22 candidates survived ether treatment, all with less than a 5% sporulation efficiency.

Each candidate was outcrossed to a haploid strain containing the genotype *ama1Δ::TRP1 SUPX HO* that was transformed with a high copy plasmid coding for the *AMA1* ORF (pAMA1) to determine if any of the second site suppressor candidates are due to mutations in a single gene. Mating of these haploids produced a diploid containing a genotype *ama1Δ::kanMX6/ama1Δ::TRP1 supx/SUPX HO/HO* pAMA1 capable of sporulation. Diploids produced from this mating were sporulated, dissected and subjected to selection to induce the loss of the plasmid coding for the *AMA1* ORF (pAMA1-URA3) by replica-plating to plates containing 5-fluorouracil-6-carboxylic acid monohydrate, a chemical toxic to yeast cells containing a functional *URA3* allele. After loss of pAMA1, each haploid self-mated by *HO*-induced diploidization. If *supx* is a single recessive gene, phenotypic analysis predicts two diploids that can form spores and two diploids that cannot form spores. The second site suppressor screen was abandoned upon the failure of any of the suppressor mutations to segregate 2+:2-.

Because the second site suppressor screen (discussed above) could not identify any essential genes necessary for spore wall formation, an alternative strategy was implemented. A strain containing a hypomorphic allele of *AMA1*, while simultaneously

having less target substrate available for degradation, might allow spore formation. A mutagenic transposon library, mTn-3XHA/GFP, digested with NotI to release genomic fragments, was transformed into diploid ADY66-2xΔIR, a strain that cannot sporulate (Ross-Macdonald *et al*., 1999). Through homologous recombination, the library fragment integrates randomly into the genomic DNA of a wild-type diploid resulting in the disruption of one copy of a gene (Figure 2-3).

Individual transformants were patched onto plates lacking uracil. To induce sporulation, the plates were replica-plated onto SpoAc plates. After incubation at 30˚C for 48 hours, each SpoAc plate was replica-plated onto two YPD plates, one of which was exposed to ether vapor. Out of 13,700 individual transformants, 261 (or approximately 2%) appeared ether resistant on the first pass. After three passes, 47 candidates produced spores. Ten candidates (0.07%) reproducibly sporulated greater than 5% and 37 individual candidates (0.2%) produced 1-4% spores.

The genomic locus of each transposon integration was identified (Riley *et al*., 1990). Briefly, the genomic DNA from positively testing strains was digested with a restriction enzyme yielding many small blunt-ended fragments. An anchor bubble was created by annealing two primers, each containing about 40 nucleotides of complementary sequence and 10 nucleotides non-complementary sequence, to each other. The anchor bubble was ligated to the ends of the digested genomic fragments. PCR amplification of the genomic DNA containing an anchor bubble was performed using a primer complementary to a sequence in the transposon region (mTn primer) and a primer containing a complementary sequence to the anchor bubble region (bubble primer). In the first cycle of PCR, only the mTn primer binds the template. In

subsequent PCR cycles, the bubble primer binds to the product of the mTn primer. This ensures only the fragment containing the mTn primer binding region is amplified. The PCR products were sent for DNA sequencing. Simultaneously, spores were dissected from sporulating candidates to reveal if the candidate gene is essential as well as to determine if the transposon integration locus is segregating in a classical Mendelian manner.

Though the transposon mutagenesis screen initially appeared to possess promising results, all of the nutritional selection marker used to identify transposon candidates failed to segregate in the predicted 2+:2- pattern. Further, upon PCR amplification followed by DNA sequencing, most of the transposon insertions occurred in ribsosomal DNA repeat regions. Two positive retesters contained a transposon disrupting the *POP1* and *CDC73* open reading frames. Homozygous *ama1Δ pop1Δ* and *ama1Δ cdc73Δ* strains failed to sporulate. Thus, the mutagenic transposon screen failed to identify a putative substrate target of APC^{Ama1}.

The Clbs Are Not The Sole Targets of Ama1

Cdc28 is an essential cyclin-dependent kinase (CDK) in *S. cerevisiae* that when bound to its activating subunit, a cyclin, phosphorylates substrates promoting progression of the cell cycle (Johnston *et al*., 1977; Bloom and Cross, 2007). Advancement of the mitotic cell cycle is regulated by the abundance and degradation of specific cyclin proteins (Bloom and Cross, 2007). The G1-phase cyclins (Cln1, Cln2 and Cln3) promote bud emergence, spindle pole body duplication and activation of S-phase cyclins (Clb5 and Clb6) that advance DNA replication. The B-type cyclins, Clb1, Clb2, Clb3 and Clb4, are required for late mitotic events such as mitotic exit and cytokinesis. The progression of the cell cycle must be sequential for cells to be viable. For example, cell division prior to completion of chromosome separation would be deleterious for the cell.

Meiosis is characterized by one round of DNA replication followed by two rounds of chromosome segregation without an intervening S-phase between the first and second meiotic divisions. Dahmann and Futcher demonstrated that Clb1, Clb3 and Clb4 are necessary for meiotic progression (Dahmann and Futcher, 1995). Deletion of any two of these three cyclin proteins prevents a second meiotic division from occurring and results in the production of diploid dyad spores (Dahmann and Futcher, 1995). Transcriptional arrays of sporulating cells determined *CLB2* transcription is meiotically suppressed (Chu *et al*., 1998). Consequently, Clb1, Clb3, Clb4 are considered the meiotic Clb proteins (Dahmann and Futcher, 1995).

If the meiotic Clb proteins are the critical targets of APC^{Ama1}, perhaps their deletion in an *ama1Δ* homozygous mutant would remove the block to spore wall synthesis. Cooper and colleagues (2000) suggested Ama1 activates the APC to direct the

ubiquitylation of Clb1 though this result has not been duplicated (Cooper *et al*., 2000; Oelschlaegel *et al.*, 2005). Several homozygous diploid mutant strains were constructed using standard gene replacement methods: *ama1Δ*, *clb1Δ*, *clb3Δ,* and *clb4Δ* (including all possible combinations). Deletion of the *CLB* genes either singly or in combination with *AMA1* did not restore spore formation. Thus, Clb1, Clb3 and Clb4 are not the sole targets of APC^{Ama1}.

If the critical target of APC^{Ama1} is Cdc28 activity, inactivation of Cdc28 during meiosis should permit sporulation in an *ama1Δ* mutant. Since *CDC28* is an essential gene, it is necessary to use a conditional allele of *CDC28*. Benjamin and colleagues (2000) constructed such an allele of *CDC28*, *cdc28-as1* (analog-sensitive), in order to differentiate between early and late functions of Cdc28 during the meiotic cell cycle (Benjamin *et al*., 2000). This analog-sensitive allele is fully functional, along with its activating cyclin subunit, during most conditions but can be conditionally rendered non-functional upon addition of a specific chemical compound, 1-NM-PP1. To determine the effects of inactivation of Cdc28 on spore formation, a chemical inhibitor was added every hour to an isolated aliquot from a sporulating *cdc28-as1* culture. Addition of the chemical inhibitor before or during the first meiotic division blocked sporulation. Inactivation of *CDC28* during or after the second meiotic division did not impede spore formation (inhibitor added 5-7 hours into sporulation time course) in wild-type cells.

A double homozygous mutant, *ama1Δ cdc28-as1*, was constructed to determine if belated inactivation (after the first meiotic division) of Cdc28-as1 in an *ama1Δ* homozygous mutant permits sporulation. Addition of the chemical inhibitor to an isolated aliquot of sporulating cells after the first meiotic division did not suppress the *ama1Δ*

phenotype. McDonald and colleagues (2005) published an analogous series of experiments using a temperature-sensitive allele of *CDC28*, *cdc28-4*, and presented data demonstrating inactivation of Cdc28 in an *ama1Δ* homozygous mutant permits spore formation. Since the McDonald and co-workers (2005) result contradicts my results utilizing *cdc28-as1*, *cdc28-4* was obtained from the Winter Laboratory so that I could see whether I could reproduce the results of McDonald and colleagues (McDonald *et al*., 2005). Inactivation of Cdc28, by analog or temperature sensitivity in an *ama1Δ* homozygous mutant produced identical results-failure to form spores. These results were communicated to Dr. Winter and upon his laboratory's closer inspection it was subsequently determined that the published experiments using *cdc28-4* were not conducted in an *ama1Δ* homozygous mutant. Thus, the cyclin-dependent kinase is not a critical target of APC^{Ama1}.

Discussion: Genetic Analyses of *AMA1*

Based on the phenotype of an *ama1*Δ homozygous mutant, I hypothesized APC^{Ama1} targets the degradation of inhibitor(s) of spore wall assembly. I pursued several genetic approaches that aimed to provide insight into critical structural features of Ama1 necessary for its function as well as identify targets of APC^{Ama1}. All of the genetic screens failed to identify targets of APC^{Ama1}. Some possible explanations for the failure of these genetic approaches include: (1) incomplete libraries were utilized in the genetic screens; (2) the APC^{Ama1} target is essential for viability; (3) the APC^{Ama1} target is redundant; (4) the APC^{Ama1} target is essential for sporulation; (5) the phenotypic readout of spore formation demanded in the genetic screens is too stringent and (6) the model on which the genetic screens are based was wrong. I will consider each explanation in turn.

A genetic screen's success begins with its starting materials. All of the screens demanded saturated libraries for meaningful analysis. This library used in the suppressor screen (pUV1) was likely not saturated because I did not recover *AMA1* (or fragment of *AMA1*) in a plasmid that suppressed the *ama1Δ* phenotype. The transposon mutagenesis library was likely not saturated as most integrations recovered occurred into ribosomal DNA regions suggesting mutagenic transposons containing ribosomal DNA were likely over-represented in the library.

If a target of APC^{Ama1} is essential for viability, only a genetic screen utilizing a diploid strain in which one copy of a putative target necessary for viability is mutated or deleted will succeed in identifying it as a target substrate. Conversely, if a target of APC^{Ama1} is redundant, there would need to be multiple deletions or mutations in several genes to suppress the *ama1Δ* phenotype. A yeast two-hybrid screen identified proteins

that bind to Ama1 and perhaps are inhibitors of spore wall formation. However, no homozygous deletion mutant of a positive Ama1-interacting protein suppressed the *ama1Δ* mutant phenotype. It remains possible that some of these Ama1-interacting proteins are indeed target substrates of APC^{Ama1} but whose degradation is not critical to initiate spore wall formation. A more conclusive analysis would be to determine if any of the Ama1-interacting proteins are degraded during sporulation in wild-type cells and if so, determine if their degradation is APC^{Ama1}-dependent by analyzing for the putative target protein's stability by western analysis in sporulating *ama1Δ* cells.

If a target of APC^{Ama1} is essential for sporulation, it would fail to be identified in any of the genetic screens because of its own sporulation phenotype. All of the genetic screens examined candidates for suppression of the *ama1Δ* phenotype by screening for survival to exposure to ether vapor, a demanding phenotypic readout requiring the formation of all four spore wall layers (Figure 1-4) (Briza *et al*., 1990; Tachikawa *et al*., 2000). There are many intermediate steps between the terminal phenotype of *ama1Δ*, exit from Meiosis II, and completion of spore wall formation (Coluccio *et al*., 2004). A genetic screen utilizing a more proximal phenotypic marker, such as formation of the β-glucan layer or expression of *DIT1-LacZ*, a mid-late meiotic gene not expressed in *ama1Δ*, might have yielded more success in the identification of a target substrate(s) of APC^{Ama1}. Unfortunately, genetic screens utilizing these phenotypic readouts are not practical in the laboratory: formation of the β-glucan layer is routinely assessed by indirect immunofluorescence, a time-intensive process, and *DIT1-LacZ* expression is weak, resulting in dubious blue-white screening.

Finally, the starting hypothesis that a homozygous *ama1Δ* diploid fails to initiate spore wall formation because Ama1 is not present in the cell to activate the APC and target an inhibitor(s) of spore wall formation for degradation, may be wrong. As explained in the next chapter, we now know that all of the genetic screens failed to identify a target of APC^{Ama1} because the target, Ssp1, has a sporulation phenotype similar to the *ama1Δ* phenotype when *SSP1* is deleted.

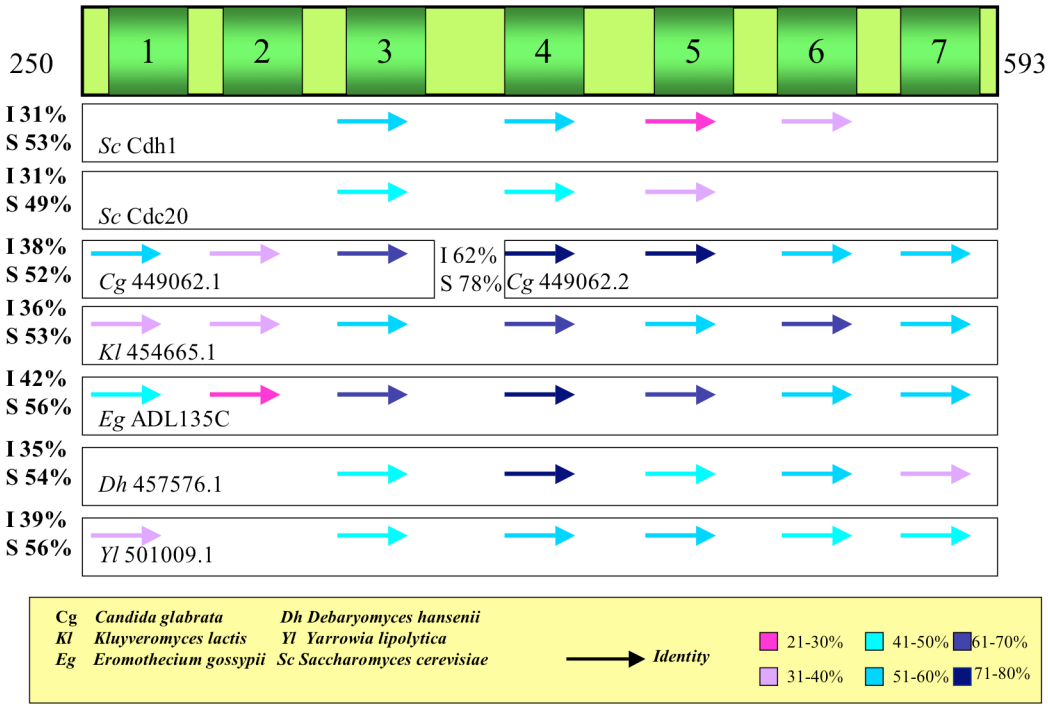

Figure 2-1. Sequence analysis of WD40 repeat region of Ama1
Ama1 is a homolog of the Cdc20 APC activator family. The WD40 repeat region of Ama1 is defined from amino acids 253 through 593 (Cooper *et al.*, 2000). BLAST analysis identifies Ama1 orthologs in closely related fungi with sequenced genomes. BLAST analysis of individual WD40 repeat regions from Ama1 identifies higher degrees of homology. The numbers of the far left indicate % identity and % similarity to the entire WD40 repeat region of Ama1. The colored arrows show the % identity of each WD40 repeat region (about 50 amino acid residues) in Ama1.

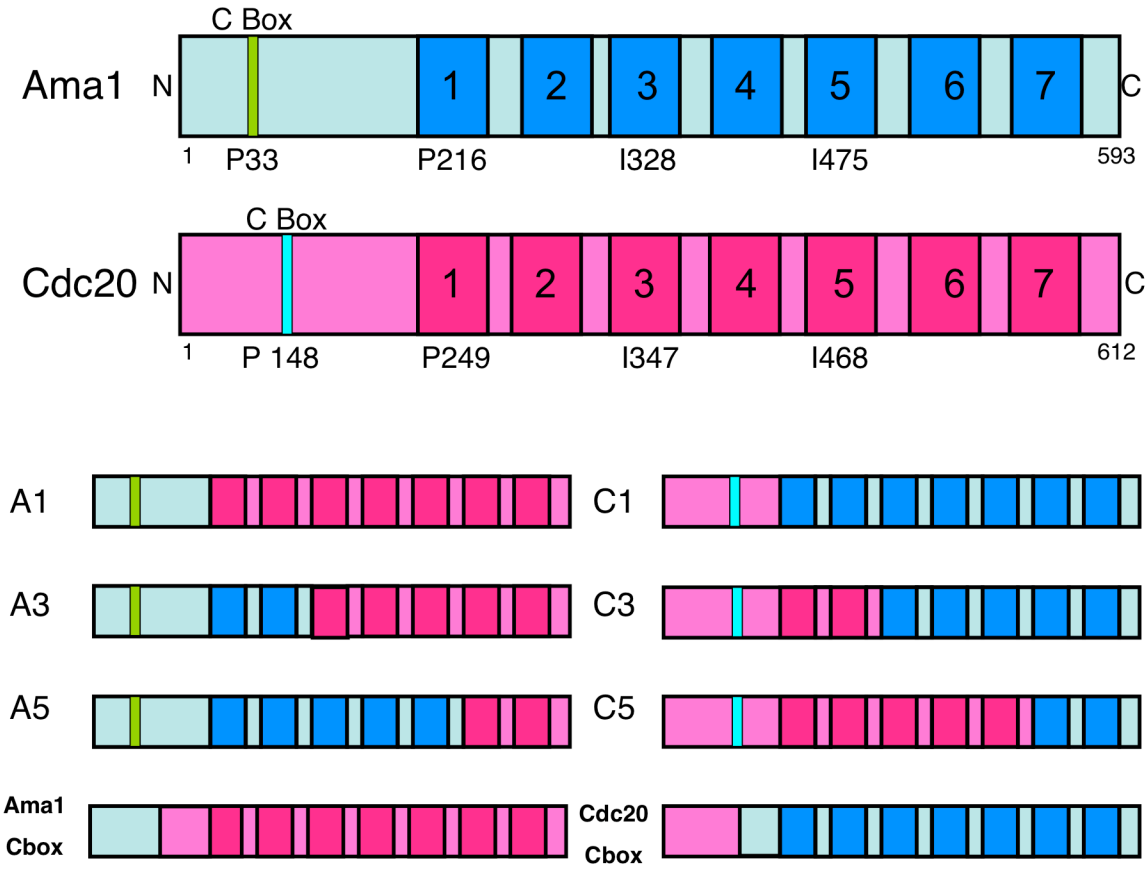

Figure 2-2. Cartoon of construction of chimeric proteins between Ama1-Cdc20 and Cdc20-Ama1.
Junctions between Ama1 and Cdc20 occurred at the first, third and fifth blades in the WD40 repeat region.

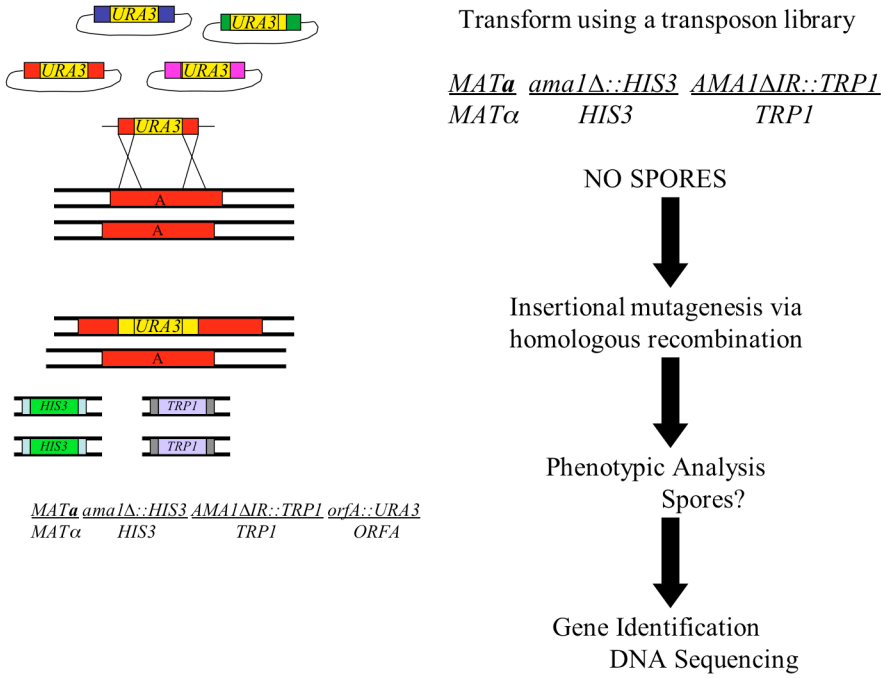

Figure 2-3. Transposon mutagenesis screen.
Cartoon reconstruction of mechanics of screen.

Table 2-1. *S. cerevisiae* strains used in this study

Strain	Genotype	Source
AN117-4B	*MATα ura3 leu2 trp1 his3Δsk arg4-NspI lys2 hoΔ::LYS2 rme1::LEU2*	(Neiman *et al.*, 2000)
AN117-16D	*MAT***a** *ura3 leu2 trp1 his3Δsk lys2 hoΔ::LYS2*	(Neiman *et al.*, 2000)
AN120	Cross of AN117-4B and AN117-16D	(Neiman *et al.*, 2000)
ADY12	*MAT***a** *ura3 leu2 trp1 his3Δsk lys2 hoΔ::LYS2 ama1Δ::CgTRP1*	This study
ADY13	*MATα ura3 leu2 trp1 his3Δsk arg4-NspI lys2 hoΔ::LYS2 rme1::LEU2 ama1Δ::CgTRP1*	This study
ADY14	Cross of ADY12 and ADY13	This study
ADY15	*MAT***a** *ura3 leu2 trp1 his3Δsk lys2 hoΔ::LYS2 clb1Δ::KlURA3*	This study
ADY16	*MATα ura3 leu2 trp1 his3Δsk arg4-NspI lys2 hoΔ::LYS2 rme1::LEU2 clb1Δ::KlURA3*	This study
ADY17	Cross of ADY15 and ADY16	This study
ADY18	*MAT***a** *ura3 leu2 trp1 his3Δsk lys2 hoΔ::LYS2 clb4Δ::HIS3*	This study
ADY19	*MATα ura3 leu2 trp1 his3Δsk arg4-NspI lys2 hoΔ::LYS2 rme1::LEU2 clb4Δ::HIS3*	This study
ADY20	Cross of ADY18 and ADY19	This study
ADY21	*MAT***a** *ura3 leu2 trp1 his3Δsk lys2 hoΔ::LYS2 clb1Δ::KlURA3 ama1Δ::CgTRP1*	This study
ADY22	*MATα ura3 leu2 trp1 his3Δsk arg4-NspI lys2 hoΔ::LYS2 rme1::LEU2 clb1Δ::KlURA3 ama1Δ::CgTRP1*	This study
ADY23	Cross of ADY21 and ADY22	This study
ADY24	*MAT***a** *ura3 leu2 trp1 his3Δsk lys2 hoΔ::LYS2 clb4Δ::HIS3 ama1Δ::CgTRP1*	This study
ADY25	*MATα ura3 leu2 trp1 his3Δsk arg4-NspI lys2 hoΔ::LYS2 rme1::LEU2 clb4Δ::HIS3 ama1Δ::CgTRP1*	This study
ADY26	Cross of ADY24 and ADY25	This study
ADY27	*MAT***a** *ura3 leu2 trp1 his3Δsk lys2 hoΔ::LYS2 clb1Δ::KlURA3 clb4Δ::HIS3*	This study
ADY28	*MATα ura3 leu2 trp1 his3Δsk arg4-NspI lys2 hoΔ::LYS2 rme1::LEU2 clb1Δ::KlURA3 clb4Δ::HIS3*	This study

ADY29	Cross of ADY27 and ADY29	This study
ADY30	*MAT***a** *ura3 leu2 trp1 his3Δsk lys2 hoΔ::LYS2 clb1Δ::KlURA3 clb4Δ::HIS3 ama1Δ::CgTRP1*	This study
ADY31	*MATα ura3 leu2 trp1 his3Δsk arg4-NspI lys2 hoΔ::LYS2 rme1::LEU2 clb1Δ::KlURA3 clb4Δ::HIS3 ama1Δ::CgTRP1*	This study
ADY32	Cross of ADY30 and ADY31	This study
ADY64	*MATα ura3 leu2 trp1 his3Δsk arg4-NspI lys2 hoΔ::LYS2 rme1::LEU2 ama1Δ::HIS3*	This study
ADY65	*MAT***a** *ura3 leu2 trp1 his3Δsk lys2 hoΔ::LYS2 ama1Δ::HIS3*	This study
ADY66	Cross of ADY64 and ADY65	This study
603	*MATα hoΔ::LYS2 ura3 leu2::hisG cdc28-as1*	(Henderson *et al*., 2006)
604	*MAT***a** *hoΔ::LYS2 ura3 leu2::hisG cdc28-as1*	(Henderson *et al*., 2006)
ADY91	*MAT***a** *ura3 leu2 trp1 his3Δsk lys2 hoΔ::LYS2 ama1Δ::HIS3 cdc28-as1*	This study
ADY96	*MATα ura3 leu2 trp1 his3Δsk arg4-NspI lys2 hoΔ::LYS2 rme1::LEU2 ama1Δ::HIS3 cdc28-as1*	This study
ADY99	Cross of ADY91 and ADY96	This study
EW1202	*MAT***a** *leu2-hisG trp1-hisG lys2 or his4-G ura3-SK1 hoΔ::LYS2 cdc28-4*	E. Winter
EW1204	*MATα leu2-hisG trp1-hisG lys2 or his4-G ura3-SK1 hoΔ::LYS2 cdc28-4*	E. Winter
ADY121	*MATα ura3 leu2 trp1 his3Δsk arg4-NspI lys2 hoΔ::LYS2 rme1::LEU2 cdc28-4*	This study
ADY126	*MAT***a** *ura3 leu2 trp1 his3Δsk lys2 hoΔ::LYS2 cdc28-4*	This study
ADY127	Cross of ADY121 and ADY126	This study
ADY130	*MAT***a** *ura3 leu2 trp1 his3Δsk lys2 hoΔ::LYS2 cdc28-4 ama1Δ::HIS3*	This study
ADY132	*MATα ura3 leu2 trp1 his3Δsk arg4-NspI lys2 hoΔ::LYS2 rme1::LEU2 cdc28-4 ama1Δ::HIS3*	This study
ADY123	Cross of ADY130 and ADY132	This study
ADY84	*cdc20ts ura3*	R. Sternglanz
ADY66-1xΔIR	Cross of ADY64 and ADY65 with *ura3::AMA1ΔIR::URA3*	This study

ADY64-1xΔIR	*MATα ura3 leu2 trp1 his3Δsk arg4-NspI lys2 hoΔ::LYS2 rme1::LEU2 ura3::AMA1ΔIR::URA3*	This study
ADY65-1xΔIR	*MAT***a** *ura3 leu2 trp1 his3Δsk lys2 hoΔ::LYS2 ura3::AMA1ΔIR::URA3*	This study
ADY66-2xΔIR	Cross of ADY64-1xΔIR with ADY65-1xΔIR	This study
ADY64-2xΔIR	*MATα ura3 leu2 trp1 his3Δsk arg4-NspI lys2 hoΔ::LYS2 rme1::LEU2 ura3::AMA1ΔIR::URA3 trp1::AMA1ΔIR::TRP1*	This study
ADY65-2xΔIR	*MAT***a** *ura3 leu2 trp1 his3Δsk lys2 hoΔ::LYS2 ura3::AMA1ΔIR::URA3 trp1::AMA1ΔIR::TRP1*	This study
ADY66-3xΔIR	Cross of ADY64-2xΔIR with ADY65-1xΔIR	This study
ADY66-4xΔIR	Cross of ADY64-2xΔIR with ADY65-2xΔIR	This study
L40	*leu2 ade2 trp1 LYS2::lexAop-HIS3 URA3::lexAop-LacZ*	R. Sternglanz
NKY895	*MAT***a** *ura3ΔhisG leu2::hisG ade2::TnLK lys2 ste7-1 HO*Δ *MATα ura3ΔhisG leu2::hisG ade2::TnLK lys2 ste7-1 HO*Δ	(McKee and Kleckner, 1997)

Table 2-2. Plasmids used in this study

Plasmid	Description	Source
pBTM116	LexA DNA binding domain	R. Sternglanz
pBluescript	Cloning vector	Fermentas
pBluescriptAMA1	Cloning intermediate	This study
pBTM116AMA1	LexA-Ama1$^{231-593}$	This study
mTn-3XHA/GFP Library	Transposon library containing genomic fragments representative of the entire *S. cerevisiae* genome	M. Snyder
pUV1 Library	Library of *S. cerevisiae* genomic inserts	N. M. Hollingsworth
pACTII Library	Library of *S. cerevisiae* genomic inserts	N. M. Hollingsworth
pRS306AMA1pr	*AMA1pr*	This study
pRS306AMA1	*AMA1*	This study
pRS306AMA1pr-AMA1	*AMA1pr-AMA1*	This study
pRS316AMA1pr-AMA1	*AMA1pr-AMA1*	This study
pRS426AMA1pr-AMA1	*AMA1pr-AMA1*	This study
pRS306CDC20pr	*CDC20pr*	This study
pRS306CDC20	*CDC20*	This study
pRS306CDC20pr-CDC20	*CDC20pr-CDC20*	This study
pRS306AMA1pr-CDC20	*AMA1pr-CDC20*	This study
pRS306CDC20pr-AMA1	*CDC20pr-AMA1*	This study
pRS306AMA1pr-A1	*AMA1pr*-N-Ama1P246-Cdc20 P249-C	This study
pRS306AMA1pr-A3	*AMA1pr*-N-Ama1I328-Cdc20I347-C	This study
pRS306AMA1pr-A5	*AMA1pr*-N-Ama1I475-Cdc20 I468-C	This study
pRS306AMA1pr-ACbox	*AMA1pr*NAma1P38-Cdc20P148-C	This study
pRS306AMA1pr-CACbox	*AMA1pr*N-Cdc20P148-Ama1P38-C	This study
pRS306AMA1pr-C1	*AMA1pr*N-Cdc20P249-Ama1P246-C	This study
pRS306AMA1pr-C3	*AMA1pr*N-Cdc20I347-Ama1328-C	This study
pRS306AMA1pr-C5	*AMA1pr*N-Cdc20I468-Ama1I475	This study
pRS306CDC20pr-A1	*CDC20pr*N-Ama1P246-Cdc20 P249-C	This study
pRS306CDC20pr-A3	*CDC20pr*N-Ama1I328-Cdc20I347-C	This study
pRS306CDC20pr-A5	*CDC20pr*N-Ama1I475-Cdc20 I468-C	This study
pRS306CDC20pr-C1	*CDC20pr*N-Cdc20P249-Ama1P246-C	This study
pRS306CDC20pr-C3	*CDC20pr*N-Cdc20I347-Ama1328-C	This study
pRS306CDC20pr-C5	*CDC20pr*N-Cdc20I468-Ama1I475	This study
pRS304AMA1pr-AMA1	*AMA1*	This study

pRS304AMA1pr-AMA1-IA	*AMA1*^{R593A}	This study
pRS314AMA1pr-AMA1-IA	*AMA1*^{R593A}	This study
pRS424AMA1pr-AMA1-IA	*AMA1*^{R593A}	This study
pRS306AMA1pr-AMA1-IA	*AMA1*^{R593A}	This study
pRS316AMA1pr-AMA1-IA	*AMA1*^{R593A}	This study
pRS426AMA1pr-AMA1-IA	*AMA1*^{R593A}	This study
pRS304AMA1pr-AMA1-ΔIR	*AMA1*$^{IR\Delta}$	This study
pRS314AMA1pr-AMA1-ΔIR	*AMA1*$^{IR\Delta}$	This study
pRS424AMA1pr-AMA1-ΔIR	*AMA1*$^{IR\Delta}$	This study
pRS306AMA1pr-AMA1-ΔIR	*AMA1*$^{IR\Delta}$	This study
pRS316AMA1pr-AMA1-ΔIR	*AMA1*$^{IR\Delta}$	This study
pRS426AMA1pr-AMA1-ΔIR	*AMA1*$^{IR\Delta}$	This study

Table 2-3. Construction of chimeras: primers and templates

Primer	ADO	Function
Ama1pFXhoI	ADO5	*AMA1* 5' end XhoI site
Ama1stopSpeI	ADO3	*AMA1* 3' end at SpeI site
CDC20pFXhoI	ADO9	*CDC20* 5' end XhoI site
CDC20STOP	ADO8	*CDC20* 3' end at SpeI site
N1Ama1CCdc20	ADO11	AMA1/CDC20 junction at WD1 AMA1P216/CDC20P249
N3Ama1CCdc20	ADO12	AMA1/CDC20 junction at WD3 AMA1I328/CDC20I347
N5Ama1CCdc20	ADO13	AMA1/CDC20 junction at WD5 AMA1I475/CDC20I468
NCdc20CAma1	ADO14	CDC20/AMA1 junction WD1 CDC20P249/AMA1P216
N3Cdc20CAma1	ADO15	CDC20/AMA1 junction WD3 CDC20I347/AMA1I328
N5Cdc20CAma1	ADO16	CDC20/AMA1 junction WD5 CDC20I468/AMA1475
CBOXNCDC20	ADO77	CDC20/AMA1 junction at C-box CDC20P148/AMA1-P38
CBOXNAMA1	ADO78	AMA1/CDC20 junction at C-box AMA1P38-CDC20P148
Ama1StopIA	ADO17	Change C-terminal R to A
Ama1StopΔIR	ADO151	Remove C-terminal IR

Chimera	Primer 1	Primer 2	Template	Primer 1	Primer 2	Template
AMA1	ADO5	ADO3	*AMA1*		None	
CDC20	ADO9	ADO8	*CDC20*		None	
AMA1-A1 (N-Ama1P246-Cdc20P249-C)	ADO5	ADO11	*AMA1*	ADO5	ADO8	*CDC20*
AMA1-A3 (N-Ama1I328-Cdc20I347-C)	ADO5	ADO12	*AMA1*	ADO5	ADO8	*CDC20*
AMA1-A5 (N-Ama1I475-Cdc20I468-C)	ADO5	ADO13	*AMA1*	ADO5	ADO8	*CDC20*
AMA1-C1 (N-Cdc20P249-Ama1P246-C)	ADO9	ADO14	*CDC20*	ADO9	ADO3	*AMA1*
AMA1-C3 (N-Cdc20I347-Ama1I328-C)	ADO9	ADO15	*CDC20*	ADO9	ADO3	*AMA1*
AMA1-C5 (N-Cdc20I468-Ama1I475-C)	ADO9	ADO16	*CDC20*	ADO9	ADO3	*AMA1*
AMA1-Cbox (N-Ama1P38-Cdc20P148-C)	ADO1	CBOX-NAMA1	*AMA1pr-AMA1*	PAMA1	CDC20 Stop	*AMA1pr-CDC20*
CDC20-Cbox (N-Cdc20P148-Ama1P38-C)	ADO1	CBOX-NCDC20	*AMA1pr-AMA1*	PAMA1	AMA1 Stop	*AMA1pr-AMA1*
AMA1 IA	ADO5	ADO17	*AMA1*		None	

Table 2-4. Rescue of *ama1*Δ and *cdc20ts* by Ama1 or Cdc20 is APC activator specific

Gene[a]	Sporulation[b]	Growth[c]
AMA1pr-AMA1	YES	NO
AMA1pr-CDC20	NO	YES
CDC20pr-CDC20	NO	YES
CDC20pr-AMA1	YES	NO
AMA1pr-AMA1-A1	NO	NO
AMA1pr-AMA1-A3	NO	NO
AMA1pr-AMA1-A5	NO	NO
CDC20pr-CDC20-C1	NO	NO
CDC20pr-CDC20-C3	NO	NO
CDC20pr-CDC20-C5	NO	NO

(a) For chimeric genes, A represents *AMA1* sequence and C represents *CDC20* as described in the text.
(b) Integrating plasmids carrying the designated gene either under the control of the *AMA1* or *CDC20* promoters and were transformed into ADY66. NO, no sporulation in *ama1Δ* ; YES, sporulation as measured by sporulation efficiency assessed by light microscopy analysis.
(c) Integrating plasmids carrying the designated gene either under the control of the *AMA1* or *CDC20* promoters were transformed into ADY84. NO, no growth; YES, growth as measured by growth of colonies after 3 days of incubation at 37˚C.

Table 2-5. Rescue of *ama1*Δ by *AMA1* allele and copy number

Genotype[a]	% Sporulation
ama1Δ::HIS3 *ura3::URA3* *ama1Δ::HIS3* *ura3*	0
ama1Δ::HIS3 *ura3::AMA1::URA3* *ama1Δ::HIS3* *ura3*	100
ama1Δ::HIS3 *ura3::AMA1-IA::URA3* *ama1Δ::HIS3* *ura3*	62
ama1Δ::HIS3 *ura3::AMA1-ΔIR::URA3* *ama1Δ::HIS3* *ura3*	0
ama1Δ::HIS3 *ura3/ URA3 CEN AMA1* *ama1Δ::HIS3* *ura3*	100
ama1Δ::HIS3 *ura3/ URA3 CEN AMA1-IA* *ama1Δ::HIS3* *ura3*	60
ama1Δ::HIS3 *ura3/ URA3 CEN AMA1-ΔIR* *ama1Δ::HIS3* *ura3*	0
ama1Δ::HIS3 + 2μ *ura3::AMA1::URA3* *ama1Δ::HIS3*	100
ama1Δ::HIS3 + 2μ *ura3::AMA1-IA::URA3* *ama1Δ::HIS3*	92
ama1Δ::HIS3 + 2μ *ura3::AMA1-ΔIR::URA3* *ama1Δ::HIS3*	51
1XΔIR *ama1Δ::HIS3* *trp1* *ura3::AMA1-ΔIR::URA3* *ama1Δ::HIS3* *trp1* *ura3*	0
2XΔIR *ama1Δ::HIS3* *trp1* *ura3::AMA1-ΔIR::URA3* *ama1Δ::HIS3* *trp1* *ura3::AMA1-ΔIR::URA3*	2
3XΔIR *ama1Δ::HIS3* *trp1::AMA1-ΔIR::TRP1* *ura3::AMA1-ΔIR::URA3* *ama1Δ::HIS3* *trp1* *ura3::AMA1-ΔIR::URA3*	12.5
4XΔIR *ama1Δ::HIS3* *trp1::AMA1-ΔIR::TRP1* *ura3::AMA1-ΔIR::URA3* *ama1Δ::HIS3* *trp1::AMA1-ΔIR::TRP1* *ura3::AMA1-ΔIR::URA3*	25

(a) All plasmids (integrating, *CEN* and 2μ) containing the specified gene under the control of the *AMA1* promoter were transformed into ADY66 (*ama1*Δ::*HIS3*/*ama1*Δ::*HIS3*).

Table 2-6. Yeast two-hybrid interacting proteins

Open Reading Frame	Gene	Location in Gene	Brief Description
YOL086C	*ADH1*	N-term	Alcohol dehydrogenase activity
YOR141C	*ARP8*	N-term	Nuclear actin-related protein involved in chromatin remodeling
YML116W	*ATR1*	Mid	Multidrug efflux pump of the major facilitator superfamily
YIL140W	*AXL2*		Integral plasma membrane required for axial budding in haploid cells
YNL271C	*BNI1*	Mid	Formin, nucleates the formation of linear actin filaments
YBL097W[b]	*BRN1* **ESSENTIAL**	Mid	Required for chromosome condensation and for clustering of tRNA genes at the nucleolus
YER164W	*CHD1*	N-term	Nucleosome remodeling factor that functions in regulation of transcription elongation
YGR108W	*CLB1*	N-term	B-type cyclin involved in cell-cycle progression; activate Cdc28 to promote the transition from G2 to M phase
YPL251C	*CLN2*	Entire	G1 cyclin involved in regulation of the cell cycle; activates Cdc28 kinase to promote the G1 to S phase transition
YFR046C	*CNN1*	N-mid	Kinetochore protein of unknown function; phosphorylated by both Clb5-Cdk1 and Clb2-Cdk1
YLR361C	*DCR2*	C-term	Phosphoresterase involved in down-regulation of the unfolded protein response
YDR039C	*ENA2*	N-term	P-type ATPase sodium pump
YPL249C[a]	*GYP5*	Mid	GTPase activating protein for yeast Rab family members, involved in ER to Golgi trafficking
YJR140C	*HIR3*	C-term	Subunit of the HIR complex, a nucleosome assembly complex involved in regulation of histone gene transcription
YGL194C	*HOS2*	C-term	Histone deacetylase required for gene activation; a meiosis-specific repressor of sporulation specific genes that contain

			deacetylase activity
YKL101W[a]	*HSL1*	Mid	Nim1-related protein kinase that regulates the morphogenesis and septin checkpoints; known APC^{Cdh1} substrate
YBR245C[a]	*ISW1*	Mid	Involved in chromatin remodeling and RNA elongation; member of the imitation-switch class of ATP-dependent chromatin remodeling complexes
YJR070C	*LIA1*	N-mid	Deoxyhypusine monooxygenase activity; microtubule cytoskeleton organization and biogenesis
YAL024C	*LTE1*	Mid	Putative GDP/GTP exchange factor for Tem1, a key regulator of mitotic exit
YOR232W	*MGE1*	N-term	Protein of the mitochondrial matrix involved in protein import into mitochondria
YLR320W	*MMS22*	N-term	Protein required for accurate meiotic chromosome segregation
YPR047W	*MSF1*	N-mid	Mitochondrial aminoacyl-tRNA-synthetase
YHR124W	*NDT80*	Mid-C-term	Meiosis-specific transcription factor required for exit from pachytene and for full meiotic recombination and activation of middle sporulation genes
YPL226W	*NEW1*	N-term	Ribosome biogenesis
YIL115C[b]	*NUP159* **ESSENTIAL**	Mid-C-term	Nucleoporin found exclusively of the cytoplasmic side required for mRNA export
YDR265W	*PEX10*	C-term	Peroxisomal membrane E3 ubiquitin ligase required for protein import into peroxisome matrix
YDR379W	*RGA2*	Mid	GTPase-activating protein for the polarity-establishment protein Cdc42
YBR073W	*RDH54*	Mid	DNA-dependent ATPase, involved in recombinational repair of DNA double strand breaks during mitosis and meiosis
YLR357W	*RSC2*	N-mid	Component of the RSC chromatin remodeling complex; required for expression of mid-late sporulation-specific genes
YDR303C	*RSC3*	C-term	Component of the RSC chromatin

	ESSENTIAL		remodeling complex
YDR159W	*SAC3*	C-term	Nuclear pore-associated protein involved in transcription and mRNA export from the nucleus
YDR389W[a]	*SAC7*	C-term +	GTPase activating protein for Rho1p, involved in signaling to the actin cytoskeleton
YLR430W[b]	*SEN1* **ESSENTIAL**	C-term	Presumed helicase required for RNA polymerase II transcription termination and processing of RNAs
YOR165W	*SEY1*	N-term	Protein of unknown function containing 2 GTP-binding motifs
YJL127C	*SPT10*	Mid	Putative histone acetylase
YMR179W	*SPT21*	C-term	Protein required for normal transcription at several loci
YGR002C[b]	*SWC4* **ESSENTIAL**	Mid	Protein involved in chromatin modification and remodeling and histone exchange and acetylation
YJL187C[a]	*SWE1*	N-mid	Protein kinase that regulates the G2 to M transition by inhibition of Cdc28 kinase activity
YER098W	*UBP9*	Mid	Ubiquitin carboxyl-terminal hydrolase, ubiquitin-specific protease
YML093W[b]	*UTP14* **ESSENTIAL**	Mid	Subunit of U3-containing small subunit processome complex involved in the production of 18S rRNA and assembly of small ribosomal subunit
YOR272W[b]	*YTM1* **ESSENTIAL**	C-term	Constituent of 66S pre-ribosomal particles, required for maturation of the large ribosomal subunit
YFL034W[a]		C-term	Protein of unknown function
YKL050C		N-term	Protein of unknown function
YNR047W		Mid	Protein of unknown function
NTS1-2		Mid	

[a]Represented more than once.
[b]Essential gene

Chapter 3: Reformatting of article published in Molecular Biology of the Cell, 2008

The APC targeting subunit Ama1 links meiotic exit to cytokinesis during sporulation in *Saccharomyces cerevisiae*

Aviva E. Diamond[1*], Jae-Sook Park[1], Ichiro Inoue[2], Hiroyuki Tachikawa[2], and Aaron M. Neiman[1]

[1] Department of Biochemistry and Cell Biology, Stony Brook University, Stony Brook New York, 11794-5215; [2]Laboratory of Biological Chemistry, Graduate School of Agricultural and Life Science, The University of Tokyo, 1-1-1 Yayoi, Bunkyo-ku, Tokyo 113-8657, Japan.

***** Responsible for Figures 3-4; 3-5; 3-6; 3-7.

Abstract

Ascospore formation in yeast is accomplished through a cell division in which daughter nuclei are engulfed by newly formed plasma membranes, termed prospore membranes. Closure of the prospore membrane must be coordinated with the end of Meiosis II to ensure proper cell division. *AMA1* encodes a meiosis-specific activator of the Anaphase Promoting Complex (APC). The activity of APC^{Ama1} is inhibited prior to Meiosis II, but the substrates specifically targeted for degradation by Ama1 at the end of meiosis are unknown. We show here that *ama1Δ* mutants are defective in prospore membrane closure. Ssp1, a protein found at the leading edge of the prospore membrane, is stabilized in *ama1Δ* mutants. Inactivation of a conditional form of Ssp1 can partially rescue the sporulation defect of the *ama1Δ* mutant, indicating that an essential function of Ama1 is to lead to the removal of Ssp1. Depletion of Cdc15 causes a defect in meiotic exit. We find that prospore membrane closure is also defective in Cdc15 and that this defect can be overcome by expression of a form of Ama1 in which multiple consensus CDK phosphorylation sites have been mutated. These results demonstrate that APC^{Ama1} functions to coordinate the exit from Meiosis II with cytokinesis.

Introduction

Upon starvation for nitrogen in the presence of a non-fermentable carbon source, diploid cells of the yeast *Saccharomyces cerevisiae* exit vegetative growth and enter a program of meiosis and sporulation to generate haploid spores (Esposito and Klapholz, 1981; Neiman, 2005). The process of spore formation is driven by a cell division in which the daughter cells are formed in the cytoplasm of the mother cell. As cells enter Meiosis II, the cytoplasmic faces of the spindle pole bodies are modified so that they become centers of membrane nucleation (Moens, 1971; Moens and Rapport, 1971). Four membranes, termed prospore membranes, are formed, one at each spindle pole (Moens, 1971; Neiman, 1998). As haploid chromosome sets separate within the nucleus in Meiosis II, each of the prospore membranes grows to engulf the region of the nucleus adjacent to it. Closure of a prospore membrane around a nascent haploid nucleus completes cell division and is equivalent to cytokinesis in mitotic growth. Once the prospore membrane has closed, the prospore then matures by the deposition of spore wall material into the luminal space between the two membranes derived from the prospore membrane (Lynn and Magee, 1970).

As the prospore membrane expands, its growth is guided in part by proteins found at the lip of the growing membrane, termed the leading edge protein coat (Moreno-Borchart *et al.*, 2001). Three components of this coat are known, Don1, Ady3, and Ssp1 (Knop and Strasser, 2000; Moreno-Borchart *et al.*, 2001; Nickas and Neiman, 2002). The function of Don1 is unknown, though it may be the most peripheral member of the complex, as it requires both Ady3 and Ssp1 for localization to the leading edge (Moreno-Borchart *et al.*, 2001; Nickas and Neiman, 2002). Ady3 may function primarily in

promoting mitochondrial segregation into the spore (Suda *et al.*, 2007). The critical constituent of the leading edge complex is Ssp1. This protein is required for localization of both Ady3 and Don1 to the leading edge (Moreno-Borchart *et al.*, 2001). Moreover, in the absence of *SSP1*, prospore membrane growth is abnormal and spore formation is blocked (Nag *et al.*, 1997; Moreno-Borchart *et al.*, 2001).

Ectopic over-expression of *SSP1* in vegetative cells has been shown to block cell growth by interfering with the fusion of secretory vesicles to the plasma membrane (Maier *et al.*, 2007). During sporulation Ssp1 is degraded around the time of prospore membrane closure and mutations that stabilize the protein inhibit sporulation (Maier *et al.*, 2007). These results have led to the proposal that removal of Ssp1 from the leading edge regulates the timing of cytokinesis during sporulation (Maier *et al.*, 2007).

The anaphase promoting complex (APC) is a multisubunit E3 ubiquitin ligase essential for progression through mitosis (Morgan, 1999). The activity of this complex is regulated by accessory subunits of the Cdc20/Fizzy family that direct it to specific substrates (Morgan, 1999). In vegetatively growing *S. cerevisiae*, Cdc20 and Cdh1 regulate APC activity (Visintin *et al.*, 1997). While both Cdc20 and Cdh1 direct the degradation of multiple, overlapping targets, each controls the degradation of a specific target essential for cell division; mitotic cyclins for Cdh1 and securin for Cdc20 (Thornton and Toczyski, 2003). During meiosis, Cdc20 is again important for controlling APC activity (Katis *et al.*, 2004; Oelschlaegel *et al.*, 2005). No meiotic role for Cdh1 has been described, however a third family member, *AMA1*, is expressed specifically in meiotic cells (Chu *et al.*, 1998; Cooper *et al.*, 2000).

Deletion of *AMA1* does not block meiosis, but rather the formation of spores; prospore membranes are formed, but the subsequent formation of spore walls is blocked (Coluccio *et al.*, 2004). This result suggests that the critical target(s) of APC^{Ama1} are protein(s) whose degradation is required to allow spore wall assembly. The identity of these putative targets is unknown.

Ama1 is subject to regulation at several levels. Both transcriptional control and meiosis-specific splicing ensure that the protein is expressed only during sporulation (Chu *et al.*, 1998; Cooper *et al.*, 2000). Although Ama1 can associate with the APC and direct the degradation of securin both *in vivo* and *in vitro*, in a wild-type meiosis APC^{Cdc20} is primarily responsible for securin degradation (Oelschlaegel *et al.*, 2005). The activity of APC^{Ama1} is held in check by the Mnd2 subunit of the APC and by the activity of the Clb-Cdc28 kinase (Oelschlaegel *et al.*, 2005; Penkner *et al.*, 2005). Failure to restrict APC^{Ama1} leads to premature loss of cohesin and chromosome missegregation (Oelschlaegel *et al.*, 2005; Penkner *et al.*, 2005). Although APC^{Ama1} may contribute to the turnover of Pds1 and cyclins during meiosis, the actions of Mnd2 and Clb-Cdc28 ensure that APC^{Ama1} remains inactive until late Meiosis II when Mnd2 dissociates from the APC and Clb-kinase activity decreases, consistent with the primary function of APC^{Ama1} in post-meiotic cells (Dahmann and Futcher, 1995; Rabitsch *et al.*, 2001; Coluccio *et al.*, 2004; Oelschlaegel *et al.*, 2005; Carlile and Amon, 2008).

Meiosis also differs from mitosis in the circuitry that regulates exit from the division. In mitotic cells, exit requires the activity of the Cdc14 protein (Wood and Hartwell, 1982; Taylor *et al.*, 1997). Two separate pathways, termed FEAR and MEN, collaborate to regulate Cdc14 (Dumitrescu and Saunders, 2002). *CDC14* is also

necessary in meiosis, but regulation of Cdc14 in meiosis is largely or wholly mediated by the FEAR network (Marston *et al.*, 2003; Kamieniecki *et al.*, 2005). The MEN component *CDC15* is required for sporulation, but this appears to be independent of *CDC14* (Pablo-Hernando *et al.*, 2007). In meiotic cells depleted of Cdc15, chromosome segregation proceeds normally as judged by 4,6-diamidino-2-phenylindole (DAPI) staining, but prospore membrane growth is abnormal. Also, spindle disassembly at the end of Meiosis II is abnormal and microtubules accumulate rather than disappear (Pablo-Hernando *et al.*, 2007). This last result suggests that a late step in exit from meiosis is defective in this mutant.

The terminal phenotype of *ama1Δ* mutants led to the suggestion that *AMA1* may be required to trigger spore wall assembly after the completion of meiosis (Coluccio *et al.*, 2004). We report here that *ama1Δ* mutants are defective at a slightly earlier stage of spore formation, the closure of the prospore membrane. This defect in cytokinesis may account for the spore wall assembly defect in the mutant. The *ama1Δ* mutant stabilizes the leading edge protein complex so that the Ssp1 protein persists in post-meiotic cells and the ring structure of the complex remains intact. The stabilization of Ssp1 is likely directly responsible for the *ama1Δ* cytokinesis defect, because inactivation of a conditional allele of *SSP1* can partially rescue the *ama1Δ* sporulation defect. A *cdc15* mutant defective in exit from Meiosis II also displays defects in prospore membrane closure. This closure defect can be suppressed by expression of a mutant form of Ama1 in which all the Cdc28 consensus phosphorylation sites have been mutated. These observations suggest that the primary function of APC^{Ama1} is to coordinate exit from Meiosis II with cytokinesis during spore formation.

Materials and Methods

Strains and Growth Medium

Unless otherwise noted, standard media and genetic techniques were used (Rose and Fink, 1990). The strains used in this study are listed in Table 3-1. All strains are in the SK-1 background except for AN390 and the JSP strains, which are hybrids between SK-1 and the S288c background. ADY12 and ADY13 were constructed by polymerase chain reaction (PCR)-mediated knockout of *AMA1* in AN117-4B and AN117-16D, respectively, by using pFA6a CgTRP1 as a template for PCR and oligonucleotides (oligos) F1AMA1 and R1AMA1 in AN117-4B and AN117-16D. ADY64 and ADY65 were constructed in the same manner except pFa6A MX6HIS3 (Longtine *et al.*, 1998) was the PCR template. To create TC37 and TC38, oligos HT362 and HT87 were used to amplify the hemagglutinin (HA)-tagging cassette in pFA6a-3xHA-HisMX6 (Longtine *et al.*, 1998) and the product was used to transform strain AN117-4B and AN117-16D, respectively. All PCR-mediated integrations were confirmed by genomic PCR with appropriate primers. ADY183 and ADY184 were obtained as segregants from a cross of TC38 and ADY64. ADY183-AMA1 and ADY184-AMA1 are ADY183 and ADY184 transformed with EcoRV-digested pRS306AMA1. To construct strains ADY216, ADY217, ADY218, and ADY220 the degron cassette in plasmid pKL187PSSP1 was amplified using primers SSP1DegronF and SSP1DegronR and transformed into ADY12, ADY13, AN117-4B, and AN117-16D, respectively. The plasmid pKL142 (Sanchez-Diaz *et al.*, 2004), carrying *GAL* promoter driven *UBR1,* was linearized by digestion with PmeI and integrated into strains ADY216, ADY217, ADY218, ADY220, AN117-4B and

AN117-16D to generate ADY221, ADY222, ADY223, ADY224, ADY229, and ADY231, respectively. To create ADY225, ADY226, ADY227, ADY228, ADY230 and ADY232 the plasmid p926 was linearized with NdeI and used to transform ADY221, ADY222, ADY223, ADY224, ADY229 and ADY231, respectively. ADY239 and ADY240 were created by transforming ADY12 and ADY13, with p926 followed by pKL142.

For the FLIP studies, ADY64 was crossed with a strain containing a green fluorescent protein (GFP)-tagged *TEF2* allele from the GFP tagged collection (Huh *et al.*, 2003), and mating of *ama1*Δ::*HIS3 TEF2*::GFP::*his5*$^{+}$ segregants from this cross produced JSP22. To generate the *CLB2pr-CDC15* strains, the GFP collection strain carrying TEF2::GFP was crossed with AN117-4B and a segregant from this cross, JSP62, was crossed to a *CLB2pr-CDC15* haploid (Pablo-Hernando *et al.*, 2007). JSP64 and JSP65 are segregants from this latter cross. Transformation of JSP64 and JSP65 with PstI linearized YIplac128-AMA1pr-AMA1 or YIplac128-AMA1pr-AMA1-m8 (Oelschlaegel *et al.*, 2005) was used to generate the haploid parents for JSP99 and JSP104.

Plasmids

Plasmids used in this study are listed in Table 3-2. To construct pRS426-R20, the coding region of monomeric red fluorescent protein (mRFP) in a template pTmRFP (Gao *et al.*, 2005) was amplified using primers HNO941 and HNO942, the product was digested with XbaI and EcoRI and used to replace the GFP sequence in similarly digested pGFP-N-FUS-*SPO20*$^{151\text{-}273}$ (Nakanishi *et al.*, 2004). An EcoRI- XhoI fragment carrying

the coding region of mRFP-*SPO20*$^{151\text{-}273}$ was then cloned from this construct into pRS426-TEF (Mumberg *et al.*, 1995). pKL187PSSP1 is a modified pKL187 (Sanchez-Diaz *et al.*, 2004) containing the *SSP1* promoter in place of the *CUP1* promoter. A 700-base pair fragment carrying the *SSP1* promoter was amplified from pRS314-SSP1-HA using primers SSP1FPromoterMfe1 and SSP1RpromoterEcoR1. The PCR product was digested with Mfe1 and EcoR1 and ligated to the vector backbone of similarly digested pKL187. p926 (gift from A. Amon) is pRS306-Pgpd1-GAL4.ER (Benjamin *et al.*, 2003), an integrative plasmid containing a GAL4-endoplasmic reticulum (ER) fusion under the control of the *GPD1* promoter. pRS306-AMA1pr-AMA1 was constructed as follows. To remove the sporulation-specific intron (base pairs 1184-1276), a 5' fragment of *AMA1* open reading frame (ORF) was amplified with primers FAMA1EcoRI (+631) and RNdeI and blunt-end ligated into pBluescript at the EcoRV restriction enzyme site to create pBluescriptAma1A. This was followed by amplification of a 3' *AMA1* ORF fragment with primers FAMA1Nde1 and RAMA1Pst1stop. This fragment was digested with NdeI and PstI and ligated to similarly digested pBluescriptAma1A. The removal of the intron sequence yielded a conservative amino acid change at position 236 from a cysteine to a serine. This intronless sequence lacks the 5' end of the coding sequence. To place the full-length *AMA1* sequence under its own promoter, we used overlap polymerase chain reaction (PCR). We amplified a 5' fragment of *AMA1* using primers ADO5 and ADO10. This product was mixed with a vector carrying the intronless *AMA1* 3' sequence and amplified with primers ADO3 and ADO5, which yielded a 2Kb DNA fragment. Separately, oligos PAMA1F and PAMA1R were used to amplify 500 base pairs of the upstream sequence of the *AMA1* gene and this promoter region was cloned

into the XhoI and Kpn1 sites of pRS306 to create pRS306-AMA1pr. The full-length intronless *AMA1* ORF was then inserted into a pRS306-AMA1pr, at the XhoI and SpeI sites creating plasmid pRS306-AMA1pr-AMA1. The *AMA1* in this plasmid was shown to be functional based on its ability to complement the *ama1*Δ phenotype (Table 2-4). Plasmids pRS306-AMA1pr-AMA1-IA and pRS306-AMA1pr-AMA1-ΔIR were constructed by reamplifying the intronless *AMA1* ORF using the oligo pairs Ama1pFXhoI and Ama1StopIA, or Ama1pFXhoI and Ama1StopΔIR, respectively. The Ama1StopIA and Ama1StopΔIR oligos incorporate the mutations at the extreme C-terminus of the coding region. The PCR fragments carrying the mutant alleles were then cloned into pRS306-AMA1-pr as XhoI-SpeI fragments. pRS426-AMA1pr-AMA1-ΔIR was created by moving a KpnI and SpeI fragment carrying the gene from pRS306-AMA1pr-AMA1-ΔIR into pRS426 (Christianson *et al.*, 1992).

Sporulation Assays

Cells were sporulated in liquid medium as described previously (Neiman, 1998). Briefly, strains were grown at 30° C overnight in YPD or in selective medium if they contained plasmids. The cultures were then diluted to a cell density of 0.2 at OD_{660} in YP media containing 2% potassium acetate and incubated at 30° C overnight. Cells were then washed once in distilled water and then resuspended in sporulation medium (2% potassium acetate) at a cell density of 1.2 at OD_{660} and these cultures were incubated at 30°C. For experiments using the *degronssp1*, 25nM ß-estradiol (Sigma-Aldrich, St. Louis, MO) was added to the sporulating cells at the time of transfer to sporulation

medium. Cells were cultured at 23° C for two hours and then moved to restrictive temperature.

Ether Tests

Cells were sporulated at permissive (25°C) and restrictive (35°C) temperatures for the degron cassette in the presence or absence of 25 nM β-estradiol (Sigma-Aldrich). Serial dilutions of sporulated cells from each culture condition were spotted onto two duplicate YPD plates, and one plate was exposed to ether vapor for 5 minutes by inversion over an ether-soaked paper filter. Plates were photographed after incubation at 30˚C for one d.

Immunoblotting and Immunofluorescence

For the Western analysis of Ssp1, cell extracts were prepared as described (Moreno-Borchart *et al.*, 2001). Briefly, cells were lysed, and proteins were separated by SDS-polyacrylamide gel electrophoresis (PAGE) and transferred onto nitrocellulose. Ssp1 was detected using anti-HA antibody 12CA5 (Roche Diagnostics, Indianapolis, IN) at 1 µg/ml. Monoclonal anti-porin (Invitrogen, Carlsbad, CA) and polyclonal goat anti-Clb5 antibodies (Santa Cruz Biotechnologies, Santa Cruz, CA) were also used at 1 µg/ml. For detection, the secondary antibody IR Dye 680 goat anti-mouse and IR Dye 800 donkey anti-goat (LI-COR Biosciences, Lincoln, NE) were used at 1:10,000 dilution of a 0.5 mg/ml stocks. Membranes were scanned using Odyssey Infrared Imaging System (LI-COR Biosciences), and the signal intensities for all three proteins measured (Ssp1 and porin were measured on the same membrane, Clb5 from a separate membrane with equal volumes of each sample loaded). To allow comparison of levels between wild type

and *ama1Δ* cells, the porin signals in each lane were normalized to the value in the wild type time zero lane and then the Ssp1 and Clb5 intensities at each time point were normalized to the porin signal at that same time point. Indirect immunofluorescence of the β-glucan layer was performed as described previously (Tachikawa *et al.*, 2001).

Time-lapse Fluorescence microscopy

Time-lapse imaging was done as follows. Sporulation media containing 1.5 % agarose-S was dropped on the glass surface of a glass-bottomed dish. Solidified media were removed from the dish, and cells were spotted on a flat surface of media, put again on a dish to sandwich cells between glass and media. Images were captured on an Axiovert 100 microscope (Carl Zeiss, Thorwood, NY) at 2-min intervals for wild type and 4-min intervals for the *ama1Δ* mutant using of IPLab 3.6.5a software (Scanalytics, Rockville, MD). At each time point, 12 Z-sections were collected at 0.5-μm intervals. The temperature was kept at 28° C. Deconvolution was performed using an EPR system (Scanalytics) and three-dimensional stacks using IPLab 3.6.5a.

Fluorescence Loss in Photobleaching (FLIP) Assays

For FLIP microscopy, strains AN390 and JSP22 were first transformed with pRS424-R20 and pRS426-R20, respectively. A thin-layer of 1.5% agarose containing 1% potassium acetate and 2mM $NaHCO_3$ was prepared. A 1.5-cm square of this agarose was cut out, and sporulated cells were spotted onto this square. The agarose square was then placed cell-side down onto a glass bottom Petri dish (MatTek, Ashland, MA) and cells were observed on a LSM 510 inverted microscope (Zeiss).

For photobleaching, a 488-nm argon laser was used at 100% power. A cytoplasmic area was photobleached for 8 s with 75 pulses per bleaching. To analyze fluorescence intensity, LSM 510 META software version 3.2 (Carl Zeiss) was used.

For the FLIP assay, cells displaying mRFP-Spo20$^{51-91}$ fluorescence (a prospore membrane marker) were selected. An area of the mother cell cytoplasm outside of the prospore membrane was photobleached four times over a period of 14 min, and the GFP fluorescence of Tef2-GFP was monitored every 15 s. Using the software, the fluorescence intensities were then measured in several areas in the cell: 1) the site of bleaching in the cytoplasm, 2) a cytoplasmic area separate from the bleached area and outside of the prospore membrane, 3) an area inside the prospore membrane, and 4) an area of cytoplasm in an unbleached, neighboring cell.

Results

The Leading Edge Complex Persists in *ama1Δ* Mutants

Time-lapse video microscopy was used to examine the growth of the prospore membrane in wild-type cells using a fusion of RFP to the lipid binding domain of Spo20 to visualize the membranes (Nakanishi *et al.*, 2004). These studies demonstrated that as prospore membranes expanded they progressed through a series of discrete morphological stages (Figure 3-1). They begin as small horseshoe-shaped structures that expand into small round structures and initially maintain that round shape as they expand. As Meiosis II progresses, the membranes elongated into a tubular shape. After extending as tubes, the membranes widened in the middle to form an oval before a rapid transition back to a round shape. This final change in shape may correspond to the closure of the prospore membrane.

To examine the relationship between morphological change and closure, a Don1-GFP fusion was used to examine the leading edge protein complex in parallel with membrane growth. The movies revealed that disassembly of the leading edge ring, as seen by dispersal of Don1-GFP fluorescence, happens a few minutes prior to the final rounding up of the prospore membrane (Figure 3-2A). Removal of the core leading edge protein Ssp1 from the leading edge has been proposed to be required for prospore membrane closure (Maier *et al.*, 2007), consistent with the idea that the rounding up of the membrane correlates with cytokinesis.

When *ama1Δ* mutants were examined in the same way, different behaviors of the prospore membrane and Don1-GFP were seen. Membrane expansion was initially

normal, but the duration of the tubular phase was greatly extended (Figure 3-2B). Moreover, even though in many cells the membranes eventually rounded up, the Don1-GFP staining never dispersed as in wild type. Rather, discrete foci of Don1-GFP fluorescence, and occasionally intact rings, persisted throughout the time course. At later times, abnormal prospore membrane structures began to accumulate in the mutant. Don1 localization is dependent on *SSP1* (Moreno-Borchart *et al.*, 2001). Therefore, Don1-GFP serves as a marker for Ssp1 localization in these cells. If disassembly of the leading edge complex and rounding up of the prospore membrane are linked to closure, these observations suggest that cytokinesis is defective in the *ama1Δ* mutant.

FLIP Assay for Closure Reveals a Defect in *ama1Δ* Mutants

To directly assess whether *AMA1* has a role in cytokinesis we developed a FLIP assay for membrane closure based on the ability of a GFP-tagged protein to diffuse between the presumptive ascal and spore cytoplasms. A strain expressing both a GFP-tagged *TEF2* gene, encoding translation elongation factor 2, as well as *mRFP-Spo20*$^{51-91}$ was sporulated. During Meiosis II, a small region of the cytoplasm outside of the prospore membranes was repeatedly photobleached with pulses from a laser and the fluorescence intensity of the Tef2-GFP signal at spots both inside and outside of the prospore membranes was monitored over time (Figure 3-3A). Cells were examined at different stages of prospore membrane growth, as defined by the shape and size of the membrane.

In wild-type cells with small round or tubular prospore membranes, photobleaching of a spot outside of the prospore membrane led to loss of GFP

fluorescence throughout the entire cell, indicating that the Tef2-GFP protein was free to diffuse between cytoplasm located inside and outside of the prospore membrane (Table 3-3 and Figure 3-3A). However in cells where the prospore membrane had made the transition from tubular to oval or round shaped, GFP fluorescence within the prospore membrane was no longer sensitive to photobleaching in the cytoplasm outside of the prospore membrane (Table 3-3 and Figure 3-3A). Thus, the change in prospore membrane shape correlates precisely with the separation of the mother cell cytoplasm into distinct ascal and prospore compartments. In combination with the video microscopy, these results also provide additional evidence that disassembly of the leading edge complex is correlated with cytokinesis.

This FLIP assay was then used to examine membrane closure in the *ama1Δ* mutant. As in wild-type cells, Tef2-GFP diffused freely throughout the cytoplasm in *ama1Δ* cells with small or tubular prospore membranes (Figure 3-3B). However, in *ama1Δ* cells only ~30% of the round or oval prospore membranes were closed off to the ascal cytoplasm (Table 3-3 and Figure 3-3B). At least half of the membranes examined clearly remained open. The remaining 20% gave ambiguous results, in which loss of fluorescence due to photobleaching was intermediate between the obviously open or closed membranes. This may represent cells where closure is incomplete, leaving a small diffusion-limiting opening, or simply be a result of the technical difficulty of photobleaching the ascal cytoplasm alone in cells with abnormal prospore membranes. That some of the prospore membranes do close suggests either that there may be an *AMA1*-independent means of removing the leading edge complex, for example, by some functional overlap with *CDC20*, or possibly an alternative pathway to membrane closure.

Nonetheless, the abundance of open prospore membranes demonstrates that *ama1Δ* mutants are defective in the cytokinesis at the end of Meiosis II.

Ssp1 Protein Levels Persist in the *ama1Δ* Mutant

Our microscopy results indicate that *ama1Δ* mutants are defective both in prospore membrane closure and in disassembly of the leading edge complex. The leading edge component Ssp1 has been shown to antagonize membrane fusion when expressed in vegetative cells leading to the suggestion that closure of the prospore membrane requires removal of Ssp1 from the leading edge (Maier *et al.*, 2007). In this light, one simple explanation for our results would be that APC^{Ama1} promotes degradation of Ssp1 and this degradation allows prospore membrane closure.

To determine if *AMA1* influences the stability of the Ssp1 protein, the levels of a HA-tagged Ssp1 protein were examined across sporulation time courses in wild-type and *ama1Δ* strains (Figure 3-4). To correlate protein levels with the events of meiosis, cells were fixed at each time point, stained with DAPI and the nuclear morphology was examined in the fluorescence microscope. In wild type cells, Ssp1 protein began to accumulate after 3 h in sporulation medium, coincident with the onset of the meiotic divisions. Consistent with earlier reports (Maier *et al.*, 2007), Ssp1 levels peaked after 6 h and then fell sharply as the population reached the end of meiosis. By contrast, in the *ama1Δ* cells, Ssp1 levels increased as in wild type, but the protein accumulated to a much greater extent than in wild-type cells. At later time points, after the bulk of cells in the population had completed Meiosis II, Ssp1 levels declined in the *ama1Δ* mutant strain, but even after 12 h the level of Ssp1 was comparable to the peak level in wild-type cells.

Thus, although some degradation of Ssp1 is seen, loss of *AMA1* leads to an accumulation and a persistence of the Ssp1 protein at the end of meiosis (Figure 3-4B).

Because *ama1Δ* mutants have been reported to have defects in meiotic progression in some backgrounds (Cooper *et al.*, 2000), it was possible that this accumulation and persistence of Ssp1 was an indirect consequence of a meiotic defect in the *ama1Δ* strain. To examine this possibility, we also measured the abundance of Clb5, a protein degraded at the completion of Meiosis II (Carlile and Amon, 2008), in the two strains (Figure 3-4C). The levels of Clb5 were comparable in both strains throughout the time course, indicating that the accumulation of Ssp1 is not a consequence of a more general defect in protein turnover at the end of Meiosis II in the *ama1Δ* mutant.

The *ama1Δ* Sporulation Defect Can Be Partially Rescued by a Conditional *SSP1*

If *AMA1*-mediated turnover of Ssp1 is required for prospore membrane closure and this cytokinesis defect is responsible for the subsequent spore wall formation phenotypes of *ama1Δ,* then mutation of *SSP1* might be expected to rescue the *ama1Δ* sporulation defect. Because *SSP1* is essential for proper prospore membrane assembly, a conditional allele of *SSP1* is required so that Ssp1 protein can be inactivated after prospore membranes have formed and expanded. A point mutation creating a conditional allele of *ssp1* has been reported previously (Esposito *et al.*, 1970; Maier *et al.*, 2007), but in our strain background the phenotype of this mutant was very mild, and no restoration of sporulation was observed when it was combined with *ama1Δ* (Diamond, unpublished observations). We therefore sought to engineer a conditional allele of *SSP1* by using a degron cassette (Sanchez-Diaz *et al.*, 2004). Fusion of one copy of ubiquitin followed by

a temperature-sensitive form of dihydrofolate reductase (DHFR) to the amino terminus of a heterologous protein can be used to generate proteins whose stability is temperature-dependent *in vivo* (Sanchez-Diaz *et al.*, 2004). Cleavage of the ubiquitin moiety reveals an amino-terminal arginine residue on the $DHFR^{ts}$ and, upon shift to elevated temperature, the $DHFR^{ts}$ fusion protein is degraded by the N-end rule pathway. Efficient turnover in this system also requires over-expression of the ubiquitin ligase *UBR1* (Sanchez-Diaz *et al.*, 2004). To induce *UBR1* in our strains, both a *GAL* promoter driven *UBR1* and a plasmid expressing a fusion of the Gal4 transcription factor to the hormone-binding domain of the human estrogen receptor were integrated into the genome. This Gal4 fusion can induce transcription only in the presence of steroid ligands such as β-estradiol (Picard, 1999). A strain expressing the fusion form of *SSP1* (hereafter *degssp1*) as its only source of Ssp1, and carrying both the *GAL-UBR1* and *GAL4-ER* plasmids, displays conditional sporulation; sporulation is blocked only when *UBR1* is induced with β-estradiol and the temperature is raised (Figure 3-5A).

The *degssp1*allele was then combined with a deletion of *AMA1*. Cells were sporulated in the presence of β-estradiol at 23°C for 2 h to allow them to enter sporulation and then shifted to 35°C and incubated overnight. Sporulation was assayed both by ether test (Figure 3-5B) and by direct examination in the light microscope (Figure 3-5C). Under this regimen, wild-type cells displayed good sporulation at both temperatures, an *ama1Δ* strain failed to produce spores at either temperature, and the *degssp1*strain displayed temperature-sensitive sporulation. By contrast, the *ama1Δ degssp1* strain displayed very weak sporulation at low temperature that was markedly improved by raising the temperature to 35°C. Tests of different temperature regimes and

incubation times before temperature upshift indicated that the protocol used in these experiments provided the best level of sporulation in the double mutant (Diamond, unpublished observations). Although this level of sporulation was only ~10% of the wild type, no spores were ever seen in the *ama1Δ* mutant alone. Thus, this represents a significant suppression of *ama1Δ* by *degssp1*. Reproducibly, at 35°C, slightly higher sporulation was seen in the *ama1Δ degssp1* strain than in the strain carrying *degssp1* alone (Figure 3-5C). Thus, reciprocally, deletion of *AMA1* improves sporulation of *degssp1* cells. The accumulation of Ssp1-HA seen in *ama1Δ* mutants (Figure 3-4) suggests that this improvement of *degssp1* sporulation may be due to stabilization of degSsp1 that has escaped from N-end rule mediated degradation.

When *ama1Δ* cells are sporulated they fail to synthesize spore wall components. As spore wall assembly is required for the generation of visible spores, the incomplete rescue of *ama1Δ* by *degssp1* could represent strong suppression of the cytokinesis defect masked by a subsequent spore wall synthesis phenotype. To address this possibility, spore wall synthesis in the *ama1Δ degssp1* mutant was examined using anti- β-1,3-glucan antibodies (Figure 3-5E). Examination of anti- β-1,3-glucan staining in the mutant demonstrated that the number of β-1,3-glucan containing prospores varied between asci. The distribution of β-glucan staining was comparable to the distribution of visible spores as seen in differential interference contrast (DIC) microscopy (Diamond, unpublished observations). Because β-glucan deposition in the spore wall layer is required for acquisition of refractility and occurs early in spore wall formation (Tachikawa *et al.*, 2001; Coluccio *et al.*, 2004), this result suggests that those prospores that bypass the cytokinesis block in the *ama1Δ degssp1* strain go on to complete spore wall synthesis.

A Motif Important for Interaction with the APC is Essential for Ama1 Function

Cdc20/Fizzy family members carry two motifs, a C-box and a carboxy-terminal isoleucine and arginine (IR) that are important for interaction with the APC (Schwab *et al.*, 2001; Vodermaier *et al.*, 2003). The IR motif has been shown to bind to the APC subunit Cdc27, and mutation of the IR motif in Cdh1 or Cdc20 blocks their interaction with the APC *in vitro* and inactivates Cdh1 *in vivo* (Vodermaier *et al.*, 2003; Kraft *et al.*, 2005; Oelschlaegel *et al.*, 2005). Similarly, mutation of the carboxy-terminal arginine residue of Ama1 to an alanine blocks its ability to interact with the APC *in vitro* (Oelschlaegel *et al.*, 2005). We examined the phenotype of this arginine to alanine mutation ($AMA1^{R593A}$) *in vivo*. Despite the strong effect of this mutation *in vitro*, cells expressing $AMA1^{R593A}$ from the chromosome as the only form of *AMA1* showed only a mild sporulation defect (Figure 3-6). By contrast, deletion of both the carboxy-terminal isoleucine and arginine residues (*IRΔ*) strongly reduced sporulation. When this $AMA1^{IR\Delta}$ allele was over-expressed from a high copy plasmid, the mutant was able to partially rescue the sporulation defect of *ama1Δ*. These observations demonstrate that the carboxy-terminal IR motif is important, although not essential, for Ama1 function *in vivo*. This suggests that interaction with the APC is necessary for Ama1 to promote sporulation but that, in contrast to the *in vitro* studies, *in vivo* the IR motif enhances but is not absolutely required for this interaction.

An Activated Form of Ama1 Can Promote Cytokinesis in a Meiotic Exit-Defective Mutant.

The protein kinase Cdc15 is a component of a pathway, the MEN, that is required for completion of mitosis in vegetative cells (Hartwell *et al*., 1970; Bardin *et al*., 2003). Cdc15 protein can be depleted from sporulating cells by placing the gene under control of the sporulation-repressed *CLB2* promoter (Kamieniecki *et al.*, 2005; Pablo-Hernando *et al.*, 2007). Although homozygous *CLB2pr-CDC15* cells progress through meiosis with normal kinetics, the cells fail to form spores and display other phenotypes, including defective spindle disassembly, that suggest a failure to properly exit from Meiosis II (Pablo-Hernando *et al.*, 2007).

APC^{Ama1} activity is inhibited during meiosis by both the Mnd2 subunit of APC and by Clb-Cdc28 kinase and both of these antagonistic activities are down-regulated as cells complete meiosis (Dahmann and Futcher, 1995; Oelschlaegel *et al.*, 2005; Carlile and Amon, 2008). If, as a consequence of the failure to exit meiosis properly, a *CLB2pr-CDC15* mutant does not release the inhibition of APC^{Ama1}, we would expect to find a prospore membrane closure defect in these cells. To test this possibility, we used the FLIP assay to examine prospore membrane closure in a *CLB2pr-CDC15* strain. As reported previously (Pablo-Hernando *et al.*, 2007), the *CLB2pr-CDC15* cells displayed a prospore membrane growth defect, with many cells displaying only one or two membranes that are full size by the end of Meiosis II. Because small membranes are usually open in wild-type cells, we limited our analysis of closure to the largest membrane in each cell. In the *CLB2pr-CDC15* strain, 53% of these membranes were

closed and 24% were open, with the remaining membranes in the indeterminate class (Table 3-4). Thus, depletion of Cdc15 results in a prospore membrane closure defect.

If the closure defect in *CLB2pr-CDC15* cells is due to inhibition of APC^{Ama1} then relief of this inhibition should restore prospore membrane closure in the mutant. Combining a deletion of *MND2* with *CLB2pr-CDC15* is problematic because unregulated APC^{Ama1} activity in the *mnd2* strain results in defects early in meiosis (Oelschlaegel *et al.*, 2005; Penkner *et al.*, 2005). By contrast, mutation of eight consensus Cdc28 phosphorylation sites in the Ama1 protein to alanines ($Ama1^{m8}$) does not cause any obvious phenotype (Oelschlaegel *et al.*, 2005). We therefore integrated either *AMA1* or *AMA1-m8* into the *CLB2pr-CDC15* strain and examined prospore membrane closure by using the FLIP assay.

Integration of two extra copies of *AMA1* into these cells did not significantly alter the fraction of prospore membranes that were closed. However, introduction of the *AMA1-m8* allele, increased the fraction of membranes that close in the *CLB2pr-CDC15* cells to 80%. Although modest, a chi-squared test indicates that the fraction of closed prospore membranes in the presence of *AMA1-m8* is significantly different from either of the other two strains ($p < 0.001$). These results indicate that the closure defect in the *CLB2pr-CDC15* cells is caused by a failure to activate APC^{Ama1} possibly due to direct phosphorylation of Ama1 by the Cdc28 kinase.

In addition to the prospore membrane closure defect, *CLB2pr-CDC15* cells display defects in prospore membrane growth, meiotic spindle disassembly, and fail to form spores (Pablo-Hernando *et al.*, 2007). Expression of *AMA1-m8* did not rescue any

of these other phenotypes (Suda and Park, unpublished observations). Thus, the lack of APC^{Ama1} activity is responsible only for the closure defect in these cells.

Discussion

Studies of the leading edge component Ssp1 have demonstrated that the protein is degraded at around the time of prospore membrane closure and that failure to degrade the protein blocks spore formation (Maier *et al.*, 2007). Using a FLIP assay, we provide direct evidence that morphological changes in the prospore membrane that correlate with removal of the leading edge complex are coincident with closure of the prospore membrane. In an *ama1Δ* mutant, Ssp1 degradation and leading edge complex disassembly is delayed and cytokinesis is impaired. This provides direct support for the idea that removal of Ssp1 from the leading edge is required for membrane closure (Maier *et al.*, 2007).

A conserved IR dipeptide at the extreme carboxy-terminus is a hallmark of Cdc20/Fizzy proteins (Vodermaier *et al.*, 2003). However, the effects of mutations in this motif vary *in vivo*. Deletion of this motif in budding yeast Cdh1 creates a null allele (Kraft *et al.*, 2005), whereas cells carrying a deletion of the IR residues of Cdc20 are viable, with only modest effects on function of the protein (Thornton *et al.*, 2006). Ama1 falls between these extremes. Deletion of the IR tail does greatly reduce sporulation, but over-expression of this allele can restore activity. The differences between these different APC targeting subunits in sensitivity to carboxy-terminal mutations suggest that in addition to the conserved C-box and IR motifs they may each make unique contacts with the APC that affect the relative importance of the conserved motifs.

Activity of APC^{Ama1} is regulated by both the Mnd2 subunit of the APC and Clb-Cdc28 kinase activity (Oelschlaegel *et al.*, 2005; Penkner *et al.*, 2005). In the presence of Mnd2, Ama1 cannot promote ubiquitylation of substrates either *in vivo* or *in vitro*

(Oelschlaegel *et al.*, 2005). The Mnd2 protein, however, dissociates from the APC during anaphase II, suggesting that the activity of APC^{Ama1} might be up-regulated at that time (Oelschlaegel *et al.*, 2005). Similarly, Clb-Cdc28 kinase activity down-regulates APC^{Ama1} and Clb-Cdc28 kinase activity drops at the end of Meiosis II (Dahmann and Futcher, 1995; Oelschlaegel *et al.*, 2005; Carlile and Amon, 2008). Our finding that mutation of the consensus Cdc28 phosphorylation sites of Ama1 allows prospore membrane closure in the *CLB2pr-CDC15* mutant suggests that Cdc28 directly phosphorylates Ama1. Relief of these two different inhibitions might trigger APC^{Ama1} activity at the end of meiosis. This is analogous to the manner in which APC^{Cdh1} activity in mitotic cells is restricted until anaphase by the combination of Cdc28 phosphorylation of Cdh1 and the binding of the APC^{Cdh1} inhibitor Acm1 (Zachariae *et al.*, 1998; Martinez *et al.*, 2006; Ostapenko *et al.*, 2008).

In the case of Cdh1, phosphorylation seems to be the predominant brake on APC^{Cdh1} activity, as mutation of the phosphorylation sites creates a constitutively active, lethal allele (Zachariae *et al.*, 1998). By contrast, though we provide evidence that mutation of the Cdc28 consensus phosphorylation sites in Ama1 results in an allele that is dominantly active late in meiosis, in an otherwise wild-type cell, the *AMA1-m8* mutant does not produce a phenotype (Oelschlaegel *et al.*, 2005). Mutation of *MND2*, however, is sufficient to activate APC^{Ama1} (Oelschlaegel *et al.*, 2005; Penkner *et al.*, 2005). One interpretation of these observations is that *MND2* provides the primary restraint on APC^{Ama1} activity early in meiosis and that inhibition by Clb-kinase late in meiosis, as Mnd2 activity is lost, allows the activation of APC^{Ama1} to be timed more precisely to exit from Meiosis II. In light of the report that different Clb-Cdc28 complexes are active at

different times of meiosis (Carlile and Amon, 2008), it will be of interest to determine if APC^{Ama1} is subject to down-regulation by Clb-kinases generally or only those that are active during Meiosis II.

Our finding that depletion of Cdc15 results in a cytokinesis defect that can be relieved by a non-phosphorylatable allele of *AMA1* is consistent with the idea that completion of meiosis leads to activation of APC^{Ama1}. These observations, and previous work indicating that removal of Ssp1 from the prospore membrane is important for prospore membrane closure (Maier *et al.*, 2007) suggest a model in which Ama1 functions to coordinate exit from Meiosis II with cytokinesis. The disappearance of Mnd2 and Clb-Cdc28 kinase activity at the end of meiosis activates APC^{Ama1} leading to the destruction of Ssp1 and disassembly of the leading edge complex. The removal of Ssp1 then allows the prospore membrane to close (Figure 3-7).

One unresolved question is whether APC^{Ama1} regulates Ssp1 turnover directly. While the simplest model would be that APC^{Ama1} ubiquitylates Ssp1 to trigger its degradation, we and others have been unable to identify ubiquitylated forms of Ssp1 in wild-type cells (Diamond, unpublished; Maier *et al.*, 2007). Furthermore, though the *SSP1* sequence contains matches to both the consensus KEN and D boxes found in many APC substrates, both these sites lie outside the C-terminal domain that has been shown to be required for Ssp1 degradation (Maier *et al.*, 2007), and mutation of the KEN box does not produce an obvious phenotype (Diamond, unpublished). Therefore, although the simple model is appealing, it is possible that, analogous to the way in which APC^{Cdc20} regulates cohesin stability through the action of separase (Ciosk *et al.*, 1998; Uhlmann *et al.*, 1999), APC^{Ama1} acts through some additional protein to regulate Ssp1 turnover.

Another issue still to be addressed is the connection between the failure of cytokinesis in *ama1Δ* and the spore wall phenotype of the mutant. Our FLIP studies reveal that a significant fraction of the prospore membranes in *ama1Δ* cells eventually close, possibly due to slower, *AMA1*-independent turnover of Ssp1. Nonetheless, these prospores do not develop spore walls. In wild-type cells, the onset of spore wall development only occurs after cytokinesis. It may be that the normal closure process generates a signal that initiates wall assembly and this signal is not generated by the abnormal closure of membranes in the *ama1Δ* cells. Alternatively, APC^{Ama1} may have additional roles in spore wall development after cytokinesis. The APC subunit Swm1 was originally identified as a mutant with a spore wall defect (Ufano *et al.*, 1999), and an APC subunit has also been identified as a spore wall mutant in *Schizosaccharomyces pombe* (Kakihara *et al.*, 2003), suggesting that the APC is important for proper wall assembly. Moreover, *AMA1* has been found to be required for the activation of the mitogen-activated protein kinase Smk1, which regulates spore wall assembly (Krisak *et al.*, 1994; Huang *et al.*, 2005; McDonald *et al.*, 2005). This last observation strongly suggests the existence of additional APC^{Ama1} targets besides Ssp1, and may explain why inactivation of degssp1 only provides a partial suppression of the *ama1Δ* sporulation defect.

Finally, the mechanism by which prospore membrane closure is achieved also requires further exploration. In vegetative yeast cells, cytokinesis is driven by a combination of actomyosin ring mediated ingression of the plasma membrane as well as deposition of septal wall material. Neither of these mechanisms is likely to operate in prospore membrane closure as actin is not found at the leading edge, and there is no

significant deposition of wall material until well after prospore membrane closure (Coluccio *et al.*, 2004; Taxis *et al.*, 2006). However, the final separation into distinct cells in a mitotic division requires rearrangement of membrane bilayers and it topologically represents the same situation as closure of the prospore membrane. Several different membrane fusion associated functions including the exocyst, soluble *N*-ethylmaleimide-sensitive factor attachment protein receptors, and the ESCRT complex have been implicated in this final stage of cell separation during division in multicellular eukaryotes (Lauber *et al.*, 1997; Jantsch-Plunger and Glotzner, 1999; Gromley *et al.*, 2005; Carlton and Martin-Serrano, 2007). Exactly how division is achieved remains obscure.

Similarly, the mechanism of prospore membrane closure remains to be determined. Ssp1 appears to be antagonistic to membrane fusion (Maier *et al.*, 2007), and our data are consistent with the proposal that removal of Ssp1 promotes closure of the membrane, but this leaves open the question of how closure is achieved. Given the parallels to the final stages of cytokinesis in mitotic cells, the identification of proteins that directly mediate closure of the membrane could provide insight into the general mechanism of cytokinesis.

Chapter 3 Figures

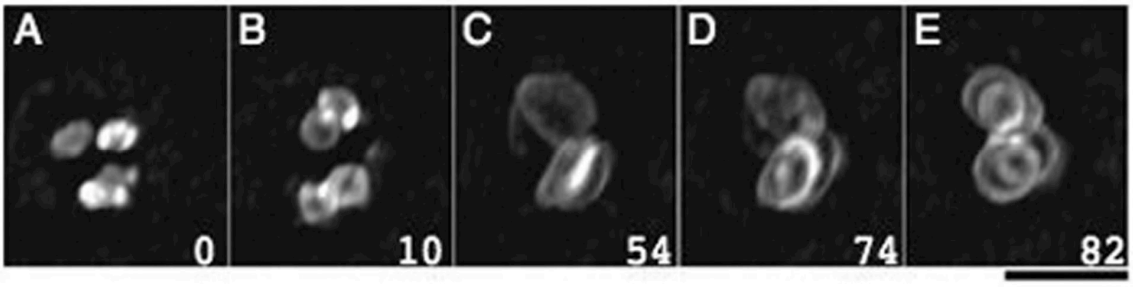

Figure 3-1. Morphological changes of the prospore membrane in wild-type cells. AN120 containing pRS424-G20 (*GFP-SPO20*$^{50-91}$) was sporulated and examined by fluorescence microscopy. Five different morphologies were observed in the following temporal order; A) a horseshoe shape, B) a small circular shape, C) a tubular shape, D) an oval shape, and E) a sphere shape. Images shown are frames from a video of prospore membrane formation of a single cell. Each image is a projection through a deconvolved image stack. The numbers indicate the time elapsed, in minutes, from the image captured in (A). Scale bar, 5 μm.

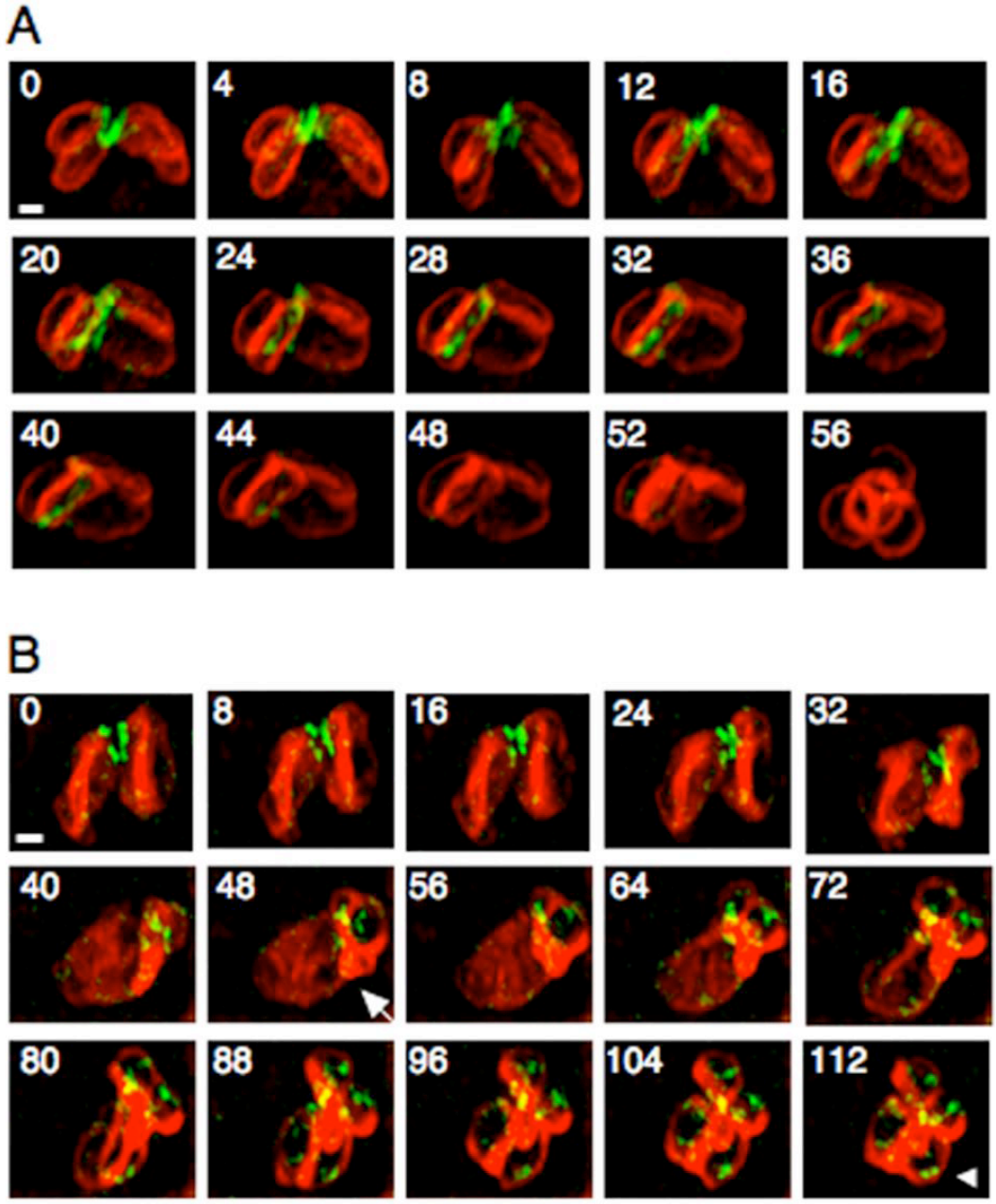

Figure 3-2. Time-lapse analysis of prospore membranes and the leading edge complex in late Meiosis II. A) AN120 (wild-type) carrying pRS424-R20 (*RFP-SPO20*$^{50-91}$) and pSB8 (*DON1-GFP*) was cultured on sporulation medium for seven hours and analyzed by time lapse fluorescence microscopy. Numbers indicate minutes elapsed from start of observation. Scale bar, 1 μm. B) ADY66 (*ama1*Δ/*ama1*Δ) carrying pRS424-R20 and pSB8 was cultured on sporulation medium for 10 hours and analyzed by time-lapse fluorescence microscopy. Numbers indicate minutes elapsed from start of observation. Arrow at 48 minutes indicates a site of abnormal prospore membrane growth. Arrowhead at 112 minutes indicates an intact Don1-GFP ring. Scale bar, 1 μm.

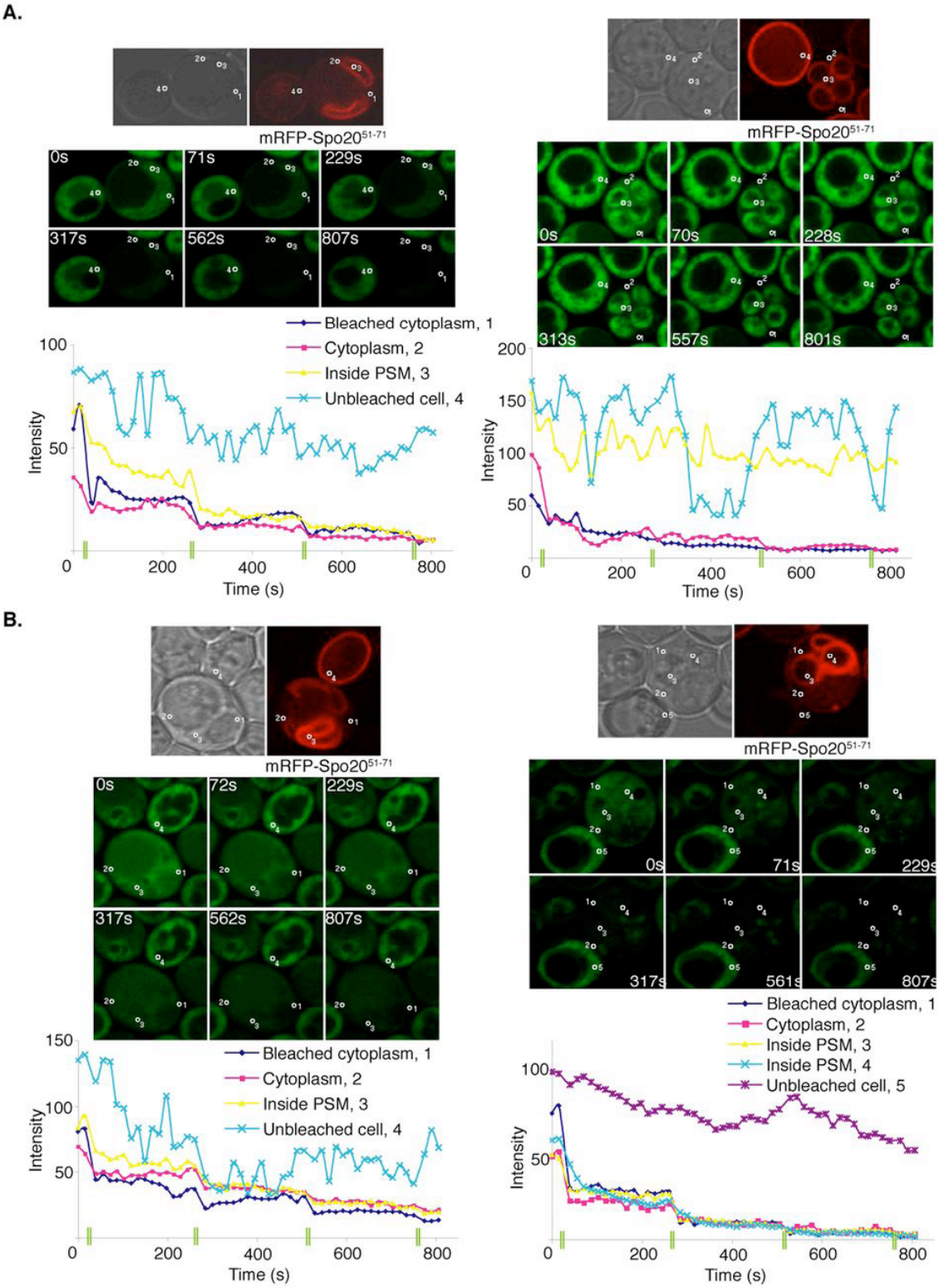
A.
mRFP-Spo20$^{51-71}$
0s
71s
229s
317s
562s
807s
Bleached cytoplasm, 1
Cytoplasm, 2
Inside PSM, 3
Unbleached cell, 4
Intensity
Time (s)
mRFP-Spo20$^{51-71}$
0s
70s
228s
313s
557s
801s
Intensity
Time (s)
B.
mRFP-Spo20$^{51-71}$
0s
72s
229s
317s
562s
807s
Bleached cytoplasm, 1
Cytoplasm, 2
Inside PSM, 3
Unbleached cell, 4
Intensity
Time (s)
mRFP-Spo20$^{51-71}$
0s
71s
229s
317s
561s
807s
Bleached cytoplasm, 1
Cytoplasm, 2
Inside PSM, 3
Inside PSM, 4
Unbleached cell, 5
Intensity
Time (s)

Figure 3-3. Morphological change of the prospore membrane coincides with prospore membrane closure. Wild type (AN390) and *ama1*Δ (JSP22) cells carrying containing pRS424-R20 (*RFP -SPO20*$^{51-91}$) were cultured and prepared for the FLIP assay as described in Methods. The prospore membranes were visualized with mRFP-Spo20$^{51-91}$. The diffuse cytoplasmic fluorescence is from Tef2-GFP.
A) Time lapse series of FLIP assay in wild-type cells. Circle 1 indicates the region of the ascal cytoplasm that was photo-bleached. Circle 2 indicates a region ascal cytoplasm opposite to the bleached area. Circle 3 indicates the cytoplasm inside a prospore membrane. Circle 4 indicates the cytoplasm of a non-bleached neighboring cell. Fluorescence intensity dropped throughout the cell containing tubular shape prospore membranes (left). Fluorescence intensity dropped only in the ascal cytoplasm of a cell containing sphere shaped prospore membranes (right).
B) Time lapse series of FLIP assay in *ama1*Δ cells. Circle 1 indicates the region of the ascal cytoplasm that was photo-bleached. Circle 2 indicates a region ascal cytoplasm opposite to the bleached area. Circle 3 indicates the cytoplasm inside a prospore membrane. Circle 4 indicates the cytoplasm of a non-bleached neighboring cell. Fluorescence intensity decreased throughout the cell in cells displaying both tubular (left) and sphere (right) phase prospore membranes. Graphs display quantification of fluorescence intensity at each monitored spot throughout the course of the assay. Vertical green lines on the x-axis indicate the times at which laser pulses were used to induce photobleaching.

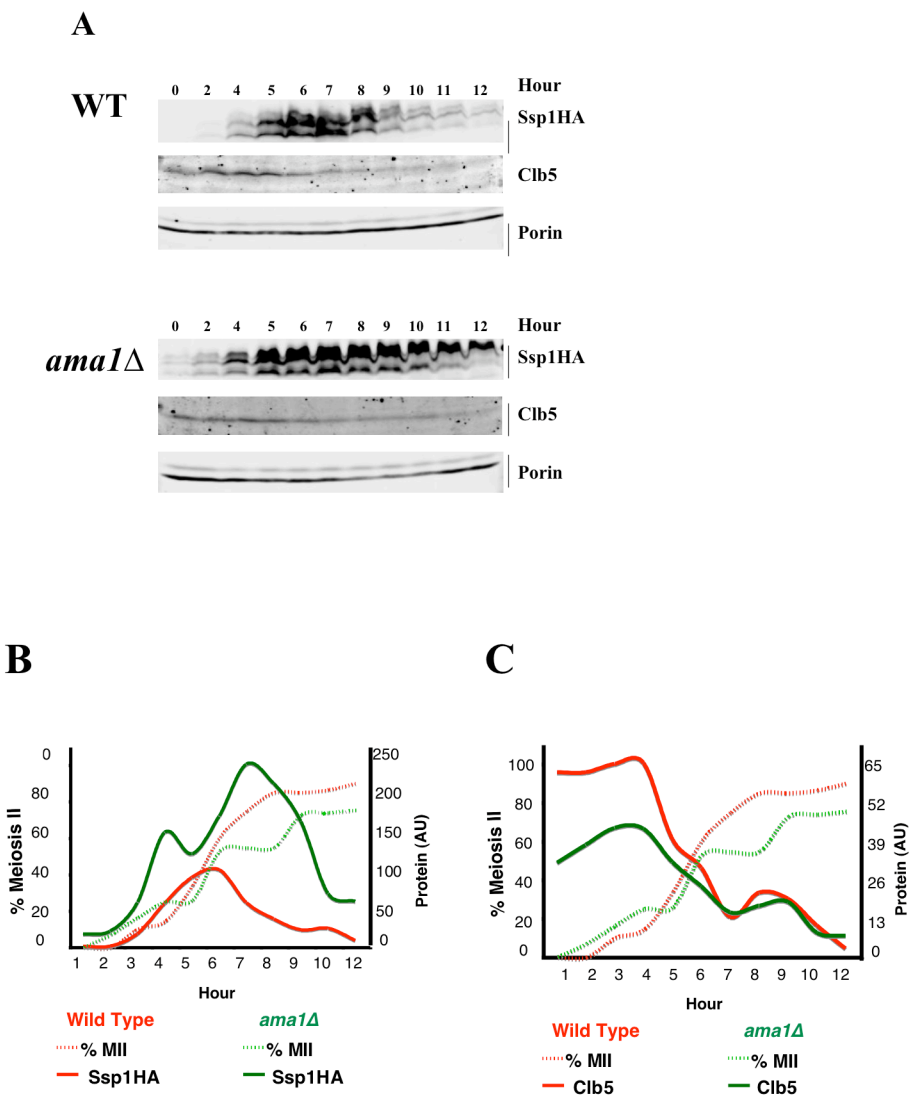

Figure 3-4. Ssp1 is degraded in an APC^{Ama1}-dependent manner
A) Western analysis of Ssp1 protein levels. Wild type and *ama1*Δ strains were sporulated and aliquots removed at specific time points both to monitor nuclear divisions and prepare samples for SDS-PAGE. Extracts were examined for the presence of Ssp1-HA, indicated with brackets, detected by anti-HA antibody as well as Clb5 and the mitochondrial porin protein. B and C) Quantification of levels of Ssp1HA and Clb5 proteins during the sporulation time course shown in (A). Dashed lines indicate percentage of cells having completed Meiosis II at each time point. Solid lines indicate levels of Ssp1-HA and Clb5 proteins in arbitrary units. Levels of Ssp1-HA and Clb5 were determined by normalization against the levels of the mitochondrial porin at each time point.

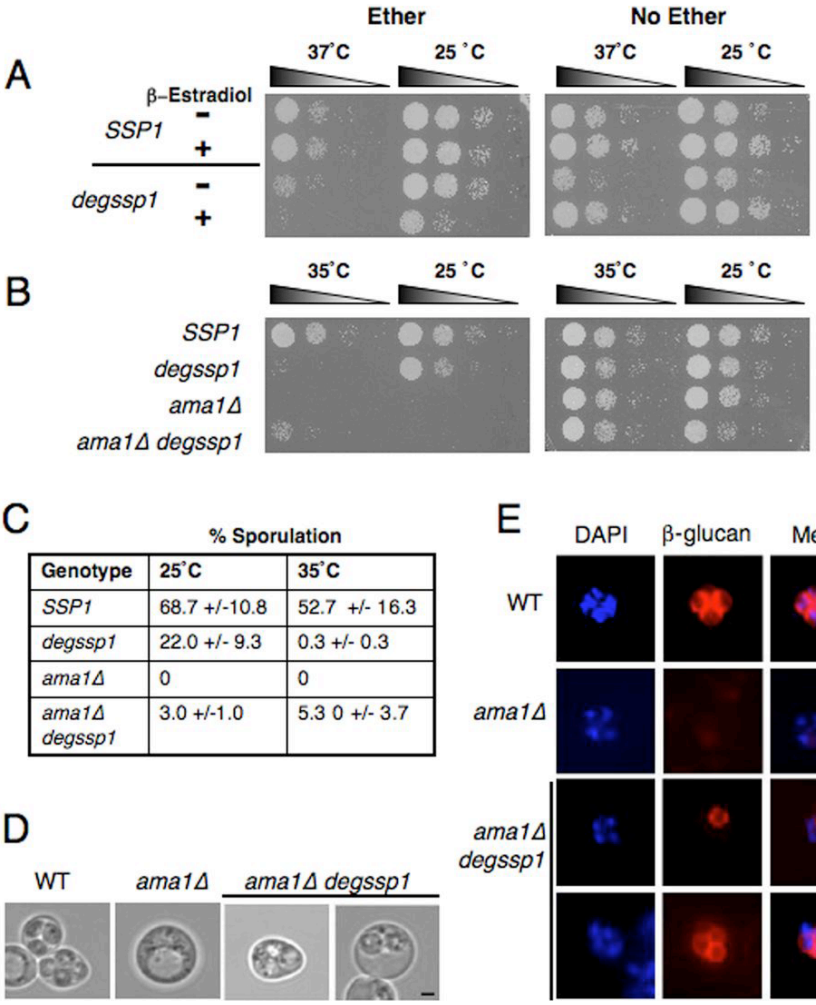

Figure 3-5. Premature degradation of Ssp1 suppresses the *ama1*Δ phenotype
A) *degssp1* is a conditional allele of *SSP1*. Wild type (ADY234) or *degssp1* (ADY235) strains carrying *GAL1::UBR1* were sporulated at permissive temperature (25˚C) and restrictive temperature (37˚C) in the presence or absence of 25nM ß-estradiol. Serial dilutions of cells in each culture condition were spotted onto YPD plates and cells in the left panel were exposed to ether vapor to kill unsporulated cells. Growth indicates the presence of spores. B) Inactivation of *SSP1* suppresses the *ama1*Δ phenotype. Wild type (ADY234) *degssp1* (ADY235), *ama1*Δ (ADY236), and *ama1*Δ *degssp1* (ADY241) strains carrying *GAL1::UBR1* were sporulated at permissive temperature in the presence of ß-estradiol. Samples were transferred at two hours to restrictive temperature (35˚C) and incubated overnight. Serial dilutions of cells in each culture condition were spotted onto YPD plates and subsequently exposed to ether vapor. C) Quantification of *degssp1* suppression of *ama1*Δ. Strains were sporulated as in (B) and percent sporulation was determined in each culture by light microscopy. Asci containing one to four visible spores were all scored as sporulated. Average values from three separate experiments are given. D) DIC images of WT (ADY234), *ama1*Δ (ADY241) and *degssp1 ama1*Δ (ADY236) strains sporulated at restrictive temperature (35˚C) in the presence of ß-estradiol. E) Anti-β-glucan staining of asci of the same strains shown in (A). Chromatin is visualized by staining with DAPI (blue). Scale bar = 2 micron

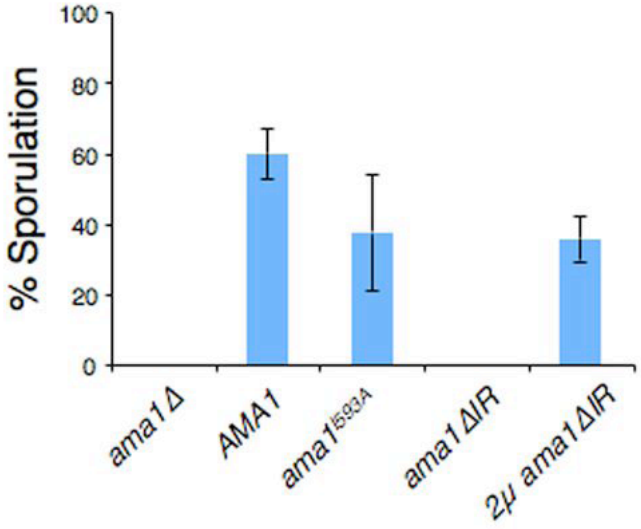

Figure 6. The carboxy-terminal APC interaction motif is essential for Ama1 function. An *ama1*Δ strain (ADY66) was transformed with the indicated *AMA1* alleles and sporulation efficiency was assessed by light microscopy. Averages are calculated from five separate experiments. Bars indicate one standard deviation from the mean.

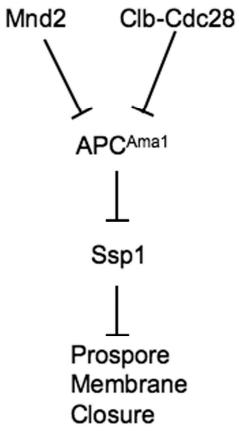

Figure 7. Model for regulatory steps linking completion of meiosis to prospore membrane closure. Mnd2 and Clb-Cdc28 act during early stages of meiosis to restrain APC^{Ama1}. Ssp1 acts as an inhibitor of membrane closure. When Mnd2 and Clb-Cdc28 activities are lost at the end of Meiosis II, APC^{Ama1} becomes active and leads to degradation of Ssp1, allowing prospore membrane closure.

Table 3-1. *S. cerevisiae* strains used in this study

Strain	Genotype	Source
AN117-4B	*MATα ura3 leu2 trp1 his3Δsk arg4-NspI lys2 hoΔ::LYS2 rme1::LEU2*	(Neiman *et al.*, 2000)
AN117-16D	*MAT***a** *ura3 leu2 trp1 his3Δsk lys2 hoΔ::LYS2*	(Neiman *et al.*, 2000)
AN120	Cross of AN117-4B and AN117-16D	(Neiman *et al.*, 2000)
ADY12	*MAT***a** *ura3 leu2 trp1 his3Δsk lys2 hoΔ::LYS2 ama1Δ::CgTRP1*	This study
ADY13	*MATα ura3 leu2 trp1 his3Δsk arg4-NspI lys2 hoΔ::LYS2 rme1::LEU2 ama1Δ::CgTRP1*	This study
ADY64	*MATα ura3 leu2 trp1 his3Δsk arg4-NspI lys2 hoΔ::LYS2 rme1::LEU2 ama1Δ::HIS3*	This study
ADY65	*MAT***a** *ura3 leu2 trp1 his3Δsk lys2 hoΔ::LYS2 ama1Δ::HIS3*	This study
ADY66	Cross of ADY64 and ADY65	This study
TC37	*MATα ura3 leu2 trp1 his3Δsk arg4-NspI lys2 hoΔ::LYS2 rme1::LEU2 SSP1::3xHA::his5*	This study
TC38	*MAT***a** *ura3 leu2 trp1 his3Δsk lys2 hoΔ::LYS2 SSP1::3xHA::his5*	This study
TC529	Cross of TC37 and TC38	This study
ADY183	*MAT***a** *ura3 leu2 trp1 his3Δsk lys2 hoΔ::LYS2 ama1Δ::HIS3 SSP1::3xHA:his5*$^{+}$	This study
ADY184	*MATα ura3 leu2 trp1 his3Δsk arg4-NspI lys2 hoΔ::LYS2 rme1::LEU2 ama1Δ::HIS3 SSP1::3xHA:his5*$^{+}$	This study
ADY185	Cross of ADY183 and ADY184	This study
ADY183-AMA1	*MAT***a** *ura3::AMA1::URA3 leu2 trp1 his3Δsk lys2 hoΔ::LYS2 ama1Δ::HIS3 SSP1::3xHA:his5*$^{+}$	This study
ADY184-AMA1	*MATα ura3::AMA1::URA3 leu2 trp1 his3Δsk arg4-NspI lys2 hoΔ::LYS2 rme1::LEU2ama1Δ::HIS3 SSP1::3xHA::his5*$^{+}$	This study
ADY185	Cross of ADY183-AMA1 and ADY184	This study
ADY186	Cross of ADY183-AMA1 and ADY184-AMA1	This study
ADY216	*MATα ura3 leu2 trp1 his3Δsk arg4-NspI lys2 hoΔ::LYS2 rme1::LEU2 ssp1::kanMX6::SSP1prDEGRON-SSP1*	This study
ADY217	*MAT***a** *ura3 leu2 trp1 his3Δsk lys2 hoΔ::LYS2 ama1Δ::CgTRP1 ssp1::kanMX6::SSP1prDEGRON-SSP1*	This study

ADY218	*MATα ura3 leu2 trp1 his3Δsk arg4-NspI lys2 hoΔ::LYS2 rme1::LEU2 ama1Δ::CgTRP1 ssp1::kanMX6::SSP1prDEGRON-SSP1*	This study
ADY220	*MAT***a** *ura3 leu2 trp1 his3Δsk lys2 hoΔ::LYS2 ssp1::kan^{R}::SSP1prDEGRON-SSP1*	This study
ADY221	*MATα ura3 leu2 trp1 his3Δsk arg4-NspI lys2 hoΔ::LYS2 rme1::LEU2 ssp1::kanMX6::SSP1prDEGRON-SSP1 UBR1::GAL1pr::HA-UBR1::HIS3*	This study
ADY222	*MAT***a** *ura3 leu2 trp1 his3Δsk lys2 hoΔ::LYS2 ama1Δ::CgTRP1 ssp1::kanMX6::SSP1prDEGRON-SSP1 UBR1::GAL1pr::HA-UBR1::HIS3*	This study
ADY223	*MATα ura3 leu2 trp1 his3Δsk arg4-NspI lys2 hoΔ::LYS2 rme1::LEU2 ama1Δ::CgTRP1 ssp1::kanMX6::SSP1prDEGRON-SSP1 UBR1::GAL1pr::HA-UBR1::HIS3*	This study
ADY224	*MAT***a** *ura3 leu2 trp1 his3Δsk lys2 hoΔ::LYS2 ssp1::kanMX6::SSP1prDEGRON-SSP1 UBR1::GAL1pr::HA-UBR1::HIS3*	This study
ADY225	*MATα ura3::GPD1prGAL4(848)ER::URA3 leu2 trp1 his3Δsk arg4-NspI lys2 hoΔ::LYS2 rme1::LEU2 ssp1::kanMX6::SSP1prDEGRON-SSP1 UBR1::GAL1pr::HA-UBR1::HIS3*	This study
ADY226	*MAT***a** *ura3::GPD1prGAL4(848)ER::URA3 leu2 trp1 his3Δsk lys2 hoΔ::LYS2 ama1Δ::CgTRP1 ssp1::kanMX6::SSP1prDEGRON-SSP1 UBR1::GAL1pr::HA-UBR1::HIS3*	This study
ADY227	*MATα ura3::GPD1GAL4(848)ER::URA3 leu2 trp1 his3Δsk arg4-NspI lys2 hoΔ::LYS2 rme1::LEU2 ama1Δ::CgTRP1 ssp1::kanMX6::SSP1prDEGRON-SSP1 UBR1::GAL1pr::HA-UBR1::HIS3*	This study
ADY228	*MAT***a** *ura3::GPD1prGAL4(848) ER::URA3 leu2 trp1 his3Δsk lys2 hoΔ::LYS2 ssp1::kanMX6::SSP1prDEGRON-SSP1 UBR1::GAL1pr::HA-UBR1::HIS3*	This study
ADY229	*MATα ura3 leu2 trp1 his3Δsk arg4-NspI lys2 hoΔ::LYS2 rme1::LEU2 UBR1::GAL1pr::HA-UBR1::HIS3*	This study
ADY230	*MATα ura3:: GPD1prGAL4 (848) ER::URA3 leu2 trp1 his3Δsk arg4-NspI lys2 hoΔ::LYS2 rme1::LEU2 UBR1::GAL1pr::HA-UBR1::HIS3*	This study
ADY231	*MAT***a** *ura3 leu2 trp1 his3Δsk lys2 hoΔ::LYS2 UBR1::GAL1pr::HA-UBR1::HIS3*	This study
ADY232	*MAT***a** *ura3::GPD1prGAL4(848)ER::URA3 leu2 trp1 his3Δsk lys2 hoΔ::LYS2 UBR1::GAL1pr::HA-UBR1::HIS3*	This study

ADY233	Cross of ADY216 and ADY220	This study
ADY234	Cross of ADY230 and ADY232	This study
ADY235	Cross of ADY225 and ADY228	This study
ADY236	Cross of ADY226 and ADY227	This study
ADY239	*MAT***a** *ura3*::*GPD1GAL4(848)ER::URA3 leu2 trp1 his3Δsk lys2 hoΔ::LYS2 ama1Δ::CgTRP1 UBR1::GAL1pr::HA-UBR1::HIS3*	This study
ADY240	*MATα ura3*::*GPD1GAL4(848)ER::URA3 leu2 trp1 his3Δsk arg4-NspI lys2 hoΔ::LYS2 rme1::LEU2 ama1Δ::CgTRP1 UBR1::GAL1pr::HA-UBR1::HIS3*	This study
ADY241	Cross of ADY239 and ADY240	This study
AN390	*MAT***a**/*MATα ura3*/*ura3 trp1*/*trp1 his3*/*his3 TEF2::GFP::his5*$^{+}$/*TEF2::GFP::his5*$^{+}$	(Coluccio *et al.*, 2008)
JSP22	*MAT***a**/*MATα ura3*/*ura3 TRP1*/*trp1 his3*/*his3 TEF2::GFP::his5*$^{+}$/*TEF2::GFP::his5*$^{+}$ *LEU2*/*leu2Δ0 arg4-NspI*/*ARG4 ama1Δ*::*HIS3*/ *ama1Δ*::*HIS3*	This study
JSP65	*MAT***a** *CLB2pr::CDC15::kanMX6 TEF2::GFP::his5*$^{+}$ *arg4-NspI leu2Δ0 ura3 trp1*	This study
JSP64	*MATα CLB2pr::CDC15:: kan*^{R} *TEF2::GFP::his5*$^{+}$ *leu2Δ0 ura3 trp1*	This study
JSP118	Cross of JSP65 and JSP64	This study
JSP89	*MAT***a** *CLB2pr::CDC15::kanMX6 TEF2::GFP::his5*$^{+}$ *arg4-NspI leu2Δ0 ura3 trp1 ura3::AMA1::URA3*	This study
JSP88	*MATα CLB2pr::CDC15::kanMX6 TEF2::GFP::his5*$^{+}$ *leu2Δ0 ura3 trp1 ura3::AMA1::URA3*	This study
JSP99	Cross of JSP89 and JSP88	This study
JSP78	*MAT***a** *CLB2pr::CDC15::kanMX6 TEF2::GFP::his5*$^{+}$ *arg4-NspI leu2Δ0 ura3 trp1 ura3::AMA1-m8::URA3*	This study
JSP77	*MATα CLB2pr::CDC15::kanMX6 TEF2::GFP::his5*$^{+}$ *leu2Δ0 ura3 trp1 ura3::AMA1-m8::URA3*	This study
JSP104	Cross of JSP78 and JSP77	This study

Table 3-2. Plasmids used in this study

Name	Description	Source
pSB8	*DON1::GFP*	(Tachikawa *et al.*, 2001)
pRS426-R20	*mRFP-SPO20*$^{51-91}$	This study
pRS424-R20	*mRFP-SPO20*$^{51-91}$	(Suda *et al.*, 2007)
pKL142	*GAL1pr::HA-UBR1*	(Kanemaki *et al.*, 2003)
p926	*GPD1prGAL4 (848) ER*	(Benjamin *et al.*, 2003)
pKL187SSP1pr	*kanMX6::SSP1prDEGRON-SSP1*	This study
pRS314-SSP1-HA	*SSP1::3XHA*	This study
pRS306-AMA1pr-AMA1	*AMA1*	This study
pRS306-AMA1pr-AMA1-IA	*AMA1*^{R593A}	This study
pRS306-AMA1pr-AMA1-ΔIR	*AMA1*$^{IR\Delta}$	This study
YIplac128-AMA1	*AMA1*	(Oelschlaegel *et al.*, 2005)
YIplac128-AMA1-m8	*AMA1-m8*	(Oelschlaegel *et al.*, 2005)

Table 3-3. Assay of prospore membrane closure by FLIP in wild type and *ama1Δ* cells

	Membrane class[b]			
	% Horseshoe, small circular, or tubular	% Oval or spherical		
Relevant genotype[a]	Closed	Closed	Open	Ind.[c]
Wild Type	0% (0/98)	100% (91/91)	0% (0/91)	0% (0/91)
ama1Δ	n.t.[d]	31% (17/55)	53% (29/55)	16% (9/55)

[a]FLIP assay was performed to measure loss or retention of fluorescence inside prospore membranes in each of the morphological classes displayed in Figure 1.
[b]Strains used in these experiments are AN390 (wild type) and JSP22 (*ama1Δ*) transformed with pRS426-R20.
[c]Indeterminate: fluorescence signal inside the prospore membrane displayed a modest response to photobleaching of the ascal cytoplasm.
[d]n.t. Not tested.

Table 3-4. Suppression of the Clb2pr-Cdc15 closure defect by Ama1-m8

Relevant Genotype[a]	Oval or spherical prospore membrane Closed	Open	Ind.[b]
CLB2pr::CDC15	53% (27/51)	23.5% (12/51)	23.5% (12/51)
CLB2pr::CDC15 ura3::AMA1	45% (23/51)	49% (25/51)	6% (3/51)
CLB2pr::CDC15 ura3::AMA1-m8	80% (41/51)	14% (7/51)	6% (3/51)

[a]Strains used in these experiments are JSP118 (wild type) and JSP99 (*CLB2pr::CDC15 ura3::AMA1*) and JSP104 (*CLB2pr::CDC15 ura3::AMA1-m8*) transformed with pRS424-R20.
[b]Indeterminate: fluorescence signal inside the prospore membrane displayed a modest response to photobleaching of the ascal cytoplasm.

Chapter 4: Conclusions and Future experiments

Spore formation in budding yeast is a good model system to study specialized cell differentiation and eukaryotic gametogenesis. During sporulation, a single diploid cell forms four haploid spores (gametes) encased in an ascus. *AMA1* encodes a meiosis-specific activator of the APC, an E3 ubiquitin ligase that targets substrates for degradation. APC^{Ama1} coordinates exit from meiosis with cytokinesis. Important details elucidating the regulation of APC^{Ama1} activity and mechanism of APC^{Ama1} function remain to be explored and may reveal insight into cytokinesis in general.

Is Ssp1 degraded?

This thesis presents data from several experimental approaches that support the model that removal of Ssp1 from the leading edge is required for prospore membrane closure and the onset of spore wall assembly (Maier *et al*., 2007). During Meiosis II, each prospore membrane expands to engulf a daughter nucleus (Neiman, 1998). APC^{Ama1} activity is restrained until late metaphase II because of an Ama1-specific antagonist, Mnd2 (Oelschlaegel *et al*., 2005). At the end of Meiosis II, coincident with removal of Mnd2 from the APC, APC^{Ama1} is activated (Oelschlaegel *et al*., 2005). In this model, APC^{Ama1} targets Ssp1 for degradation directly leading to prospore membrane fusion and cytokinesis.

Three independent experimental approaches collaborate in support of a model that asserts APC^{Ama1}-dependent degradation of Ssp1 links meiotic exit to cytokinesis and the onset of spore wall assembly. Time lapse video microscopy experiments show the

leading edge disappears in sporulating wild-type cells at the time corresponding to prospore membrane closure. In contrast, the leading edge appears to be stabilized in sporulating *ama1Δ* homozygous mutant cells. Fluorescence loss in photobleaching studies demonstrate the morphological changes that occur during formation of the prospore membrane correlate with removal of the leading edge complex and are coincident with cytokinesis in wild-type cells. Conversely, sporulating *ama1Δ* homozygous mutant cells present a variable phenotype consisting of open, closed and indeterminate closure of the prospore membrane suggesting an impairment of cytokinesis. Western analysis demonstrates that Ssp1 protein is destabilized in sporulating wild-type cells at the end of Meiosis II, a time that corresponds to prospore membrane closure. Ssp1 protein steady-state levels are stabilized in sporulating *ama1Δ* homozygous mutant cells and persist at a level comparable to the peak Ssp1 protein level seen in wild-type cells. This is likely not due to a failure of sporulating *ama1Δ* homozygous mutant cells to exit meiosis because Clb5, a protein known to be degraded at the time of meiotic exit, is similarly destabilized in both wild-type and *ama1Δ* homozygous mutant cells (Carlile and Amon, 2008). Finally, genetic evidence demonstrates inactivation of Ssp1 at the end of Meiosis II, corresponding to a time of disappearance of the leading edge in sporulating wild-type cells, allows spore formation to occur in *ama1Δ* homozygous mutant cells.

This thesis does not provide direct evidence Ssp1 is degraded in an APC^{Ama1}-dependent manner. Western analysis shows that Ssp1 steady state protein levels are stabilized in sporulating *ama1*Δ homozygous mutant cells and disappear in sporulating wild-type cells. The persistence of Ssp1 protein in sporulating *ama1*Δ homozygous

mutant cells could be the result of two possibilities: 1) Ssp1 protein is being degraded, presumably by APC^{Ama1}, or 2) Ama1 may activate transcription of *SSP1* mRNA, directly or indirectly, and the pool of Ssp1 protein in sporulating *ama1*Δ homozygous mutant cells is continuously being replenished. Consequently, regulation of Ssp1 degradation would be controlled in an Ama1-independent manner. Several experimental approaches examining protein stability and degradation could further support the model that Ssp1 is degraded in an APC^{Ama1}-dependent manner. A pulse-chase experiment in sporulating *ama1Δ* homozygous mutant cells in which pulsed (labeled) Ssp1 protein levels persist after a chase would provide evidence that steady state Ssp1 protein levels are a consequence of a failure to degrade Ssp1 and not caused by the continuous translation of abundant *SSP1* mRNA into protein. However, pulse-chase experiments are likely not to be successful in sporulating budding yeast cells because sporulation requires the absence of a non-fermentable carbon source that is supplied to cells when they are labeled (pulsed). Another possibility would be to inhibit translation of *SSP1* mRNA by the addition of cyclohexamide to sporulating cells. If Ssp1 protein levels remain similarly stabilized in both cyclohexamide-treated and untreated sporulating *ama1Δ* homozygous mutant cells, Ssp1 steady state protein levels are likely due to a failure of APC^{Ama1}-dependent degradation of Ssp1 protein.

Is Ssp1 a direct target of APC^{Ama1}?

All APC targets are ubiquitylated predicting that if Ssp1 is a direct target of APC^{Ama1}, Ssp1 should be ubiquitylated in an APC^{Ama1}-dependent manner. Consistent with the report of Maier and colleagues (2007), I was not able to demonstrate Ssp1

ubiquitylation in sporulating cells (Maier *et al.*, 2007). These results suggest two possibilities: 1) Ssp1 is not a direct target of APC^{Ama1}, or 2) the ubiquitylated form of Ssp1 is too short-lived or rare to be detected. *SSP1* is meiotically induced and Ssp1 protein is degraded rapidly in wild-type sporulating cells at the time of cytokinesis. As a result, there is only a brief period of time during sporulation when Ssp1 protein accumulates, and only a small fraction of this accumulated pool of Ssp1 might be ubiquitylated.

In vitro studies, analogous to those done by Oelschlaegel and colleagues (2005) demonstrating APC^{Ama1} can target securin for degradation, may show APC^{Ama1} can direct the ubiquitylation and degradation of Ssp1 (Oelschlaegel *et al.*, 2005). Further, addition of the Ama1 inhibitory protein, Mnd2, can test if the ubiquitylation and degradation of Ssp1 can be reversed in *in vitro* assays. *In vivo* experiments that regulate APC activity by utilizing conditional alleles of APC subunits or inhibit APC activity by the addition of specific APC inhibitor chemicals may provide further evidence supporting Ssp1 is degraded in APC^{Ama1}-dependent manner. However, a broad inactivation of the APC is not specific to APC^{Ama1} and will also inactivate APC^{Cdc20} and APC^{Cdh1}, likely complicating the interpretation of results.

To further investigate the relationship between APC^{Ama1} and Ssp1, it would be helpful to examine APC^{Ama1} and Ssp1 function in vegetative cells. Published experiments demonstrate ectopic over-expression of *SSP1* is lethal in vegetative cells because of its anti-fusion function (Maier *et al.,* 2007). Oelschlaegel and co-workers (2005) demonstrated that ectopic over-expression of *AMA1* cDNA is lethal in *mnd2Δ* vegetative cells, perhaps because of its unrestrained targeting of substrates for degradation

(Oelschlaegel *et al*., 2005). It will be of interest to determine if over-expression of *AMA1* cDNA can suppress the lethal phenotype caused by over-expression of *SSP1*in vegetative cells. Preliminary experiments in the SK1 strain background demonstrate *SSP1* over-expression in wild-type vegetative cells does not cause lethality and *AMA1* cDNA over-expression presents a slow-growing, rather than lethal, phenotype suggesting APC^{Ama1} is active despite the inhibitory activity of Mnd2. This proposed experiment might succeed in cells with a strain background other than SK1 such as W303.

Regulation of APC^{Ama1} activity

The relationship between APC^{Ama1} activity and Clb-Cdk activity still needs to sorted out. It remains to be determined whether APC^{Ama1} regulates Clb-Cdk activity by targeting some Clb proteins for degradation or if Clb-Cdk activity regulates APC^{Ama1} activity by phosphorylation of Ama1. In order to prevent unregulated proteolysis, *AMA1* transcription, splicing, and Ama1 post-translational modifications are tightly regulated (Chu *et al*., 1998; Cooper *et al*., 2000). Clb-Cdc28 kinase activity is down-regulated at the end of Meiosis II coincident with the up-regulation of APC^{Ama1} activity (Dahmann and Futcher, 1995; Oelschlaegel *et al*., 2005; Carlile and Amon, 2008).

Though a plethora of studies explore the regulation of Cdk activity during the mitotic cell cycle, less is known about Cdk activity during meiosis. Carlile and Amon recently provided an extensive study of the regulation of cyclin proteins (Clb1, Clb3, Clb4 and Clb5) during the more complex meiotic cycle (Carlile and Amon, 2008). The cyclins, and Cdk activity, are regulated differently during each meiotic division, as well as vastly different from the mitotic cell cycle. Clb1-Cdk activity is restricted to Meiosis I,

though Clb1 protein levels remain high during the second meiotic division, and Clb3-Cdk activity is restricted to the second meiotic division, though *CLB3* mRNA transcripts are present during the first meiotic division (Carlile and Amon, 2008). Clb4-Cdk activity is lost partway through the second meiotic division, though Clb4 protein levels persist. Finally, they found Clb5-Cdk activity (an S-phase cyclin) varies directly with Clb5 protein levels in meiotic cells. In light of the Carlile and Amon results, the experiments demonstrating the cyclin proteins are not the critical targets of APC^{Ama1} (Chapter 2) remain meaningful. Experiments utilizing regulatable forms of *CDC28* (*cdc28-as1* and *cdc28-4*) in *ama1Δ* cells clearly demonstrate the cyclin proteins are not the critical targets of the APC^{Ama1}. Although the Clb proteins are not the critical targets of APC^{Ama1}, it remains to be determined if APC^{Ama1} targets any Clb protein for degradation to coordinate meiotic exit with the onset of spore wall formation.

APC^{Ama1} and Meiotic Exit

In vegetative cells, mitotic exit is controlled by the FEAR (Cdc14 early anaphase release) and MEN (mitotic exit network) signaling pathways (Dumitrescu and Saunders, 2002). During early anaphase, Cdc14, a phosphatase, is relocalized from the nucleolus to the nucleus (Wood and Hartwell, 1982; Taylor *et al*., 1997). Subsequently, a component of the MEN, Cdc15, functions by phosphorylating nucleolar proteins to maintain Cdc14 in its active, released state in the nucleus (D'Amours and Amon, 2004). Cdc14 removes inhibitory phosphates from Cdh1, an activator of the APC, that prevent its binding to the APC. Consequently, APC^{Cdh1} targets cyclin proteins for degradation thereby reducing

Clb-Cdk1 activity necessary for mitotic exit (Zachariae *et al*., 1998; Martinez *et al*., 2006).

CDC14 is essential in meiosis, but unlike in mitosis, its regulation primarily depends on the FEAR network and not the MEN (Marston *et al*., 2003; Kamieniecki *et. al*., 2005). Cdc15 can be depleted from sporulating cells by placing the gene under the control of the sporulation-repressed *CLB2* promoter (Kamieniecki *et al*., 2005; Pablo-Hernando *et al*., 2007). Sporulating *CLB2pr-CDC15* cells complete anaphase but in contrast to wild-type cells, *CLB2pr-CDC15* cells do not exhibit proper spindle disassembly and microtubules accumulate rather than disperse (Pablo-Hernando *et al*., 2007). Sporulating *ama1Δ* cells complete meiosis but have difficulty with prospore membrane closure and arrest prior to the onset of spore wall formation. The terminal phenotypes of *ama1Δ* and *CLB2pr-CDC15* suggest *CDC15* may function upstream of *AMA1*. The FLIP experiments in Chapter 3 indicate the closure defect in sporulating *CLB2pr-CDC15* cells may be caused by a failure to activate APC^{Ama1}, possibly due to direct phosphorylation of Ama1 by Cdc28. As mitotic exit requires removal of inhibitory phosphates from Cdh1 by Cdc14, activation of APC^{Ama1} may also require inhibitory phosphate removal by Cdc14 to promote meiotic exit. In order to further unravel the molecular mechanism of Ama1 activity, the role of Cdc15 during meiosis requires further exploration. Although Cdc15 is not required for the release of Cdc14 from the nucleolus at the end of anaphase II, Cdc15 is required to maintain Cdc14 in its released state and for the transport of Cdc14 from the nucleus to the cytoplasm (Pablo-Hernando *et al*., 2007). It will be of interest to resolve if Ssp1 is stabilized in *CLB2pr-CDC15* mutant cells as well as mutants containing a conditional allele of *CDC14*.

Bibliography

Adams, I.R. and Kilmartin, J.V. (2000). Spindle pole body duplication: a model for centrosome duplication? Trends Cell Biol *10*, 4095-4104.

Almeida, A., Bolanos, J.P., and Moreno, S. (2005). Cdh1/Hct1-APC is essential for the survival of postmitotic neurons. J Neurosci *25*, 8815-8821.

Asakawa, H., Kitamura, K., and Shimoda C. (2001). A novel Cdc20-related WD-repeat protein, Fzr1, is required for spore formation in *Schizosaccharomyces pombe*. Mol Genet Genomics *265*, 424-435.

Bajgier, B.K., Malzone, M., Nickas M., and Neiman, A.M. (2001). Spo21 is required for meiosis-specific modification of the spindle pole body in yeast. Mol Biol Cell *12*, 1611-1621.

Bardin, A.J., Boselli, M.G., and Amon, A. (2003). Mitotic exit regulation through distinct domains within the protein kinase Cdc15. Mol Cell Biol *23*, 5018-5030.

Benjamin, K.R., Zhang, C., Shokat, K.M., and Herskowitz, I. (2003). Control of landmark events in meiosis by the CDK Cdc28 and the meiosis-specific kinase Ime2. Genes Dev *17*, 1524-1539.

Blanco, M.A., Pelloquin, L., and Moreno, S. (2001). Fission yeast *mfr1* activates APC and coordinates meiotic nuclear division with sporulation. J Cell Sci *114*, 2135-2143.

Bloom, J. and Cross, F.R. (2007). Multiple levels of cyclin specificity in cell-cycle control. Nat Rev Mol Cell Biol *8* 149-160.

Briza, P., Winkler G., Kalchhauser H., and Breitenbach, M. **(**1986). Dityrosine is a prominent component of the yeast ascospore wall. A proof of its structure. J Biol Chem *261,* 4288–4294.

Briza, P., Ellinger A., Winkler G., and Breitenbach, M. **(**1988). Chemical composition of the yeast ascospore wall. The second outer layer consists of chitosan. J Biol Chem *263,* 11569–11574.

Briza, P., Breitenbach, M., Ellinger, A., and Segall, J. **(**1990). Isolation of two developmentally regulated genes involved in spore wall maturation in *Saccharomyces cerevisiae*. Genes Dev. *4*,1775–1789.

Briza, P., Eckerstorfer, M., and M. Breitenbach, M. **(**1994). The sporulation specific enzymes encoded by the *DIT1* and *DIT2* genes catalyze a two-step reaction leading to a soluble LL-dityrosine-containing precursor of the yeast spore wall. Proc Natl Acad Sci USA *91*, 4524–4528.

Buonomo S.B., Clyne, R.K., Fuchs, J., Loidl, J., Uhlmann, F., and Nasmyth, K. (2000). Disjunction of homologous chromosomes in meiosis I depends on the proteolytic cleavage of the meiotic cohesin Rec8 by separin. Cell *103*, 387-398.

Burton, J.L. and Solomon, M.J. (2001). D box and KEN box motifs in budding yeast Hsl1p are required for APC-mediated degradation and direct binding to Cdc20p and Cdh1p. Genes Dev *15*, 2381-2395.

Burton J.L., Tsakraklides, V., and Solomon M.J. (2005). Assembly of an APC-Cdh1-substrate complex is stimulated by engagement of a destruction box. Mol Cell *18*, 533-542.

Byers, B. (1981). Cytology of the yeast life cycle, p. 59-96. *In* J. N. Strathern, E.W. Jones, and J.R. Broach (ed.) The molecular biology of the yeast *Saccharomyces*: life cycle and inheritance. Cold Spring Harbor Laboratory Press, Cold Spring Harbor, N.Y.

Carlile, T.M. and Amon, A. (2008). Meiosis I is established through division-specific translational control of a cyclin. Cell *133*, 280-291.

Carlton, J.G. and Martin-Serrano, J. (2007). Parallels between cytokinesis and retroviral budding: a role for the ESCRT machinery. Science *316*, 1908-1912.

Carroll C.W. and Morgan, D. (2002). The Doc1 subunit is a processivity factor for the anaphase-promoting complex. Nat Cell Biol *4*, 880-887.

Castro, A., Vigneron, S., Bernis, C., Labbe, J.C., and Lorca, T. (2003). Xkid is degraded in a D-box, KEN-box, and A-box-independent pathway. Mol Cell Biol *23*, 4126-4138.

Christianson, T.W., Sikorski, R.S., Dante, M., Shero, J.H., and Hieter, P. (1992). Multifunctional yeast high-copy-number shuttle vectors. Gene *110*, 119-122.

Chu, S., DeRisi, J., Eisen, M., Mulholland, J., Botstein, D., Brown, P.O., and Herskowitz, I. (1998). The transcriptional program of sporulation in budding yeast. Science *282*, 699-705.

Chu, T., Henrion G., Haegeli, V., and Stickland S. (2001). Cortex, a Drosophila gene required to complete oocyte meiosis, is a member of the Cdc20/fizzy protein family. Genetics *29*, 141-152.

Ciechanover, A., Finley, D., and Varshavsky, A. (1984). Ubiquitin dependence of selective protein degradation demonstrated in the mammalian cell cycle mutant ts85. *Cell* 37, 57–66.

Ciosk, R., Zachariae, W., Michaelis, C., Shevchenko, A., Mann, M., and Nasmyth, K. (1998). An *ESP1/PDS1* complex regulates loss of sister chromatid cohesion at the metaphase to anaphase transition in yeast. Cell *93*, 1067-1076.

Cohen-Fix, O., Peter, J.M., Kirschner, M.W., and Koshland, D. (1996) Anaphase initiation in *Saccharomyces cerevisiae* is controlled by the APC-dependent degradation of the anaphase inhibitor, Pds1p. Genes and Dev *10*, 3081-3093.

Coluccio, A., Bogengruber, E., Conrad, M.N., Dresser, M.E., Briza, P., and Neiman, A.M. (2004). Morphogenetic pathway of spore wall assembly in *Saccharomyces cerevisiae*. Eukaryot Cell *3*, 1464-1475.

Coluccio, A.E., Rodriguez, R., Kernan, M., and Neiman, A.M. (2008). The *Saccharomyces cerevisiae* spore wall allows spores to survive passage through the digestive tract of the fly *Drosophila melanogaster*. PLOS One *3*, e2873.

Cooper, K.F., Mallory, M.J., Egeland, D.B., Jarnik, M., and Strich, R. (2000). Ama1p is a meiosis-specific regulator of the anaphase promoting complex/cyclosome in yeast. Proc Natl Acad Sci U S A *97*, 14548-14553.

Dahmann, C. and Futcher, B. (1995). Specialization of B-type cyclins for mitosis or meiosis in *S. cerevisiae*. Genetics *140*, 957-963.

D'Amours, D. and Amon, A. (2004). At the interface between signaling and executing anaphase-Cdc14 and the FEAR network. Genes Dev *18*, 2581-2595.

Davidow, L.S., Goetsch, L., and Byers, B. (1980). Preferential occurrence of nonsister spores in two-spored asci of *Saccharomyces cerevisiae*: evidence for regulation of spore-wall formation by the spindle pole body. Genetics *94*, 581-595.

Davis, E.S., Wille, L., Chestnut, B.A., Sadler, P.L., Shakes, D.C., and Golden, A. (2002). Multiple subunits if the *Caenorhabditis elegans* anaphase-promoting complex are required for chromosome segregation during meiosis I. Genetics *160*, 805-813.

Dube P., Herzog, F., Gieffers, C., Sander, B., Riedel, D., Muller, S.A., Engel, A., Peters, J.M., and Stark, H. (2005). Localization of the coactivator Cdh1 and the cullin subunit Apc2 in a cryo-electron microscopy model of vertebrate APC/C. Mol Cell *20*, 867-879.

Dumitrescu, T.P. and Saunders, W.S. (2002). The FEAR Before MEN: networks of mitotic exit. Cell Cycle *1*, 304-307.

Enyenihi, A.H. and Saunders, W.S. **(**2003). Large-scale functional genomic analysis of sporulation and meiosis in *Saccharomyces cerevisiae*. Genetics *163***,** 47–54. Esposito, M.S. and Esposito, R.E. (1969). The genetic control of sporulation in *Saccharomyces*. I. The isolation of temperature-sensitive sporulation-deficient mutants. Genetics *61*, 79-89.

Esposito, M.S., Esposito, R.E., Arnaud, M., and Halvorson, H.O. (1970). Conditional mutants of meiosis in yeast. J Bacteriol *104*, 202-210.

Esposito, R.E. and Klapholz, S. (1981). Meiosis and ascospore development. In: The Molecular Biology of the Yeast *Saccharomyces*: Life Cycle and Inheritance, eds. J.N. Strathern, E.W. Jones, and J.R. Broach, Cold Spring Harbor, NY: Cold Spring Harbor Laboratory Press, 211-287.

Fang, G., Yu, H., and Kirschner, M.W. (1998). Direct binding of *CDC20* protein family members activates the anaphase promoting complex in mitosis and G1. Mol Cell *2*, 163-171

Fares, H., Goetsch, L., and Pringle, J.R. (1996). Identification of a developmentally regulated septin and involvement of the septins in spore formation in *Saccharomyces cerevisiae*. J Cell Biol *132*, 399-411.

Felder, T., Bogengruber, E., Tenreiro, S., Ellinger, A., Sa-Correia, I., and Briza, P. **(**2002). Dtrlp, a multidrug resistance transporter of the major facilitator superfamily, plays an essential role in spore wall maturation in *Saccharomyces cerevisiae*. Eukaryot Cell *1,* 799–810.

Fields, S. and Song, O. (1989). A novel genetic system to detect protein-protein interactions. Nature *340*, 245-6.

Finley, D., Ciechanover, A., and Varshavsky, A. (1984). Thermolability of ubiquitin-activating enzyme from the mammalian cell cycle mutant ts85. Cell *37*, 43-55.

Funabiki, H., Yamano, H., Kumada, K., Nagano, K., Hunt, T., and Yanagida, M. (1996) Cut2 proteolysis required for sister-chromatid segregation in fission yeast. Nature *381*, 438-441.

Gao, X.D., Tachikawa, H., Sato, T., Jigami, Y., and Dean, N. (2005). Alg14 recruits Alg13 to the cytoplasmic face of the endoplasmic reticulum to form a novel bipartite UDP-N-acetylglucosamine transferase required for the second step of N-linked glycosylation. J Biol Chem *280*, 36254-36262.

Geiffers, C., Peters, B.H., Kramer, E.R., Dotti, C.G., and Peters, J.M. (1999). Expression of the *CDH1*-associated form of the anaphase-promoting complex in postmitotic neurons. Proc Natl Acad Sci USA *96*, 11317-11322.

Gieffers, C., Dube, P., Harris, J.R., Stark, H., and Peters, J.M. (2001). Three-dimensional structure of the anaphase-promoting complex. Mol Cell *7*, 907-913.

Gladfelter, A.S., Pringle, J.R., and Lew, D.J. (2001). The septin cortex at the yeast mother-bud neck. Curr Opin Microbiol *4*, 681-689.

Glotzer, M., Murray, A.W., and Kirschner, M.W. (1991). Cyclin is degraded by the ubiquitin pathway. Nature *349*, 132-138.

Gmachl, M., Gieffers, C., Podtelejnikov, A.V., Mann, M., and Peters, J.M. (2000). The RING-H2 finger protein APC11 and the E2 enzyme UBC4 are sufficient to ubiquitinate substrates of the anaphase-promoting complex. Proc. Natl. Acad. Sci., USA *97*, 8973-8978.

Gromley, A., Yeaman, C., Rosa, J., Redick, S., Chen, C.T., Mirabelle, S., Guha, M., Sillibourne, J., and Doxsey, S.J. (2005). Centriolin anchoring of exocyst and SNARE complexes at the midbody is required for secretory-vesicle-mediated abscission. Cell *123*,75-87.

Grossberger, R., Gieffers, C., Zachariae, W., Podtelejnikov, A.V., Schleiffer, A., Nasmyth, K., Mann, M., and Peters, J.M. (1999). Characterization of the DOC1/APC10 subunit of the yeast and human anaphase-promoting complex. J Biol Chem *274*, 14500-14507.

Guth, E., Hashimoto T., and Conti, S.F. (1972). Morphogenesis of acrospores in *Saccharomyces cerevisiae*. J Bacteriol *109*, 869-880.

Hall, M.C., Torres, M.P., Schroeder, G.K., and Borchers, C.H. (2003). Mnd2 and Swm1 are core subunits of the *Saccharomyces cerevisiae* anaphase-promoting complex. J Biol Chem *278*, 16698-16705.

Harper, J.W., Burton, J.L., and Solomon, M.J. (2002) The anaphase promoting complex: it's not just for mitosis any more. Genes Dev *16*, 2179-2206.

Hartwell, L.H., Culotti, J., and Reid, B. (1970). Genetic control of the cell-division cycle in yeast. I. Detection of mutants. Proc Natl Acad Sci USA *66*, 352-359.

Hauf, S., Waizenegger, I.C., and Peters, J.M. (2001). Cohesin cleavage by separase required for anaphase and cytokinesis in human cells. Science *293*, 1320-1323.

Hayes, M.J., Kimata, Y., Wattam, S.L., Lindon, C., Mao, G., Yamano, H., and Fry, A.M. (2006). Early mitotic degradation of Nek2A depends on Cdc20-independent interaction with the APC/C. Nat Cell Biol *6*, 607-614.

Henderson, K.A., Kee, K., Maleki, S., Santini, P.A., and Keeney, S. (2006). Cyclin-dependent kinase directly regulates initiation of meiotic recombination. Cell *125*, 1321-1332.

Hershko, A. and Ciechanover, A. (1998). The ubiquitin system. Annu Rev Biochem *67*, 425-479.

Herzog, F. Mechtler, K., and Peters, J.M. (2005). Identification of cell cycle-dependent phosphorylation sites on the anaphase-promoting complex/cyclosome by mass spectrometry. Methods Enzymol *398*, 231-145.

Hilioti, Z., Chung, Y.S., Mochizuki, Y., Hardy, C.F., and Cohen-Fix, O. (2001). The anaphase inhibitor Pds1 binds to the APC/C-associated protein Cdc20 in a destruction box-dependent manner. Curr Biol *11*, 1347-1352.

Hollaway, B.L., Lehman, D.J., Primerano, D.A., Magee, P.T., and Clancy, M.J. **(**1985). Sporulation-regulated genes of *Saccharomyces cerevisiae*. Curr Genet *10,* 163–169.

Hwang, L.H. and Murray, A.W. (1997). A novel yeast screen for mitotic arrest mutants identifies *DOC1*, a new gene involved in cyclin proteolysis. Mol Biol Cell *8*, 1877-1887.

Huang, L.S., Doherty, H.K., and Herskowitz, I. (2005). The Smk1p MAP kinase negatively regulates Gsc2p, a 1,3-beta-glucan synthase, during spore wall morphogenesis in *Saccharomyces cerevisiae*. Proc Natl Acad Sci U S A *102*, 12431-12436.

Huh, W.K., Falvo, J.V., Gerke, L.C., Carroll, A.S., Howson, R.W., Weissman, J.S., and O'Shea, E.K. (2003). Global analysis of protein localization in budding yeast. Nature *425*, 686-691.

Irniger, S., Piatti, S, Michaelis, C., and Nasmyth, K. (1995). Genes involved in sister chromatid separation are needed for B-type cyclin proteolysis in budding yeast. Cell, 81, 269-278.

Ito, T., Chiba, R., Ozawa, M., Yoshida, M., Hattori, M., and Sakaki, Y. (2001). A comprehensive two-hybrid analysis to explore the yeast protein interactome. Proc Natl Acad Sci USA *98*, 4569-4584.

Jantsch-Plunger, V. and Glotzer, M. (1999). Depletion of syntaxins in the early *Caenorhabditis elegans* embryo reveals a role for membrane fusion events in cytokinesis. Curr Biol *9*, 738-745.

Johnston, G.C., Pringle, J.R., and Hartwell, L.H. (1977). Coordination of growth with cell division in the yeast *Saccharomyces cerevisiae*. Exp Cell Res *105*, 79-98.

Juo, P. and Kaplan, J.M. (2004). The anaphase-promoting complex regulates the abundance of *GLR-1* glutamate receptors in the ventral nerve cord of *C. elegans*. Curr Biol *14*, 2057-2062.

Kakihara, Y., Nabeshima, K., Hirata, A., and Nojima, H. (2003). Overlapping *omt1+* and *omt2+* genes are required for spore wall maturation in *Schizosaccharomyces pombe*. Genes Cells *8*, 547-558.

Kallio, M., Weinstein, J., Daum, J.R., Burke, D.J., and Gorbsky, G.J. (1998). Mammalian $p55^{CDC}$ mediates association of the spindle checkpoint protein Mad2 with the cyclosome/anaphase-promoting complex, and is involved in regulating anaphase onset and late mitotic events. J Cell Biol *141*, 1393-1406.

Kamieniecki, R.J., Liu, L., and Dawson, D.S. (2005). FEAR but not MEN genes are required for exit from meiosis I. Cell Cycle *4*, 1093-1098.

Kanemaki, M., Sanchez-Diaz, A., Gambus, A., and Labib, K. (2003). Functional proteomic identification of DNA replication proteins by induced proteolysis *in vivo*. Nature *423*, 720-724.

Kaplow, M.E., Mannava, L.J., Pimentel, A.C., Fermin, H.A., Hyatt, V.J., Lee, J.J., and Venkatesh, T.R. (2007). A genetic modifier screen identifies multiple genes that interact with Drosophila Rap/Fzr and suggests novel cellular roles. J Neurogenet *21*, 105-51.

Kassir, Y., Granot, D., and Simchen, G. (1988). *IME1*, a positive regulator gene of meiosis in *S. cerevisiae*. Cell *52*, 853-62.

Katis, V.L., Matos, J., Mori, S., Shirahige, K., Zachariae, W., and Nasmyth, K. (2004). Spo13 facilitates monopolin recruitment to kinetochores and regulates maintenance of centromeric cohesion during yeast meiosis. Curr Biol *14*, 2183-2196.

King, R.W., Peters, J.M., Tugendreich, S., Rolfe, M., Heiter, P., and Kirschner, M.W. (1995). A 20S complex containing CDC27 and CDC16 catalyzes the mitosis-specific conjugation of ubiquitin to cyclin B. Cell, *81*, 279-288.

King, R.W., Glotzer, M., and Kirschner, M.W. (1996). Mutagenic analysis of the destruction signal of mitotic cyclins and structural characterization of ubiquitinated intermediates. Mol Biol Cell *7*, 1343-1357.

Kitajima, T.S., Kawashima, S.A., and Watanabe, Y. (2004). The conserved kinetochore protein shugoshin protects centromeric cohesion during meiosis. Nature *427*, 510-517.

Klein, F., Mahr, P., Galova, M., Buonomo, S.B., Michaelis, C., and Nasmyth, K. (1999). A central role for cohesions in sister chromatid cohesion, formation of axial elements, and recombination during yeast meiosis. Cell *98*, 91-103.

Klis, F.M., Mol, P., Hellingwerf, K., and Brul, S. (2002). Dynamics of cell wall structure in *Saccharomyces cerevisiae*. FEMS Microbiol Rev *26*, 239–256.

Knop, M. and Schiebel, E. (1998). Receptors determine the cellular localization of a gamma-tubulin complex and thereby the site of microtubule formation. EMBO J *19*, 3657-3667.

Knop, M. and Strasser, K. (2000). Role of the spindle pole body of yeast in mediating assembly of the prospore membrane during meiosis. EMBO J *19*, 3657-3667.

Kominami, K., Seth-Smith, H., and Toda, T. (1998). Apc10 and Ste9/Srw1, two regulators of the APC-cyclosome, as well as the CDK inhibitor Rum1 are required for G_1 cell-cycle arrest in fission yeast. EMBO J *17*, 5388-5399.

Konishi, Y., Stegmuller, J., Matsuda, T., Bonni, S., and Bonni, A. (2004). Cdh1-APC controls axonal growth and patterning in the mammalian brain. Science *303*, 1026-1030.

Kraft, C., Herzog, F., Gieffers, C., Mechtler, K., Hagting, A., Pines, J., and Peters, J.M. (2003). Mitotic regulation of the human anaphase promoting complex by phosphorylation. EMBO J *22*, 6598-65609.

Kraft, C., Vodermaier, H.C., Maurer-Stroh, S., Eisenhaber, F., and Peters, J.M. (2005). The WD40 propeller domain of Cdh1 functions as a destruction box receptor for APC/C substrates. Mol Cell *18*, 543-553.

Kreger-Van Rij, N. J. (1978). Electron microscopy of germinating ascospores of *Saccharomyces cerevisiae*. Arch Microbiol *117,* 73–77.

Krisak, L., Strich, R., Winters, R.S., Hall, J.P., Mallory, M.J., Kreitzer, D., Tuan, R.S., and Winter, E. (1994). *SMK1*, a developmentally regulated MAP kinase, is required for spore wall assembly in *Saccharomyces cerevisiae*. Genes Dev *8*, 2151-2161.

Kudo, N.R., Wasmann, K., Anger, M., Schuh, M., Wirh, K.G., Helmhart, W., Kudo, H., McKay, M., Maro, B., Ellenberg, J., de Boer, P., and Nasymth, K. (2006). Resolution of chiasmata in oocytes requires separase-mediated proteolysis. Cell *126*, 135-146.

Kurasawa, Y. and Todokoro, K. (1999). Identification of human APC10/Doc1 as a subunit of the anaphase promoting complex. Oncogene *18*, 5131-5137.

Lasorella, A., Stegmuller, J., Guardavaccaro, D., Liu, G., Carro, M.S., Rothschild, G., de la Torre-Ubieta, L., Pagano, M., Bonni, A., and Lavarone, A. (2006). Degradation of Id2 by the anaphase-promoting complex couples cell cycle exit and axonal growth. Nature *442*, 471-474.

Lauber, M.H., Waizenegger, I., Steinmann, T., Schwarz, H., Mayer, U., Hwang, I., Lukowitz, W., and Jurgens, G. (1997). The *Arabidopsis* KNOLLE protein is a cytokinesis-specific syntaxin. J Cell Biol *139*, 1485-1493.

Leverson, J.D., Jazeiro, C.A., Page, A.M., Huang, H., Hieter, P., and Hunter, T. (2000). The *APC11* RING-H2 finger mediates E2-dependent ubiquitination. Mol Biol Cell *11*, 2315-2325.

Li, M., Shin, Y.H., Huang, X., Wei, Z., Klann, E., and Zhang, P. (2008). The adaptor protein of the anaphase promoting complex Cdh1 is essential in maintaining replicative lifespan and in learning and memory. Nat Cell Biol

Lim, H.H., Goh, P.Y., and Surana, U. (1998). Cdc20 is essential for the cyclosome-mediated proteolysis of both Pds1 and Clb2 during M phase in budding yeast. Curr Biol. *8*, 231-234.

Liu, W., Wu, G., Li, W., Lobur, D., and Wan, Y. (2007). Cdh1-anaphase-promoting complex targets Skp2 for destruction in transforming growth factor beta-induced growth inhibition. Mol Cell Biol *8*, 2967-2979.

Littlepage, L.E. and Ruderman, J.V. (2002). Identification of a new APC/C recognition domain, the A box, which is required for the Cdh1-dependent destruction of the kinase Aurora-A during mitotic exit. Genes Dev *16*, 2274-2285.

Longtine, M.S., McKenzie, A., 3rd, Demarini, D.J., Shah, N.G., Wach, A., Brachat, A., Philippsen, P., and Pringle, J.R. (1998). Additional modules for versatile and economical PCR-based gene deletion and modification in *Saccharomyces cerevisiae*. Yeast *14*, 953-961.

Longtine, M.S. and Bi, E. (2003). Regulation of septin organization and function in yeast. Trends Cell Biol *13*, 403-409.

Lynn, R.R. and Magee, P.T. (1970). Development of the spore wall during ascospore formation in *Saccharomyces cerevisiae*. J Cell Biol *44*, 688-692.

Maestre, C., Delgado-Esteban, M., Gomez-Sanchez, J.C., Bolanos, J.P., and Almeida, A. (2008). Cdk5 phosphorylates Cdh1 and modulates cyclin B1 stability in excitotoxicity. EMBO J *27*, 2736-2745.

Maier, P., Rathfelder, N., Finkbeiner, M.G., Taxis, C., Mazza, M., Le Panse, S., Haguenauer-Tsapis, R., and Knop, M. (2007). Cytokinesis in yeast meiosis depends on the regulated removal of Ssp1p from the prospore membrane. EMBO J *26*, 1843-1852.

Marston, A.L., Lee, B.H., and Amon, A. (2003). The Cdc14 phosphatase and the FEAR network control meiotic spindle disassembly and chromosome segregation. Dev Cell *4*, 711-726.

Marston, A.L., Tham, W.H., Shah, H., and Amon, A. (2004). A genome-wide screen identifies genes required for centromeric cohesion. Science *303*, 1367-1370.

Marston, A.L. and Amon, A. (2004). Meiosis: cell-cycle controls shuffle and deal. Nat Rev Mol Cell Biol *12,* 983-97.

Martinez, J.S., Jeong, D.E., Choi, E., Billings, B.M., and Hall, M.C. (2006). Acm1 is a negative regulator of the *CDH1*-dependent anaphase-promoting complex/cyclosome in budding yeast. Mol Cell Biol *26*, 9162-9176.

McKee, A.H. and Kleckner, N. (1997). A general method for identifying recessive diploid-specific mutations in *Saccharomyces cerevisiae*, its application to the isolation of mutants blocked at intermediate stages of meiotic prophase and characterization of a new gene *SAE2*. Genetics *146*, 797-816.

McDonald, C.M., Cooper, K.F., and Winter, E. (2005). The Ama1-directed anaphase promoting complex regulates the Smk1 mitogen-activated protein kinase during meiosis in yeast. Genetics *171*, 901-911.

Michaelis, C., Ciosk, R., and Nasmyth, K. (1997). Cohesins: chromosomal proteins that prevent premature separation of sister chromatids. Cell *91*, 35-45.

Mitchell, A.P. **(**1994). Control of meiotic gene expression in *Saccharomyces cerevisiae*. Microbiol Rev *58*, 56–70.

Moens, P.B. (1971). Fine structure of ascospore development in the yeast *Saccharomyces cerevisiae*. Can J Microbiol *17*, 507-510.

Moens, P.B. and Rapport, E. (1971). Spindles, spindle plaques, and meiosis in the yeast *Saccharomyces cerevisiae* (Hansen). J Cell Biol *50*, 344-361.

Moens P.B, Esposito, R.E., and Esposito, M.S. (1974). Aberrant nuclear behavior at meiosis and anucleate spore formation by sporulation-deficient (*SPO*) mutants of *Saccharomyces cerevisiae*. Exp Cell Res *83*, 166-174.

Moreno-Borchart, A.C., Strasser, K., Finkbeiner, M.G., Shevchenko, A., and Knop, M. (2001). Prospore membrane formation linked to the leading edge protein (LEP) coat assembly. EMBO J *20*, 6946-6957.

Morgan, D.O. (1999). Regulation of the APC and the exit from mitosis. Nat Cell Biol *1*, E47-53.

Mumberg, D., Muller, R., and Funk, M. (1995). Yeast vectors for the controlled expression of heterologous proteins in different genetic backgrounds. Gene *156*, 119-122.

Nag, D.K., Koonce, M.P., and Axelrod, J. (1997). *SSP1*, a gene necessary for proper completion of meiotic divisions and spore formation in *Saccharomyces cerevisiae*. Mol Cell Biol *17*, 7029-7039.

Nakanishi, H., de los Santos, P., and Neiman, A.M. (2004). Positive and negative regulation of a SNARE protein by control of intracellular localization. Mol Biol Cell *15*, 1802-1815.

Neiman, A.M. (1998). Prospore membrane formation defines a developmentally regulated branch of the secretory pathway in yeast. J Cell Biol *140*, 29-37.

Neiman, A.M., Katz, L., and Brennwald, P.J. (2000). Identification of domains required for developmentally regulated SNARE function in *Saccharomyces cerevisiae*. Genetics *155*, 1643-1655.

Neiman, A.M. (2005). Ascospore formation in the yeast *Saccharomyces cerevisiae*. Microbiol Mol Biol Rev *69*, 565-584.

Nickas, M.E. and Neiman, A.M. (2002). Ady3p links spindle pole body function to spore wall synthesis in *Saccharomyces cerevisiae*. Genetics *160*, 1439-1450.

Nickas, M.E., Schwartz, C., and Neiman, A.M. (2003). Ady3p and Spo74 are components of the meiotic spindle pole body that promote growth of the prospore membrane in *Saccharomyces cerevisiae*. Eukaryot Cell *2*, 431-445.

Oelschlaegel, T., Schwickart, M., Matos, J., Bogdanova, A., Camasses, A., Havlis, J., Shevchenko, A., and Zachariae, W. (2005). The yeast APC/C subunit Mnd2 prevents premature sister chromatid separation triggered by the meiosis-specific APC/C-Ama1. Cell *120*, 773-788.

Ohtoshi, A., Maeda, T., Higashi, H., Ashizawa, S., and Hatakeyama, M. (2000). Human p55/Cdc20 associates with cyclin A and is phosphorylated by the cyclin A-Cdk2 complex. Biophys Res Comm *268*, 530-534.

Orlean, P. (1997). Biogenesis of yeast wall and surface components, p. 229–262. *In* J.R. Pringle, J.R. Broach, and E.W. Jones (ed.), The molecular and cellular biology of the yeast *Saccharomyces*. Cell cycle and biology. Cold Spring Harbor Laboratory Press, Cold Spring Harbor, N.Y.

Ostapenko, D., Burton, J.L., Wang, R., and Solomon, M.J. (2008). Pseudosubstrate inhibition of APC^{Cdh1} by Acm1: regulation by proteolysis and Cdc28 phosphorylation. Mol Cell Biol *15*, 4653-4664.

Pablo-Hernando, M.E., Arnaiz-Pita, Y., Nakanishi, H., Dawson, D., del Rey, F., Neiman, A.M., and Vazquez de Aldana, C.R. (2007). Cdc15 is required for spore morphogenesis independently of Cdc14 in *Saccharomyces cerevisiae*. Genetics *177*, 281-293.

Pak, J. and Segall, J. **(**2002). Regulation of the premiddle and middle phases of expression of the *NDT80* gene during sporulation of *Saccharomyces cerevisiae*. Mol Cell Biol *22*, 6417–6429.

Passmore, L.A., McCormack, E.A., Au, S.W., Paul, A., Willison, K.R., Harper, J.W., and Barford, D. (2003). Doc1 mediates the activity of the anaphase-promoting complex by contributing to substrate recognition. EMBO J *22*, 786-796.

Passmore, L.A. and Barford, D. (2004). Getting into position: the catalytic mechanisms of protein ubiquitylation. Biochem J *379*, 513-525.

Passmore, L.A., Booth, C.R., Venien-Bryan, C., Ludtke, S.J., Fioretto, C., Johnson, L.N., Chiu, W., and Barford, D. (2005). Structural analysis of the anaphase-promoting complex reveals multiple active sites and insights into polyubiquitylation. Mol Cell *20*, 855-866.

Penkner, A.M., Prinz, S., Ferscha, S., and Klein, F. (2005). Mnd2, an essential antagonist of the anaphase-promoting complex during meiotic prophase. Cell *120*, 789-801.

Percival-Smith, A. and Segall, J. **(**1984). Isolation of DNA sequences preferentially expressed during sporulation in *Saccharomyces cerevisiae*. Mol Cell Biol *4*, 142–150.

Pesin, J.A. and Orr-Weaver, T.L. (2007). Developmental role and regulation of cortex, a meiosis-specific anaphase-promoting complex/cyclosome activator. PLoS Genet *11*, e202.

Peters, J.M. (2006). The anaphase promoting complex/cyclosome: a machine designed to destroy. Nat Rev Mol Cell Biol *9*, 644-656.

Petronczki, M., Siomos, M.F., and Nasmyth, K. (2003). *Un ménage a quatre*: the molecular biology of chromosome segregation in meiosis. Cell *112*, 423-440.

Pfleger, C.M. and Kirchner, M.W. (2000). The KEN box: an APC recognition signal distinct fro the D box targeted by Cdh1. Genes Dev *14*, 655-665.

Pfleger, C.M., Lee, E., and Kirschner, M.W. (2001). Substrate recognition by the Cdc20 and Cdh1 components of the anaphase-promoting complex. Genes Dev *15*, 2396-2407.

Picard, D. (1999). Regulation of heterologous proteins by fusion to a hormone binding domain. *In*: Nuclear receptors; a practical approach, ed. D. Picard, Oxford: Oxford University Press, 261-274.

Pinsky, B.A. and Biggins, S. (2005). The spindle checkpoint: tension versus attachment. Trends Cell Biol *15*, 486-493.

Primig, M., Williams, R.M., Winzeler, E.A., Tevzadze, G.G., Conway, A.R., Hwang, S.Y., Davis, R.W., and Esposito, R.E. (2000). The core meiotic transcriptome in budding yeasts. Nat Gene *26,* 415–423.

Rabitsch, K.P., Toth, A., Galova, M., Schleiffer, A., Schaffner, G., Aigner, E., Rupp, C., Penkner, A.M., Moreno-Borchart, A.C., Primig, M., Esposito, R.E., Klein, F., Knop, M., and Nasmyth, K. (2001). A screen for genes required for meiosis and spore formation based on whole-genome expression. Curr Biol *11*, 1001-1009.

Reis, A., Levasseur, M., Chang, H.Y., Elliot,t D.J., and Jones, K.T. (2006). The CRY box: a second APCcdh1-dependent degron in mammalian cdc20. EMBO Rep *10*, 1040-5.

Riley, J., Butler, R., Ogilvie, D., Finniear, R., Jenner, D., Powell, S., Anand, S., Smith, J.C., and Markham, A.F. (1990). A novel, rapid method for the isolation of terminal sequences from yeast artificial chromosome (YAC) clones. Nucleic Acids Res *18*, 2887-2890.

Rockmill, B., Lambie, E.J., and Roeder, G.S. (1991). Spore enrichment. Methods Enzymol *194*, 146-149.

Rose, M.D. and Fink, G.R. (1990). Methods in Yeast Genetics. Cold Spring Harbor Laboratory Press: Cold Spring Harbor, NY.

Ross-Macdonald, P., Coelho, P.S., Roemer, T., Agarwal, S., Kumar, A., Jansen, R., Cheung, K.H., Sheehan. A., Symoniatis, D., Umansky, L., Heidtman, M., Nelson, F.K., Iwasaki, H., Hager, K., Gerstein, M., Miller, P., Roeder, G.S., and Snyder, M. (1999). Large-scale analysis of the yeast genome by transposon tagging and gene disruption. Nature *402*, 413-418.

Salah, S.M. and Nasmyth, K. (2000). Destruction of the securin Pds1p occurs at the onset of anaphase during both meiotic divisions in yeast. Chromasoma *109*, 27-34.

Sanchez-Diaz, A., Kanemaki, M., Marchesi, V., and Labib, K. (2004). Rapid depletion of budding yeast proteins by fusion to a heat-inducible degron. Sci STKE *2004*, PL8.

Schott, E.J. and Hoyt, M.A. (1998). Dominant alleles of *Saccharomyces cerevisiae CDC20* reveal its role in promoting anaphase. Genetics *148*, 599-610.

Schwab, M., Lutum A.S., and Seufert, W. (1997). Yeast Hct1 is a regulator of Clb2 cyclin proteolysis. Cell *90*, 683-693.

Schwab, M., Neutzner, M., Mocker, D., and Seufert, W. (2001). Yeast Hct1 recognizes the mitotic cyclin Clb2 and other substrates of the ubiquitin ligase APC. EMBO J *20*, 5165-5175.

Shirayama, M., Toth, A., Galova, M., and Nasmyth, K. (1999). APC^{Cdc20} promotes exit from mitosis by destroying the anaphase inhibitor Pds1 and cyclin Clb5. Nature *402*, 203-207.

Shonn, M.A., McCarroll, R., and Murray, A. (2002). Spo13 protects meiotic cohesions at centromeres in meiosis I. Genes Dev *16*, 1659-1671.

Sorensen, C.S., Lukas, C., Kramer, E.R., Peters, J.M., Bartek, J., and Lukas, J. (2001). A conserved cyclin-binding domain determines functional interplay between anaphase-promoting complex-Cdh1 and cyclin A-Cdk2 during cell cycle progression. Mol Cell Biol *20*, 3692-3703.

Smits, G.J., van den Ende, H., and Klis, F.M. **(**2001). Differential regulation of cell wall biogenesis during growth and development in yeast. Microbiology *147*, 781–794.

Stegmuller, J. and Bonni, A. (2005). Moving past proliferation: New roles for Cdh1-APC in postmitotic neurons. Trends Neurosci. 28, 596-601.

Stegmuller, J., Konishi, Y., Huynh, M.A., Yuan, Z., Dibacco, S., and Bonni, A. (2006). Cell-intrinsic regulation of axonal morphogenesis by the Cdh1-APC target-SnoN. Neuron *50*, 389-400.

Stegmuller, J., Huynh, M.A., Yuan, Z., Konishi, Y., and Bonni, A. (2008). TGFbeta-Smad2 signaling regulates the Cdh1-APC/SnoN pathway of axonal morphogenesis. J Neurosci *28*, 1961-1969.

Strochein, S.L., Bonni, S., Wrana, J.L., and Luo, K. (2001). Smad3 recruits the anaphase-promoting complex for ubiquitination and degradation of SnoN. Genes Dev *15*, 2822-2836.

Suda, Y., Nakanishi, H., Mathieson, E.M., and Neiman, A.M. (2007). Alternative modes of organellar segregation during sporulation in *Saccharomyces cerevisiae*. Eukaryot Cell *6*, 2009-2017.

Sudakin, V., Ganoth, D., Dahan, A., Heller, H., Hershko, J., Luca, F.C., Ruderman, J.V., and Hershko, A. (1995). The cyclosome, a large complex containing cyclin-selective ubiquitin ligase activity, targets cyclins for destruction at the end of mitosis. Mol Biol Cell *6*, 185-197.

Sullivan, M. and Morgan, D.O. (2007). A novel destruction sequence targets the meiotic regulator Spo13 for anaphase-promoting complex-dependent degradation in anaphase I. J Biol Chem *282*, 19710-5.

Sym, M., Engebrecht J., and Roeder, G.S. (1993). *ZIP1* is a synaptonemal complex protein required for meiotic chromosome synapsis, Cell *72*, 365–378.

Swan, A. and Schupbach, T. (2007). The Cdc20 (Fzy)/Cdh1-related protein, Cort, cooperates with Fzy in cyclin destruction and anaphase progression in meiosis I and II in *Drosophila*. Dev *134*, 891-9.

Tachikawa, H., Bloecher, A., Tatchell, K., and Neiman, A.M. (2001). A Gip1-Glc7p phosphatase complex regulates septin organization and spore wall formation. J Cell Biol *155*, 797-808.

Tanaka, T., Cosma, M.P., Wirth, K., and Nasmyth, K. (1999). Identification of cohesin association sites at centromeres and along chromosome arms. Cell *98*, 847-858.

Tang, Z., Li, B., Bharadwaj, R., Zhu, H., Ozkan, E., Hakala, K., Deisenhofer, J., and Yu, H. (2001). APC2 cullin protein and APC11 RING protein comprise the minimal ubiquitin ligase module of the anaphase-promoting complex. Mol Biol Cell *12,* 3839-3851.

Taylor, G.S., Liu, Y., Baskerville, C., and Charbonneau, H. (1997). The activity of Cdc14p, an oligomeric dual specificity protein phosphatase from *Saccharomyces cerevisiae*, is required for cell cycle progression. J Biol Chem *272*, 24054-24063.

Taxis, C., Maeder, C., Reber, S., Rathfelder, N., Miura, K., Greger, K., Stelzer, E.H., and Knop, M. (2006). Dynamic organization of the actin cytoskeleton during meiosis and spore formation in budding yeast. Traffic *12*, 1628-1642.

Teng, F.Y. and Tang, B.L. (2005). APC/C regulation of axonal growth and synaptic functions in postmitotic neurons: the Liprin-alpha connection. Cell Mol Life Sci *62*, 1571-1578.

Thornton, B.R., Ng, T.M., Matyskiela, M.E., Carroll, C.W., Morgan, D.O., and Toczyski, D.P. (2006). An architectural map of the anaphase-promoting complex. Genes Dev *20*, 449-460.

Thornton, B.R. and Toczyski, D.P. (2003). Securin and B-cyclin/CDK are the only essential targets of the APC. Nat Cell Biol *5*, 1090-1094.

Thornton, B.R. and Toczyski D. P. (2006). Precise destruction: an emerging picture of the APC. Genes Dev, *20*, 3069-3078.

Tinker-Kulberg, R.L. and Morgan, D.O. (1999). Pds1 and Esp1 control both anaphase and mitotic exit in normal cells and after DNA damage. Genes Dev *13,* 1936-1949.

Toth, A., Rabitsch, K.P., Galova, M., Schleiffer, A, Buonomo, S.B., and Nasmyth, K. (2000). Functional genomics identifies monopolin: a kinetochore protein required for segregation of homologs during meiosis I. Cell *103*, 1155-1168.

Uetz, P., Giot, L., Cagney, G., Mansfield, T.A., Judson, R.S., Knight, J.R., Lockshon, D., Narayan, V., Srinivasan, M., Pochart, P., Qureshi-Emili, A., Li, Y., Godwin, B., Conover, D., Kalbfleisch, T., Vijayadamodar, G., Yang, M., Johnston, M., Fields, S., and Rothberg, J.M. (2000). A comprehensive analysis of protein-protein interactions in *Saccharomyces cerevisiae*. Nature *403*, 623–627.

Ufano, S., San-Segundo, P., del Rey, F., and Vazquez de Aldana, C.R. (1999). *SWM1*, a developmentally regulated gene, is required for spore wall assembly in *Saccharomyces cerevisiae.* Mol Cell Biol *19*, 2118-2129.

Uhlmann, F. and Nasmyth, K. (1998). Cohesion between sister chromatids must be established during DNA replication. Curr Biol *8*, 1095-1101.

Uhlmann, F., Lottspeich, F., and Nasmyth, K. (1999). Sister-chromatid separation at anaphase onset is promoted by cleavage of the cohesin subunit Scc1. Nature *400*, 37-42.

Uhlmann F., Wernic, D., Poupart, M.A., Koonin, E.V., and Nasmyth, K. (2000). Cleavage of cohesin by the CD clan protease separin triggers anaphase in yeast. Cell *103*, 375-386.

Van Roessel, P., Eliott, D.A., Robinson, I.M., Prokop, A., and Brand, A.H. (2004). Independent regulation of synaptic size and activity by the anaphase-promoting complex. Cell *119*, 707-718.

Visintin, R., Prinz, S., and Amon, A. (1997). *CDC20* and *CDH1*: a family of substrate specific activators of APC-dependent proteolysis. Science *278*, 460-463.

Vodermaier, H.C., Gieffers, C., Maurer-Stroh, S., Eisenhaber, F., and Peters, J.M. (2003). TPR subunits of the anaphase-promoting complex mediate binding to the activator protein CDH1. Curr Biol *13*, 1459-1468.

Wan, Y. and Kirschner, M.W. (2001) Identification of multiple *CDH1* homologs in vertebrates conferring different substrate specificities. Proc Natl Acad Sci USA *98*, 13066-13071.

Wendt, K.S., Vodermaier, H.C., Jacob, U., Gieffers, C., Gmachl, M., Peters, J.M., Huber, R., and Sondermann, P. (2001). Crystal structure of the APC/DOC1 subunit of the human anaphase-promoting complex. Nat Struct Biol *8*, 784-788.

Wigge, P.A., Jensen O.N., Holmes, S., Soues, M., Mann, M., and Kilmartin, J.V. (1998). Analysis of the *Saccharomyces* spindle pole by matrix-assisted laser desorption/ionization (MALDI) mass spectrometry. J Cell Biol *141*, 967-977.

Wirth, K.G., Ricci, R., Gimenez-Abian, J.F., Taghybeeglu, S., Kudo, N.R., Jochum, W., Vasseur-Cognet, M., and Nasmyth, K. (2004). Loss of the anaphase-promoting complex in quiescent cells causes unscheduled hepatocyte proliferation. Genes Dev *18*, 88-98.

Wood, J.S. and Hartwell, L.H. (1982). A dependent pathway of gene functions leading to chromosome segregation in *Saccharomyces cerevisiae*. J Cell Biol *94*, 718-726.

Yamamoto, A., Guacci, V., and Koshland, D. (1996). Pds1p, an inhibitor of anaphase in budding yeast, plays a critical role in the APC checkpoint pathway(s). J Cell Biol *133*, 99-110.

Yamano, H., Kominami, K., Harrison, C., Kitamura, K., Kitayama, S., Dhut, S., Hunt, T., and Toda, T. (2004). Requirement of the SCFPop1/Pop2 ubiquitin ligase for degradation of the fission yeast S phase. J Biol Chem *279*, 18974-18980.

Yanagida, M. (2000). Cell cycle mechanisms of sister chromatid separation of Cut1/separin and Cut2/securin. Genes Cells *5*, 1-8.

Yoon, H.J., Feoktistova, A., Wolfe, B.A., Jennings, J.L., Link, A.J., and Gould, K.L. (2002). Proteomics analysis identifies new components of the fission and budding yeast anaphase promoting complexes. Curr Biol *12*, 2048-2054.

Yu, H., Peters, J.M., King, R.W., Page, A.M., Hieter, P., and Kirschner, M.W. (1998). Identification of a cullin homology region in a subunit of the anaphase-promoting complex. Science *279*, 1219-1222.

Zachariae, W. and Nasmyth, K. (1996). TPR proteins required for anaphase progression mediate ubiquitination of mitotic B-type cyclins in yeast. Mol Biol Cell *7*, 791-801.

Zachariae, W., Schwab, M., Nasmyth, K., and Seufert, W. (1998a). Control of cyclin ubiquitination by CDK-regulated binding of Hct1 to the anaphase promoting complex. Science *282*, 1721-1724.

Zachariae, W., Shevchenko, A., Andrews, P.D., Ciosk, R., Galova, M., Stark, M.J., Mann, M., and Nasmyth, K. (1998b). Mass spectrometric analysis of the anaphase-promoting complex from yeast: Identification of a subunit related to the cullins. Science *279*, 1216-1219.

Zou, H., McGarry, T.J., Bernal, T., and Kirschner, M.J. (1999). Identification of a vertebrate sister-chromatid separation inhibitor involved in transformation and tumorigenesis. Science *285*, 418-422.

Appendix 1: *S. cerevisiae* strains used in this study

Strain	Genotype	Source
AN117-4B	*MATα ura3 leu2 trp1 his3Δsk arg4-NspI lys2 hoΔ::LYS2 rme1::LEU2*	(Neiman *et al.*, 2000)
AN117-16D	*MAT***a** *ura3 leu2 trp1 his3Δsk lys2 hoΔ::LYS2*	(Neiman *et al.*, 2000)
AN120	Cross of AN117-4B and AN117-16D	(Neiman *et al.*, 2000)
ADY4	*MATα ura3 leu2 trp1 his3Δsk arg4-NspI lys2 hoΔ::LYS2 rme1::LEU2 cit1Δ::CgTRP1*	This study
ADY5	*MATα ura3 leu2 trp1 his3Δsk arg4-NspI lys2 hoΔ::LYS2 rme1::LEU2 cit2Δ::CgTRP1*	This study
ADY6	Cross of ADY4 and ADY7	This study
ADY7	*MAT***a** *ura3 leu2 trp1 his3Δsk lys2 hoΔ::LYS2 cit1Δ::CgTRP1*	This study
ADY8	*MAT***a** *ura3 leu2 trp1 his3Δsk lys2 hoΔ::LYS2 cit2Δ::CgTRP1*	This study
ADY9	Cross of ADY5 and ADY8	This study
ADY10	*MAT***a**/ *ura3 leu2 trp1 his3Δsk lys2 hoΔ::LYS2 cit1Δ::HIS3 cit2Δ::CgTRP1* *MATα ura3 leu2 trp1 his3Δsk arg4-NspI lys2 hoΔ::LYS2 rme1::LEU2 cit1Δ:: HIS3 cit2Δ::CgTRP1*	This study
ADY11	*MATα clb1Δ::URA3 URA3-GAL-CLB2 clb3Δ::TRP1 clb4Δ::HIS3 ade1*	B. Futcher (IFG2#3)
ADY12	*MAT***a** *ura3 leu2 trp1 his3Δsk lys2 hoΔ::LYS2 ama1Δ::CgTRP1*	This study
ADY13	*MATα ura3 leu2 trp1 his3Δsk arg4-NspI lys2 hoΔ::LYS2 rme1::LEU2 ama1Δ::CgTRP1*	This study
ADY14	Cross of ADY12 and ADY13	This study
ADY15	*MAT***a** *ura3 leu2 trp1 his3Δsk lys2 hoΔ::LYS2 clb1Δ::KlURA3*	This study
ADY16	*MATα ura3 leu2 trp1 his3Δsk arg4-NspI lys2 hoΔ::LYS2 rme1::LEU2 clb1Δ::KlURA3*	This study
ADY17	Cross of ADY15 and ADY16	This study
ADY18	*MAT***a** *ura3 leu2 trp1 his3Δsk lys2 hoΔ::LYS2 clb4Δ::HIS3*	This study
ADY19	*MATα ura3 leu2 trp1 his3Δsk arg4-NspI lys2 hoΔ::LYS2 rme1::LEU2 clb4Δ::HIS3*	This study
ADY20	Cross of ADY18 and ADY19	This study

ADY21	*MAT***a** *ura3 leu2 trp1 his3Δsk lys2 hoΔ::LYS2 clb1Δ::KlURA3 ama1Δ::CgTRP1*	This study
ADY22	*MATα ura3 leu2 trp1 his3Δsk arg4-NspI lys2 hoΔ::LYS2 rme1::LEU2 clb1Δ::KlURA3 ama1Δ::CgTRP1*	This study
ADY23	Cross of ADY21 and ADY22	This study
ADY24	*MAT***a** *ura3 leu2 trp1 his3Δsk lys2 hoΔ::LYS2 clb4Δ::HIS3 ama1Δ::CgTRP1*	This study
ADY25	*MATα ura3 leu2 trp1 his3Δsk arg4-NspI lys2 hoΔ::LYS2 rme1::LEU2 clb4Δ::HIS3 ama1Δ::CgTRP1*	This study
ADY26	Cross of ADY24 and ADY25	This study
ADY27	*MAT***a** *ura3 leu2 trp1 his3Δsk lys2 hoΔ::LYS2 clb1Δ::KlURA3 clb4Δ::HIS3*	This study
ADY28	*MATα ura3 leu2 trp1 his3Δsk arg4-NspI lys2 hoΔ::LYS2 rme1::LEU2 clb1Δ::KlURA3 clb4Δ::HIS3*	This study
ADY29	Cross of ADY27 and ADY29	This study
ADY30	*MAT***a** *ura3 leu2 trp1 his3Δsk lys2 hoΔ::LYS2 clb1Δ::KlURA3 clb4Δ::HIS3 ama1Δ::CgTRP1*	This study
ADY31	*MATα ura3 leu2 trp1 his3Δsk arg4-NspI lys2 hoΔ::LYS2 rme1::LEU2 clb1Δ::KlURA3 clb4Δ::HIS3 ama1Δ::CgTRP1*	This study
ADY32	Cross of ADY30 and ADY31	This study
ADY33	*MAT***a** *ura3 leu2 trp1 his3Δsk lys2 hoΔ::LYS2 mdh1Δ::CgTRP1*	This study
ADY34	*MATα ura3 leu2 trp1 his3Δsk arg4-NspI lys2 hoΔ::LYS2 rme1::LEU2 mdh1Δ::CgTRP1*	This study
ADY35	Cross of ADY33 and ADY34	This study
ADY42	*MAT***a** *ura3 leu2 trp1 his3Δsk lys2 hoΔ::LYS2 mdh1Δ::CgTRP1 mdh2Δ::HIS3*	This study
ADY43	*MATα ura3 leu2 trp1 his3Δsk arg4-NspI lys2 hoΔ::LYS2 rme1::LEU2 mdh1Δ::CgTRP1mdh2Δ::HIS3*	This study
ADY44	Cross of ADY42 and ADY43	This study
ADY45	*MAT***a** *ura3 leu2 trp1 his3Δsk lys2 hoΔ::LYS2 mdh1Δ::CgTRP1 mdh3Δ::KlURA3*	This study
ADY46	*MATα ura3 leu2 trp1 his3Δsk arg4-NspI lys2 hoΔ::LYS2 rme1::LEU2 mdh1Δ::CgTRP1 mdh3Δ::KlURA3*	This study
ADY47	Cross of ADY45 and ADY46	This study

ADY51	*MAT***a** *ura3 leu2 trp1 his3Δsk lys2 hoΔ::LYS2 mdh1Δ::CgTRP1 mdh2Δ:: HIS3 mdh3Δ::KlURA3*	This study
ADY52	*MATα ura3 leu2 trp1 his3Δsk arg4-NspI lys2 hoΔ::LYS2 rme1::LEU2 mdh1Δ::CgTRP1 mdh2Δ::HIS3 mdh3Δ::KlURA3*	This study
ADY53	Cross of ADY51 and ADY52	This study
ADY54	*MAT***a** *ura3 leu2 trp1 his3Δsk lys2 hoΔ::LYS2 mae1Δ::KlURA3*	This study
ADY55	*MATα ura3 leu2 trp1 his3Δsk arg4-NspI lys2 hoΔ::LYS2 rme1::LEU2 mae1Δ::KlURA3*	This study
ADY56	Cross of ADY54 and ADY55	This study
ADY57	*MAT***a** *ura3 leu2 trp1 his3Δsk lys2 hoΔ::LYS2 mae1Δ::KlURA3 mdh2Δ::HIS3*	This study
ADY58	*MATα ura3 leu2 trp1 his3Δsk arg4-NspI lys2 hoΔ::LYS2 rme1::LEU2 mae1Δ::KlURA3 mdh2Δ::HIS3*	This study
ADY59	Cross of ADY57 and ADY58	This study
ADY60	*MAT***a** *ura3 leu2 trp1 his3Δsk lys2 hoΔ::LYS2 mae1Δ::KlURA3 mdh2Δ::HIS3 mdh1Δ::KlURA3*	This study
ADY61	*MATα ura3 leu2 trp1 his3Δsk arg4-NspI lys2 hoΔ::LYS2 rme1::LEU2 mae1Δ::KlURA3 mdh2Δ::HIS3mdh1Δ::KlURA3*	This study
ADY64	*MATα ura3 leu2 trp1 his3Δsk arg4-NspI lys2 hoΔ::LYS2 rme1::LEU2 ama1Δ::HIS3*	This study
ADY65	*MAT***a** *ura3 leu2 trp1 his3Δsk lys2 hoΔ::LYS2 ama1Δ::HIS3*	This study
ADY66	Cross of ADY64 and ADY65	This study
ADY84	*cdc20ts ura3*	R. Sternglanz
ADY87	*MATα hoΔ::LYS2 ura3 leu2::hisG cdc28-as1*	Scott Keeney (N. M. Hollingsworth 603)
ADY88	*MAT***a** *hoΔ::LYS2 ura3 leu2::hisG cdc28-as1*	Scott Keeney (N. M. Hollingsworth 604)
ADY89	Cross of ADY87 and ADY88	This study
ADY91	*MAT***a** *ura3 leu2 trp1 his3Δsk lys2 hoΔ::LYS2 ama1Δ::HIS3 cdc28-as1*	This study
ADY96	*MATα ura3 leu2 trp1 his3Δsk arg4-NspI lys2 hoΔ::LYS2 rme1::LEU2 ama1Δ::HIS3 cdc28-as1*	This study
ADY99	Cross of ADY91 and ADY96	This study

ADY103	*MAT***a** *hoΔ::hisG lys2 ura3 leu2 his3 trp1ΔFA SMK1-3XHA-HIS3MX6*	L. Huang
ADY104	*MATα ura3 leu2 trp1 his3Δsk arg4-NspI lys2 hoΔ::LYS2 rme1::LEU2 SMK1-3XHA-HIS3MX6*	This study
ADY105	*MAT***a** *ura3 leu2 trp1 his3Δsk lys2 hoΔ::LYS2 ama1Δ::HIS3 SMK1-3XHA-HIS3MX6*	This study
ADY108	Cross of ADY104 and ADY105	This study
ADY110	*MAT**a** leu2-hisG trp1-hisG lys2 or his4-G ura3-SK1 hoΔ::LYS2 cdc28-4*	E. Winter 1202
ADY111	*MATα leu2-hisG trp1-hisG lys2 or his4-G ura3-SK1 hoΔ::LYS2 cdc28-4*	E. Winter 1204
ADY121	*MATα ura3 leu2 trp1 his3Δsk arg4-NspI lys2 hoΔ::LYS2 rme1::LEU2 cdc28-4*	This study
ADY123	Cross of ADY130 and ADY132	This study
ADY126	*MAT***a** *ura3 leu2 trp1 his3Δsk lys2 hoΔ::LYS2 cdc28-4*	This study
ADY127	Cross of ADY121 and ADY126	This study
ADY130	*MAT***a** *ura3 leu2 trp1 his3Δsk lys2 hoΔ::LYS2 cdc28-4 ama1Δ::HIS3*	This study
ADY132	*MATα ura3 leu2 trp1 his3Δsk arg4-NspI lys2 hoΔ::LYS2 rme1::LEU2 cdc28-4 ama1Δ::HIS3*	This study
ADY134	yTAPYOR242CSSP2	Euroscarf
ADY135	*MATα ura3 leu2 trp1 his3Δsk arg4-NspI lys2 hoΔ::LYS2 rme1::LEU2 CNM67::GFP(his5+)*	This study
ADY136	*MATα ura3 leu2 trp1 his3Δsk arg4-NspI lys2 hoΔ::LYS2 rme1::LEU2 CNM67::HA(his5+)*	This study
ADY137	*MATα ura3 leu2 trp1 his3Δsk arg4-NspI lys2 hoΔ::LYS2 rme1::LEU2 CNM67::MYC(his5+)*	This study
ADY138	*MAT***a** *ura3 leu2 trp1 his3Δsk lys2 hoΔ::LYS2 CNM67::GFP(his5+)*	This study
ADY139	*MAT***a** *ura3 leu2 trp1 his3Δsk lys2 hoΔ::LYS2 CNM67::HA(his5+)*	This study
ADY140	*MAT***a** *ura3 leu2 trp1 his3Δsk lys2 hoΔ::LYS2 CNM67::RFP(his5+)*	This study
ADY141	*MAT***a** *ura3 leu2 trp1 his3Δsk lys2 hoΔ::LYS2 CNM67::GST(his5+)*	This study
ADY144	*MATα ura3 leu2 trp1 his3Δsk arg4-NspI lys2 hoΔ::LYS2 rme1::LEU2 CNM67::GST(his5+)*	This study
ADY145	*MATα ura3 leu2 trp1 his3Δsk arg4-NspI lys2 hoΔ::LYS2 rme1::LEU2 CNM67::RFP(his5+)*	This study

ADY146	*MAT***a** *ura3 leu2 trp1 his3Δsk lys2 hoΔ::LYS2 CNM67::MYC(his5+)*	This study
ADY147	*MAT***a** *ura3 leu2 trp1 his3Δsk lys2 hoΔ::LYS2 ssp2Δ::HIS3*	This study
ADY148	*MATα ura3 leu2 trp1 his3Δsk arg4-NspI lys2 hoΔ::LYS2 rme1::LEU2 ssp2Δ::HIS3*	This study
ADY149	Cross of ADY147 and ADY148	This study
ADY150	*MAT***a** *ura3 leu2 trp1 his3Δsk lys2 hoΔ::LYS2 ssp2Δ::CgTRP1*	This study
ADY151	*MATα ura3 leu2 trp1 his3Δsk arg4-NspI lys2 hoΔ::LYS2 rme1::LEU2 ssp2Δ::CgTRP1*	This study
ADY152	Cross of ADY150 and ADY151	This study
ADY153	*MAT***a** *ura3 leu2 trp1 his3Δsk lys2 hoΔ::LYS2 ssp2Δ::KlURA3*	This study
ADY154	*MATα ura3 leu2 trp1 his3Δsk arg4-NspI lys2 hoΔ::LYS2 rme1::LEU2 ssp2Δ::KlURA3*	This study
ADY155	Cross of ADY153 and ADY154	This study
ADY156	*MAT***a** *ura3 leu2 trp1 his3Δsk lys2 hoΔ::LYS2 SSP2::GFP (his5+)*	This study
ADY157	*MATα ura3 leu2 trp1 his3Δsk arg4-NspI lys2 hoΔ::LYS2 rme1::LEU2 SSP2::GFP (his5+)*	This study
ADY158	Cross of ADY156 and ADY157	This study
ADY159	*MAT***a** *ura3 leu2 trp1 his3Δsk lys2 hoΔ::LYS2 SSP2::GST (his5+)*	This study
ADY160	*MATα ura3 leu2 trp1 his3Δsk arg4-NspI lys2 hoΔ::LYS2 rme1::LEU2 SSP2::GST (his5+)*	This study
ADY161	Cross of ADY159 and ADY160	This study
ADY162	*MAT***a** *ura3 leu2 trp1 his3Δsk lys2 hoΔ::LYS2* P_{SPO20}*ProteinA::SSP2 (his5+)*	This study
ADY163	*MATα ura3 leu2 trp1 his3Δsk arg4-NspI lys2 hoΔ::LYS2 rme1::LEU2* P_{SPO20}*ProteinA::SSP2 (his5+)*	This study
ADY164	Cross of ADY162 and ADY163	This study
ADY165	*MAT***a** *ura3 leu2 trp1 his3Δsk lys2 hoΔ::LYS2* P_{MPC54}*YFP::SSP2 (URA3)*	This study
ADY166	*MATα ura3 leu2 trp1 his3Δsk arg4-NspI lys2 hoΔ::LYS2 rme1::LEU2* P_{MPC54}*YFP::SSP2 (URA3)*	This study
ADY167	Cross of ADY165 and ADY166	This study
ADY168	*MAT***a** *ura3 leu2 trp1 his3Δsk lys2 hoΔ::LYS2 SSP2::GFP (his5+)*	This study

ADY169	*MATα ura3 leu2 trp1 his3Δsk arg4-NspI lys2 hoΔ::LYS2 rme1::LEU2 SSP2::GFP (his5+)*	This study
ADY170	Cross of ADY168 and ADY169	This study
ADY171	*MAT***a** *ura3 leu2 trp1 his3Δsk lys2 hoΔ::LYS2 SSP2::HA (his5+)*	This study
ADY172	*MATα ura3 leu2 trp1 his3Δsk arg4-NspI lys2 hoΔ::LYS2 rme1::LEU2 SSP2::HA (his5+)*	This study
ADY173	Cross of ADY171 and ADY172	This study
ADY174	*MAT***a** *ura3 leu2 trp1 his3Δsk lys2 hoΔ::LYS2 SSP2::MYC (his5+)*	This study
ADY175	*MATα ura3 leu2 trp1 his3Δsk arg4-NspI lys2 hoΔ::LYS2 rme1::LEU2 SSP2::MYC (his5+)*	This study
ADY176	Cross of ADY174 and ADY175	This study
ADY177	*MAT***a** *ura3 leu2 trp1 his3Δsk lys2 hoΔ::LYS2 ssp1Δ::kanMX6 ama1Δ::HIS3*	This study
ADY178	*MATα ura3 leu2 trp1 his3Δsk arg4-NspI lys2 hoΔ::LYS2 rme1::LEU2 ssp1Δ::kanMX6 ama1Δ::HIS3*	This study
ADY179	Cross of ADY177 and ADY178	This study
ADY180	*MAT***a** *ura3 leu2 trp1 his3Δsk lys2 hoΔ::LYS2 SSP1::3xHA::his5* TC38	H. Tachikawa
ADY181	*MATα ura3 leu2 trp1 his3Δsk arg4-NspI lys2 hoΔ::LYS2 rme1::LEU2 SSP1::3xHA::his5* TC37	H. Tachikawa
ADY182	Cross of ADY180 and ADY181 TC529	H. Tachikawa
ADY183	*MAT***a** *ura3 leu2 trp1 his3Δsk lys2 hoΔ::LYS2 ama1Δ::HIS3 SSP1::3xHA:his5*$^{+}$	This study
ADY184	*MATα ura3 leu2 trp1 his3Δsk arg4-NspI lys2 hoΔ::LYS2 rme1::LEU2 ama1Δ::HIS3 SSP1::3xHA::his5*	This study
ADY183-AMA1	*MAT***a** *ura3::AMA1::URA3 leu2 trp1 his3Δsk lys2 hoΔ::LYS2 ama1Δ::HIS3 SSP1::3xHA:his5*$^{+}$	This study
ADY184-AMA1	*MATα ura3::AMA1::URA3 leu2 trp1 his3Δsk arg4-NspI lys2 hoΔ::LYS2 rme1::LEU2 ama1Δ::HIS3 SSP1::3xHA::his5*$^{+}$	This study
ADY185	Cross of ADY183-AMA1 and ADY184	This study
ADY186	Cross of ADY183-AMA1 and ADY184-AMA1	This study

ADY197	*MAT**a** hoΔ::LYS2 ura3 leu2::hisG trp1::hisG his3::hisG GAL-NDT80::TRP1URA3::pGPD1GAL4(848) ER::URA3*	N. M. Hollingsworth (14154)
ADY198	*MAT**a** ura3 leu2 trp1 his3Δsk lys2 hoΔ::LYS2 GAL-NDT80::TRP1 URA3::pGPD1GAL4(848)ER::URA3*	This study
ADY199	*MATα ura3 leu2 trp1 his3Δsk arg4-NspI lys2 hoΔ::LYS2 rme1::LEU2 GAL-NDT80::TRP1 URA3::pGPD1GAL4(848)ER::URA3*	This study
ADY200	Cross of ADY198 and ADY199	This study
ADY204	*MAT**a** ura3 leu2 trp1 his3Δsk lys2 hoΔ::LYS2 GAL-NDT80::TRP1 URA3::pGPD1GAL4(848) ER::URA3 SSP1::3XHA (his5+)*	This study
ADY205	*MATα ura3 leu2 trp1 his3Δsk arg4-NspI lys2 hoΔ::LYS2 rme1::LEU2 GAL-NDT80::TRP1 URA3::pGPD1GAL4(848)ER::URA3 SSP1::3XHA (his5+)*	This study
ADY206	Cross of ADY204 and ADY205	This study
ADY207	*MAT**a** ura3 leu2 trp1 his3Δsk lys2 hoΔ::LYS2 GAL-NDT80::TRP1 URA3::pGPD1GAL4(848) ER::URA3 SSP1::3XHA (his5+)*	This study
ADY208	Cross of ADY205 and ADY207	This study
ADY209	*MAT**a** ade2-1 ura3-1 his3-11,15 trp1-1 leu2-3,112 can1-100 UBR1::GAL-HA-UBR1 (HIS3)* (W303)	EUROSCARF
ADY210	*MAT**a** ura3 leu2 trp1 his3Δsk lys2 hoΔ::LYS2 ama1::his5+-spo20pr-HA-AMA1* *MATα ura3 leu2 trp1 his3Δsk arg4-NspI lys2 hoΔ::LYS2 rme1::LEU2 ama1::his5+-spo20pr-HA-AMA1* TC541	H. Tachikawa
ADY211	*MAT**a** ura3 leu2 trp1 his3Δsk lys2 hoΔ::LYS2 SSP1::GFP his5+* *MATα ura3 leu2 trp1 his3Δsk arg4-NspI lys2 hoΔ::LYS2 rme1::LEU2 SSP1::GFP his5+* TC534	H. Tachikawa
ADY212	*MAT**a** ura3 leu2 trp1 his3Δsk lys2 hoΔ::LYS2 ura3 ama1Δ::kanMX6*	This study
ADY213	*MATα ura3 leu2 trp1 his3Δsk arg4-NspI lys2 hoΔ::LYS2 rme1::LEU2 ama1Δ::kanMX6 GAL-NDT80::TRP1 URA3::pGPD1GAL4(848)ER::URA3 SSP1::3XHA (his5+)*	This study
ADY214	Cross of ADY212 and ADY213	This study
ADY216	*MATα ura3 leu2 trp1 his3Δsk arg4-NspI lys2 hoΔ::LYS2 rme1::LEU2 ssp1::kanMX6::SSP1prDEGRON-SSP1*	This study
ADY217	*MAT**a** ura3 leu2 trp1 his3Δsk lys2 hoΔ::LYS2 ama1Δ::CgTRP1 ssp1::kanMX6::SSP1prDEGRON-SSP1*	This study

ADY218	*MATα ura3 leu2 trp1 his3Δsk arg4-NspI lys2 hoΔ::LYS2 rme1::LEU2 ama1Δ::CgTRP1 ssp1::kanMX6::SSP1prDEGRON-SSP1*	This study
ADY220	*MAT***a** *ura3 leu2 trp1 his3Δsk lys2 hoΔ::LYS2 ssp1::kanMX6::SSP1prDEGRON-SSP1*	This study
ADY221	*MATα ura3 leu2 trp1 his3Δsk arg4-NspI lys2 hoΔ::LYS2 rme1::LEU2 ssp1::kanMX6::SSP1prDEGRON-SSP1 UBR1::GAL1pr::HA-UBR1::HIS3*	This study
ADY222	*MAT***a** *ura3 leu2 trp1 his3Δsk lys2 hoΔ::LYS2 ama1Δ::CgTRP1 ssp1::kanMX6::SSP1prDEGRON-SSP1 UBR1::GAL1pr::HA-UBR1::HIS3*	This study
ADY223	*MATα ura3 leu2 trp1 his3Δsk arg4-NspI lys2 hoΔ::LYS2 rme1::LEU2 ama1Δ::CgTRP1 ssp1::kanMX6::SSP1prDEGRON-SSP1 UBR1::GAL1pr::HA-UBR1::HIS3*	This study
ADY224	*MAT***a** *ura3 leu2 trp1 his3Δsk lys2 hoΔ::LYS2 ssp1::kanMX6::SSP1prDEGRON-SSP1 UBR1::GAL1pr::HA-UBR1::HIS3*	This study
ADY225	*MATα ura3:: GPD1prGAL4 (848) ER::URA3 leu2 trp1 his3Δsk arg4-NspI lys2 hoΔ::LYS2 rme1::LEU2 ssp1::kanMX6::SSP1prDEGRON-SSP1 UBR1::GAL1pr::HA-UBR1::HIS3*	This study
ADY226	*MAT***a** *ura3::GPD1prGAL4(848) ER::URA3 leu2 trp1 his3Δsk lys2 hoΔ::LYS2 ama1Δ::CgTRP1ssp1::kanMX6::SSP1prDEGRON-SSP1 UBR1::GAL1pr::HA-UBR1::HIS3*	This study
ADY227	*MATα ura3::GPD1GAL4(848)ER::URA3 leu2 trp1 his3Δsk arg4-NspI lys2 hoΔ::LYS2 rme1::LEU2 ama1Δ::CgTRP1 ssp1::kanMX6::SSP1prDEGRON-SSP1 UBR1::GAL1pr::HA-UBR1::HIS3*	This study
ADY228	*MAT***a** *ura3::GPD1prGAL4(848)ER::URA3 leu2 trp1 his3Δsk lys2 hoΔ::LYS2 ssp1::kanMX6::SSP1prDEGRON-SSP1 UBR1::GAL1pr::HA-UBR1::HIS3*	This study
ADY229	*MATα ura3 leu2 trp1 his3Δsk arg4-NspI lys2 hoΔ::LYS2 rme1::LEU2 UBR1::GAL1pr::HA-UBR1::HIS3*	This study
ADY230	*MATα ura3:: GPD1prGAL4 (848) ER::URA3 leu2 trp1 his3Δsk arg4-NspI lys2 hoΔ::LYS2 rme1::LEU2 UBR1::GAL1pr::HA-UBR1::HIS3*	This study
ADY231	*MAT***a** *ura3 leu2 trp1 his3Δsk lys2 hoΔ::LYS2 UBR1::GAL1pr::HA-UBR1::HIS3*	This study
ADY232	*MAT***a** *ura3::GPD1prGAL4(848)ER::URA3 leu2 trp1 his3Δsk lys2 hoΔ::LYS2 UBR1::GAL1pr::HA-UBR1::HIS3*	This study
ADY233	Cross of ADY216 and ADY220	This study
ADY234	Cross of ADY230 and ADY232	This study

ADY235	Cross of ADY225 and ADY228	This study
ADY236	Cross of ADY226 and ADY227	This study
ADY237	Cross of ADY217 and ADY218	This study
ADY238	ADY229 and ADY231	This study
ADY239	*MAT***a** *ura3*::*GPD1GAL4(848) ER::URA3 leu2 trp1 his3*Δ*sk lys2 ho*Δ*::LYS2 ama1*Δ*::CgTRP1 UBR1::GAL1pr::HA-UBR1::HIS3*	This study
ADY240	*MAT*α *ura3*::*GPD1GAL4(848) ER::URA3 leu2 trp1 his3*Δ*sk arg4-NspI lys2 ho*Δ*::LYS2 rme1::LEU2 ama1*Δ*::CgTRP1 UBR1::GAL1pr::HA-UBR1::HIS3*	This study
ADY241	Cross of ADY239 and ADY240	This study

Appendix 2: List of primers used in this study

ADO	Primer	Sequence	Brief Description
ADO1	PAMA1F	5' GTT CTT **GGT ACC** TAA GTT AAG CAC GAT TTA	Anneals to -500 *AMA1* promoter and adds KpnI site
ADO2	PAMA1R	5' GTT CTT **CTC GAG** TTT TTT TCT GAT CCA AAG	Reverse primer begins -10 *AMA1* upstream start and adds XhoI site
ADO3	AMA1STOPSPE1	5' GTT CTT **ACT AGT** TTA CCT TAT TCT TTT GTT ATG TGT TGT TTC	Reverse primer adds SpeI site just downstream *AMA1* stop codon
ADO4	AMA1US	5' GTA AAG TCA CAT ATT CCA TAC	Forward primer +740 into ORF of *AMA*1 for DNA sequencing
ADO5	AMA1PFXHO1	5' GTT CTT **CTC CAG** AAT ATG GCT ACT CCC CAT TTA	Forward primer of *AMA1* begins -3 ORF adds XhoI site
ADO6	PCDC20F	5' GTT CTT **GGT ACC** ATG ATA ATT TGA CAT TCA	Anneals to -500 *CDC20* promoter and adds KpnI site
ADO7	PCDC20R	5' GTT CTT **CTC GAG** TTG TAA TAC TTG TCT TTT GAT	Reverse primer begins -10 *CDC20* upstream start and adds XhoI site
AD08	CDC20STOP	5' GTT CTT **ACT AGT** ATT ATA TGC CTT GAC ATG	Reverse primer adds SpeI site just downstream *CDC20* stop codon
ADO9	CDC20pF	5' GTT CTT **CTC GAG** CTA ATG CCA GAA AGC TCT AGA	Forward primer of *CDC20* begins -3 ORF adds XhoI site
ADO10	AMA1USR	5' GAC GCA TGT CAC TAA ATC CCT	Reverse primer +800 bp into ORF of *AMA1* for DNA sequencing
ADO11	NAMA1CCDC20	5' TTG GAA ACC AGG TGC ATC AAG AAT TCT TTC CGG AAT ATG TGA CTT TAC TCG	Ama1/Cdc20 junction at WD1 Ama1P216-Cdc20P249
ADO12	N3AMA1CCDC20	5' TAT CAA AGT ATC TAA CCA AGA CAA TGA ACC GAT TCC TTT GAA GGA TTC AGT	Ama1/Cdc20 junction at WD3 Ama1I328-Cdc20I347
ADO13	N5AMA1CCDC20	5' ATG TAA AGA GCT CAC CTG GGA TCC GGT ATT GAT CTC ATC CAA CAA TGT GCC	Ama1/Cdc20 junction at WD5 Ama1I475-Cdc20I468
ADO14	NCDC20CAMA1	5' TCT CAG GCA AGG TGC ATC CAA TAC ACG GTA TGG ATT GGT ATT GAT TTT CCT	Cdc20/Ama1 junction at WD1 Cdc20P249-Ama1P216
ADO15	N3CDC20CAMA1	5' TTC ACC TGG TTT GAA CCA TTC TAG GCA ACA TAT ACG GAC ACC TAA GCC TGA	Cdc20/Ama1 junction at WD3 Cdc20I347-Ama1I328
ADO16	N5CDC20CAMA1	5' TAT CAA AGA CGT CAC CTG TCC CGA GGT GCA AAT TGA GCC AAC TCG TGC ACC	Cdc20/Ama1 junction at WD5 Cdc20I468-Ama1475

ADO17	AMA1STOPHIA	5’ GTT CTT **ACT AGT** TTA TCT TTT GTT ATG TGT TGT TTC	Reverse primer changes final residue R593A and adds SpeI site just downstream *AMA1* stop codon
ADO18	TRP1F	5’ ACA CAA AGG CAG CTT GGA GTA TGT CTG TTA	DNA sequencing primer just upstream of the *TRP1* ORF
ADO19	TRP1R	5’ TAA ATA CTA CTC AGT AAT AAC CTA TTT CTT AGC	DNA sequencing primer just downstream of the *TRP1* ORF
ADO20	SQCDC20N	5’ TTA AGG GCC CAG ACT AAG	Sequencing primer +500bp into *CDC20* ORF
ADO21	SQAMA1N	5’ GCC ATC AAA AAT TGC TTT GGA	Sequencing reverse primer ~600bp into *AMA1* ORF
ADO22	AMA1A-CK	5’ TCA AAA CTA CTC GAA GTT AGG	Sequencing primer at ~+1600bp to check *AMA1* ORF C-terminus
ADO23	F1-CIT1	5’ TAA AAA GAA AAT AAG GCA AAA CAT ATA GCA ATA TAA TAC TAT TTA CGA AG**C GGA TCC CCG GGT TAA TTA**	PCR-mediated of *CIT1* knockout using pFA6a
ADO24	R1-CIT1	5’ AAA TAC GTG TTT GAA TAG TCG CAT ACC CTG AAT CAA AAA TCA AAT TTT **CCG AAT TCG AGC TCG TTT AAA C**	PCR-mediated knockout of *CIT1* using pFA6a
ADO25	F2-CIT1	5’ GCT CAA AAC TTG CAG CAA CTA TTC	Confirmation primer forward 500bp upstream start *CIT1* ORF
ADO26	R2-CIT1	5’ GCG CTT TGC AGG AAT TTA AGA G	Confirmation primer reverse 200bp downstream of stop *CIT1* ORF
ADO27	F1-CIT2	5’ CAG GGA ACA ATA TCA ACA CAT ATC ATA ACA GGT TCT CAA AAC TTT TTG TTT TAA TAA TAC TAG TAA CAA GAA AA**C GGA TCC CCG GGT TAA TTA**	PCR-mediated knockout of *CIT2* using pFA6a
ADO28	R1-CIT2	5’ TCA TGA GGA AAG AAA AAT ATG CAG AGG GGT GTA AAA GTA GGA TGT AAT CCA A**GA ATT CGA GCT CGT TTA AAC**	PCR-mediated knockout of *CIT2* using pFA6a
ADO29	F2-CIT2	5’ GCG TTA CAT TCG TAT GAA ATT GG	Confirmation forward primer 250bp upstream of start *CIT2* ORF
ADO30	R2-CIT2	5’ GTA CCT AGT TAT CGC GTG ATA GC	Confirmation reverse primer 250bp downstream of stop *CIT2* ORF
ADO31	F1-MAE1	5’ TAA CGA GTT TAG TGC ACA TAA ATA CCA AGA CAAAAG GTA GAA ATA **CGG TTC GGA TCC CCG GGT TAA TTA**	PCR-mediated knockout of *MAE1* using pFA6a
ADO32	R1-MAE1	5’ ACT CTA TAT GGT TTT TTT TTT TTA AGT GCA GGC GTT GGT TAT GCT TCC TC**G AAT TCG AGC TCG TTT AAA C**	PCR-mediated knockout of *MAE1* using pFA6a

ADO33	F2-MAE1	5’ GGT CTA CAG CTT TAG CGC TA	Confirmation forward primer (200bp upstream of start) for PCR mediated knockout of *MAE1* using pFA6a
ADO34	R2-MAE1	5’ GTA GCT GTT AGG CAG TGA CC	Confirmation reverse primer (650bp downstream of stop) for PCR mediated knockout of *MAE1* using pFA6a
ADO35	F2-MDH1	5’ TCA CGC GCC AAG CGG ATT CCC AGA A	Confirmation forward primer 250bp upstream of start *MDH1* ORF
ADO36	R2-MDH1	5’ ATC ATC ATT ATC ATC ACC ATC ACA C	Confirmation reverse primer 250bp downstream of stop *MDH1* ORF
ADO37	F1-CLB1	5’ TAT TTT CGT CCG TTA TAT CAA CCA TCA AAG GAA GCT TTA ATC TTC TCA TA**C GGA TCC CCG GGT TAA TTA**	PCR-mediated knockout of *CLB1* using pFA6a
ADO38	R1-CLB1	5’ ATG ATA AAG TAA GGA AGT GAG ATT TTG GTT TTC TGT GTA GGC TAG CAC CTT **GAA TTC GAG CTC GTT TAA AC**	PCR-mediated knockout of *CLB1* using pFA6a
ADO39	F1-CLB4	5’ CTT ACT ATA CCG GAT ACT AGG CTG CCC TGA TCA AAC AAG GAA ATT GAC AG**C GGA TCC CCG GGT TAA TTA**	PCR-mediated knockout of *CLB4* using pFA6a
ADO40	R1-CLB4	5’ TGA TCC TTC CGA AAC CAA AAC TGA AGC AAA TGG TGT TAA GAT GAG TAA GT**G AAT TCG AGC TCG TTT AAA C**	PCR-mediated knockout of *CLB4* using pFA6a
ADO41	F1- MDH1	5’ CGT GGA CAT CTA CGG AAA GGA AGA AAA AAA ACA AAA GGA AAA GGA AGG AT	PCR-mediated knockout of *MDH1* using pFA6a
ADO42	R1-MDH1	5’ GCG AGT AGT CTT CCG TTC TTA TTA GTA GAA TTT TTT TTT TTT TTT CCC TA	PCR-mediated knockout of *MDH1* using pFA6a
ADO43	F2-AMA1	5’ TCC AAC GAT AAT AAT AAT ACT TG	Confirmation forward primer 75bp upstream of start *AMA1* ORF
ADO44	R2-AMA1	5’ TTC TTA CTG TTA GTT TGC TA	Confirmation reverse primer 200bp upstream of stop *AMA1*
ADO45	CLB1US	5’ CTT CTT TAC AGC ATC ATT TAT GGG T	Confirmation forward primer 500bp upstream of start ORF *CLB1*
ADO46	CLB1DS	5’ CTT GTT TCC ACC TGA AGC CAT CAT A	Confirmation reverse primer 500bp downstream of stop *CLB1* ORF
ADO47	USBH1-PCLB4	5’ GCT CTT **GGA TCC** TAG TGT ACC GGA ATG ACC TG	Forward primer just upstream of start of *CLB4* and adds BamHI site

ADO48	DSNOT1-PCLB4	5' GTC CTT **GCG GCC** GCA TGG TGT TAA GAT GAG TAA G	Reverse primer just downstream of stop of *CLB4* and adds NotI site
ADO49	DSNOT1-PCLB1	5' GTC CTT **GCG GC**C GCT CTG TGT AGG CTA GCA CCT T	Reverse primer just downstream of stop of *CLB1* and adds NotI site
ADO50	USBH1-PCLB1	5' GTC CTT **GGA TCC** GGT ATC CTG CAA GTT AGG T	Forward primer just upstream of start of *CLB1* and adds BamHI site
ADO51	UBUSECOR1	5' GTT CTT **GAA TTC** ATG CAG ATT TTC GTC AAG	Forward primer just upstream of start of *UBI4* (ubiquitin) and adds EcoRI site
ADO52	UBDSSPE1	5' GTT CTT **ACT AGT** CTA ACC ACC TCT TAG CCT TAG	Reverse primer just downstream of stop of *UBI4* (ubiquitin) and adds SpeI site
ADO53	R-PFA6ANOT1	5' GTT CTT G**CG GCC G**CA GAT CTA TAT TAC CCT G	Reverse primer similar to HT66 but includes a NotI site (pFA6a just after terminator)
ADO54	R-DSREDKPN1	5' CTT GTT **GGT ACC** CTA AAG GAA CAG ATG GTG	Reverse primer used to PCR amplify DsRED (pDsRED Clontech as template) and adds a KpnI site
ADO55	F-DSREDPAC1	5' CTT GTT **TTA ATT** AAG ATG AGG TCT TCC AAG AAT G	Forward primer used to PCR amplify DsRED (pDsRED Clontech as template) and adds a PacI site
ADO56	R3ECOR1	5' GTT CTT GAA TCC GCA CTG AGC AGC GTA ATC TG	Reverse primer anneals to pFA6aHIS5PSPO20HA and adds an EcoRI site
ADO57	F1-AMA1	5' AAC TCT TTT AAA GTT TTA CAA AAC TTT GGA TCA GAA AAA AAG AAA AAA AT**C GGA TCC CCG GGT TAA TTA**	PCR-mediated knockout of *AMA1* using pFA6a
ADO58	RAMA1NDE1	5' CTT GTT A**CA TAT G**CC ACA GAC TTG CTG TGC CTG	Reverse primer used to remove intron (1184-1276) in *AMA1* and introduce NdeI site
ADO59	FAMA1NDE1	5' CTT GTT GG**C ATA TG**T CTG AAT GAA CAT GCA AAC	Forward primer used to remove intron (1184-1276) in *AMA1* and introduce NdeI site
ADO60	FAMA1ECOR1	5' CTT GTT **GAA TTC** GTA AAG TCA CAT ATT CCA	Forward primer 600bp upstream of start *AMA1* and adds EcoRI site
ADO61	RAMA1PST1STOP	5' CTT GTT **CTG CAG** CTT TTG TTA TGT GTT GTT TGC	Reverse primer just downstream of stop *AMA1* and adds PstI site
ADO62	jxnchkama	5' AAT GTG AGC CTC TTT GAA A	DNA sequencing primer in *AMA1* ORF to check intron removal (1160bp after start coding sequence)
ADO63	URA3DS	5' CTT GTT GAA GCT CTA ATT TGT GA	Reverse primer just downstream of *URA3* stop
ADO64	F2AMA1	5' ATT ATA GAA TAT ATG GAG GGT ATC GAA ACA ACA CAT AAC AAA AGA ATA AGG **CGG ATC CCC GGG TTA ATT AA**	PCR-mediated C-terminal tagging of *AMA1* using pFA6a

ADO65	R1AMA1	5' TGC TAT TTG AAG TAT TTG GTT TGT GCG TGC AAT GAA TAT CCT TTT TTT ATA **GAA TTC GAG CTC GTT TAA AC**	PCR-mediated deletion/C-terminal tagging of *AMA1* using pFA6a
ADO66	AM23	5' TAG ATT GGT ATA TAT ACG CAT ATG TGG TGT TGA AGA AAC ATG AAA TTG CCC AGT	Forward primer used in strategy for making *STE5pr-URA3* (template is p402)
ADO67	AM24	5' CAG CAA CAG GAC TAG GAT GAG TAG CAG CAC GTT CCT TAT ATG TAG CTT TCG ACA TTT AAA AGT TGT TTC CGC TG	Reverse primer used in strategy for making *STE5pr-URA3* (template is p402)
ADO68	AM26	5' ATT CGG TAA TCT CCG AGC AGA AGG	Diagnostic forward primer (~150bp upstream of the *URA3* ATG) to check integration of the *STE5/FUS1* promoters upstream of *URA3*
ADO69	AM27	5' TGG TGG TAC GAA CAT CCA ATG AAG C	Diagnostic reverse primer (in the 5' region of *URA3* ~100bp into the gene) to check integration of the *STE5/FUS1* promoters upstream of the *URA3* gene
ADO70	AD1	5' CTT GTT **AAG CTT** AAG TCA CAG CAA GCC TGA G	Forward primer 500 bp upstream of AMA1 and adds a HindIII site
ADO71	R1SWM1	5' CCC ATA CAC CAC AAT TTC TGA CTA ATG ATC AGC ATA TAC GTC ACG TTC TGC **GAA TTC GAG CTC GTT TAA**	PCR-mediated knockout of *SWM1* using pFA6a
ADO72	N-MYC2 (SalI) used	5' GTT CTT **GTC GAC** ATG ATC CCC GGG TTA ATT AAC	Forward primer anneals to *MYC* DNA sequence in Pringle plasmid and adds SalI site (plasmid construction failed)
ADO73	SWM1RCHK	5' CGA AAT CTA TCT AGG CCG ATC A	Confirmation reverse primer of PCR-mediated knockout of *SWM1* using pFA6a (cannot find match DNA in SGD)
ADO74	F1SWM1	5' GGA GAA TAA TAT CAG AGA AGT GGG GTG AGC AAA GTA TAA CAA CCA CGA TT**C GGA TCC CCG GGT TAA TTA A**	PCR-mediated knockout of *SWM1* using pFA6a
ADO75	SWM1FCHK	5' ATA CTC AGA ACG TAG GCA CTA	Confirmation forward primer 250 bp upstream of start ORF *SWM1*
ADO76	AM23LEU	5' TAG ATT GGT ATA TAT ACG CAT ATG TGG TGT TGA AGA AAC ATG AAA TTG CCC AGT AC	Similar to AM23 but substitutes *LEU* for *URA* (From A. Amon)
ADO77	CBOXNCDC20	5' AGA CTT ATA AGC ATT TCT CGA AAC TGA TTT TGG **AAT ATA TCT**	Cdc20/Ama1 junction at C-box Cdc20P148-Ama1P38

		ATC CGC TGC	
ADO78	CBOXNAMA1	5’ GAC CTT GTT TTG CGA AGC TCC CTG TAG AAT TGG **AAT GAA ACG GTC AAC CTC**	Ama1/Cdc20 junction at C-box Ama1P38-Cdc20P148
ADO79	C-MYC2	5’ GTT CTT **CTC GAG** GGC GCG AAT GTG ATT GAT	Reverse primer anneals to *MYC* DNA sequence in Pringle plasmid and adds SalI site
ADO80	MND2FCHK	5’ ACA CTT GTC TTG CCA TAA ACA	Forward primer 200bp upstream of start *MND2*
ADO81	MND2RCHK	5’ TGA AAT GAA CTT GTC GGA CCT G	Cannot find DNA sequence in SGD
ADO82	SMK1FXHO1	5’ GTT CTT **CTC GAG** AGA AAG GAG AGA GAT AAT	Forward primer 700bp upstream of start of *SMK1* and adds a XhoI site
ADO83	KANRFCHK	5’ TCA GGC GCA ATCACG AAT AAC	Forward primer anneals to 443-461bp of *kanMX6* cassette in Pringle plasmids
ADO84	TEVSQF53	5’ GTC ATT TGA CGA ATG AAT	DNA sequencing primer to determine TEV protease sequence from pNasmyth-TEVprotease
ADO85	pUBFBamH1	5’ GTT CTT **GGA TCC** ATG CAG ATC CAC CAT CAC CAT	Forward primer just upstream of start of ubiquitin and adds a BamHI site (pUB221 and pUB223 used as templates)
ADO86	DON1RBglII	5’ GTT CTT **AGA TCT** CGT AAA ACT TAA TTC TTG	Reverse primer 100bp downstream of stop of *DON1* ORF and adds a BglII site
ADO87	pUBRPst1	5’ GTT CTT **CTG CAG** CTT CTT CAA CCC ACC AAA GGC	Reverse primer just downstream of ubiquitin and adds a PstI site (pUB221 and pUB223 used as templates)
ADO88	TEVSQF	5’ TCT AGC ATG GTG TCA GAC ACT AGT	DNA sequencing forward primer used with TEVSQR to determine TEV protease cleavage sequence from p4428 (K. Nasmyth)
ADO89	GFPNDS	5’ GTT CTT **CTC GAG** TTT GTA TAG TTC ATC CAT GCC	Cannot find relevant plasmid
ADO90	DON1FBamHI	5’ GTT CTT **GGA TCC** AAC ATG GGA AAG AAA AAT AGA	Forward primer begins just upstream of *DON1* ORF and continues into coding sequence and adds a BamHI site
ADO91	TEVSQF363	5’ TCT AGC ATG GTG TCA GAC ACT	DNA sequencing primer to determine TEV protease sequence from pTEV#3 (KM)
ADO92	AMA1F4	5’ GAA GGA AGG TCA AAT TTT CTT CCT CCA ACG ATA ATA ATA CTT GCT TAT AT**G AAT TCG AGC TCG TTT AAA C**	PCR-mediated *GAL1pr* introduction to *AMA1* using PFA6a
ADO93	AMA1R7	5’ TTG TTA GAG CTT TTG GAG TTA TAT CTG TGA TAT AAA TGG GGA GTA GCC AT**G GCG CCA**	PCR-mediated *SPO20pr* introduction to *AMA1* using pFA6a

		GCT CCA GCC CC	
ADO94	HT66speI	5’ GAA **ACT AGT** AGA TCT ATA TTA CCC TGT TAT CC	pFA6a just after terminator around BglII site
ADO95	TEVSSP1F	5’ GAA AAT CTT TAT TTT CAA GGT GGT GGT GAA AAT CTT TAT TTT CAA GGT CGG CAA AAA CCT ACG CAA GAA	Forward primer used in overlap PCR to introduce TEV protease cleavage site into *SSP1* (did not use)
ADO96	TEVSSP1R	5’ ACC TTG AAA ATA AAG ATT TTC ACC ACC ACC TTG AAA ATA AAG ATT TTC GTA AGG TGA CTT TGG AAG TTC	Reverse primer used in overlap PCR to introduce TEV protease cleavage site into *SSP1* (did not use)
ADO97	F1CDC73	5’ TCG GGG CGT TAA AAG AAT AAT TTG AGC AAG AAA CTG GTG AAA AAA TTC GGA TCC C**CG GGT TAA TTA A**	PCR-mediated knockout of *CDC73* using pFA6a
ADO98	R1CDC73	5’ CTG AAG AAA CAC TTT CAA TGG CCG AAA TAC CAT TCT TCC GTT TAT CGT AT**G AAT TCG AGC TCG TTT AAA C**	PCR-mediated knockout of *CDC73* using pFA6a
ADO99	CDC73CKF	5’ TAG CTA AGA GTC TCT TTT ACA AC	Confirmation forward primer 750bp upstream of *CDC73* start
ADO100	CDC73CKR	5’ TTA CTG ATA GAC AAG CAA CTG A	Confirmation reverse primer 250bp downstream of stop of *CDC73*
ADO101	F1POP1	5’ ACT TGA ACA TTT GGC AAG GGT GAG AAT TGA CCT CAT TAT AAT TAC AA**C GGA TCC CCG GGT TAA TTA A**	PCR-mediated knockout of *POP1* using pFA6a
ADO102	R1 POP1	5’ ATA CAT AGC TTT ATA GGA TAT CGG TCG TAC ATA TAA TTC AGT TCA GTT CA**G AAT TCG AGC TCG TTT AAA C**	PCR-mediated knockout of *POP1* using pFA6a
ADO103	POP1CKF	5’ TAG ATT GAC TTC TTT GCT GGT CA	Confirmation forward primer 250bp upstream of *POP1*
ADO104	POP1CKR	5’ CTA GGG AAT GAA TCA ATG AGC	Confirmation reverse primer 600bp downstream of *POP1* ORF
ADO105	AMA1pRXho1	5’ GTT CTT **CTC GAG** TTA CCT TAT TCT TTT GTT ATG TGT TGT TTC	Similar to ADO3 AMA1STOP but contains a SpeI site
ADO106	AMA1pFBamHI	5’ GTT CTT **GGA TCC** AAT ATG GCT ACT CCC CAT TTA TA	Similar to ADO5 AMA1PFXHO1 but contains a BamHI site
ADO107	FSSP1BamHI	5’ GTT CTT **GGA TCC** ACA ATG AGA AGC TCT GGC ACA	Forward primer of *SSP1* just upstream of start and adds BamHI site
ADO108	TEVRXhoI	5’ GTT CTT **CTC GAG**	Reverse primer anneals to TEV

		GTA CCC TTA TTG CGA GTA	protease plasmid and adds XhoI site (did not use)
ADO109	TEVSQR	5' ACT AGT GTC TGA CAC CAT GCT AGA	DNA sequencing (reverse) primer to determine TEV protease cleavage site sequence p4428 (K. Nasmyth)
ADO110	TEVFBamHIMYC	5' GTT CTT **GGA TCC** ATG GAA CAA AAG TTG ATT TCT GAA GAA GAT TTG GGA GAA AGC TTG TTT AAG	TEVprotease primers from KM sequence
ADO111	CpATEVSpeI	5' GTT CTT **ACT AGT** ACC TTG AAA ATA TAA ATT TTC GAG CGC GTC TAC TTT CGG	Reverse primer anneals to Protein A C-terminus and adds a SpeI site (did not use)
ADO112	SSP1DegronF	5' ACA ATA GTG CCT ATT ATC ATG ATA GAA GTA GAG TAG AAA AGC TAG CAA CAA TTA AGG CGC GCC AGA TCT G	Forward primer for PCR-mediated tagging of Degron to *SSP1*
ADO113	SSP1DegronR	5' GAG GTT ATT TCC CCA GAA GGA TCA TTC TCA TAT GTG CCA GAG CTT CTC ATG GCA CCC GCT CCA GCG CCT G	Reverse primer for PCR-mediated tagging of Degron to *SSP1*
ADO114	SSP1DegconfB	5' GAC AAA CTA CTG GGA AAA GTT	Confirmation primer B +520 reverse complement 501-521 for *degssp1* (did not use)
ADO115	SSP1DegconfC	5' CTG GTG CAG GCG CTG GAG CG	Confirmation forward primer C within Degron cassette for *degssp1* (did not use)
ADO116	SSP1DegconfD	5' CGC TCC AGC GCC TGC ACC AG	Confirmation reverse primer D within Degron cassette for *degssp1* (did not use)
ADO117	SSP1FPromoterMfe1	5' GTT CTT **CAA TTG** CTA CCA CCT ACG GT TCC CAA	Forward primer used to amplify *SSP1pr* at MfeI site
ADO118	SSP1RPromoterEcoRI	5' GTT CTT **GAA TTC** TGT TGC TAG CTT TTC TAC TCT	Reverse primer used to amplify *SSP1pr* at EcoRI site
ADO119	PromoterCUP1@Spe1	5' ACT AGT TAG AAA AAG ACA	Forward primer anneals 250bp upstream in *CUP1pr* of pUB221 and pUB223
ADO120	Ssp1degronATG	5' ATG AGA AGC TCT GGC ACA	Forward primer anneals at *SSP1* start of ORF
ADO121	HT66XhoI	5' GAA **CTC GAG** AGA TCT ATA TTA CCC TGT TAT CC	pFA6a just after terminator around BglII site
ADO122	FDBOXSSP1A	5' CCA AAT TTA GGG AAA GAA TGG CCA GGT GGG CAC AAA ATG GGA AAG CTA ACA ACC ACC AAG G	Forward primer utilized in overlap PCR to mutate Ssp1 D box from residue 36 RRWLQNGKN to **A**RW**A**QNGK**A**
ADO123	RDBOXSSP1A	5' CCT TGG TGG TTG TTA GCT TTC CCA TTT TGT GCC CAC CTG GCC	Reverse primer utilized in overlap PCR to mutate Ssp1 D box from residue 36 **R**RW**L**QNGK**N** to

		ATT CTT TCC CTA AAT TTG G	**A**RW**A**QNGK**A**
ADO124	FKENSSP1A	5’ CAA CCT GAA ATA AAG GCG GCG GCT CTC GAA TCA GCT GAT TCC TTG ATT TTA AGA AGC	Forward primer utilized in overlap PCR to mutate Ssp1 KEN box from residue 504 **KEN**LESN to **AAA**LES**A**
ADO125	RKENASSP1A	5’ GCT TCT TAA AAT CAA GGA ATC AGC TGA TTC GAG AGC CGC CGC CTT TAT TTC AGG TTG	Reverse primer utilized in overlap PCR to mutate Ssp1 KEN box from residue 504 **KEN**LESN to **AAA**LES**A**
ADO126	SSP1SQ511	5’ AGT AGT TTG TCA TTG AGG ACT	Primer used for DNA sequencing beginning about +500 from start codon
ADO127	SSP1SQ1291	5’ GAG CAC ACT GAT GTG CCT GAA	Primer used for DNA sequencing beginning about +1300 from start codon
ADO128	PtefUS	5’ CGA ACT ATA ATT AAC TAA AC	Primer anneals to *TEFpr*
ADO129	MTnGFP3XHA	5’ CAT CAC CTT CAC CCT CTC CAC TGA C	Oligo used to identify integration site of transposon; Internal primer annealing to the mTn region
ADO130	NpABH1	5’ GTT CTT **GGA TCC** ATG GCA GGC CTT GCG CAA CAC GAT	Primer anneals to N-terminus of Protein A and adds a BamHI site
ADO131	SSP2FF307A	5’ GAT TTT CAG AAT GCT GGA GAG GTT CTA GAA ATT ACG CC	Forward primer utilized in overlap PCR to mutate Ssp2 F307A
ADO132	SSP2RF307A	5’ GGC GTA ATT TCT AGA ACC TCT CCA GCA TTC TGA AAA TC	Reverse primer utilized in overlap PCR to mutate Ssp2 F307A
ADO133	SSP2FF327A	5’ GC GTA TCT ATA TTC GCT TAC GAT ATT TCC AGT GC	Forward primer utilized in overlap PCR to mutate Ssp2 F327A
ADO134	SSP2RF327A	5’ GC ACT GGA AAT ATC GTA AGC GAA TAT AGA TAC GC	Reverse primer utilized in overlap PCR to mutate Ssp2 F327A
ADO135	SSP2FC368A	5’ ATT ACA GAC CAG CCT GCC ATT GAC TTG TAG TAC G	Forward primer utilized in overlap PCR to mutate Ssp2 C368A
ADO136	SSP2RC368A	5’ CGT ACT ACA AGT CAA TGG CAG GCT GGT CTG TAA T	Reverse primer utilized in overlap PCR to mutate Ssp2 C368A
ADO137	SSP2SQ	5’ ATG AAA GAG CAA TCT GTC AAC	Forward primer 750bp downstream *SSP2* start (used for DNA sequencing in *SSP2* ORF)
ADO138	SSP2SQ1	5’ ACC TTC TAG ATA TAT CTT ATC	Forward primer 200bp upstream *SSP2* start (used for DNA sequencing in *SSP2* ORF)
ADO139	SSP2SQ2	5’ TTG CAA AAG CAT ATC TGT TTG	Forward primer 200bp downstream *SSP2* start (used for DNA sequencing in *SSP2* ORF)
ADO140	SSP2SQ3	5’ GTT CTC AGA ATC CCG CTC TTC	Forward primer 450bp downstream *SSP2* start (used for DNA sequencing in *SSP2* ORF)
ADO141	SSP2SQ4	5’ GCA ATC TGT CAA	Forward primer 750bp downstream

		CAG AAT AAT	*SSP2* start (used for DNA sequencing in *SSP2* ORF)
ADO142	SSP2SQ5	5' CTA GAA ATT ACG CCT ATT GTA	Forward primer 900 bp downstream of *SSP2* start (used for DNA sequencing in *SSP2* ORF)
ADO143	SSP2GFPSPE1	5' GTT CTT **ACT AGT** ATG TAC AAG AAC TAT TAT TCA	Forward primer at start of *SSP2* ORF with SpeI site (attempt to N-terminal GFP tag *SSP2*, failed)
ADO144	SSP2GFPSAL1	5' GTT CTT **GTC GAC** GAG GAA GCA AAT GAA TTG AT	Reverse primer 200bp downstream of stop of *SSP2* and adds a SalI site (attempt to N-terminal GFP tag *SSP2*, failed)
ADO145	SSP2F1	5' TCC AAC GAA GGT AAA ATA ATA ATA AAA TAC GAA GCA TTT AAT CCG GTC AAC GGA TCC CCG GGT TAA TTA A	PCR-mediated knockout of *SSP2* using pFA6a
ADO146	SSP2F4	5' TAT TTT ATA AAC AAA AAG ACA GAT ATA TTC TCG CGT ATT GAA GTC GGG AAG AAT TCG AGC TCG TTT AAA C	PCR-mediated *GAL1pr* introduction to *SSP2* using PFA6a
ADO147	SSP2R6	5' TCT TTA TGC TTT TTA TAA ACT TCT GTG TTT GAA TAA TAG TTC TTG TAC ATG TCT ACT TTC GGC GCC TG	PCR-mediated *SPO20pr-ProteinA* introduction to *SSP2* using pFA6a
ADO148	SSP2R7	5' TCT TTA TGC TTT TTA TAA ACT TCT GTG TTT GAA TAA TAG TTC TTG TAC ATG GCG CCA GCT CCA GCC CC	PCR-mediated *SPO20pr* introduction to *SSP2* using pFA6a
ADO149	SSP2RSPE1	5' GTT CTT **ACT AGT** GAG GAA GCA AAT GAA TTG AT	Reverse primer just downstream stop of *SSP2* and adds SpeI site
ADO150	SSP2FKPN1	5' GTT CTT **GGT ACC** AGA TAT ATG CCA GAT AAA GGC	Forward primer begins -6 from start of *SSP2* and adds KpnI site
ADO151	AMA1STOPΔIR	5' GTT CTT **ACT AGT** TTA TCT TTT GTT ATG TGT TGT TTC	Reverse primer deletes last two residues of Ama1protein and adds SpeI site just downstream *AMA1* stop codon

Appendix 3: Plasmids used in this study

Plasmid	Brief Description[a]	Source
pBTM116	LexA DNA binding domain	R. Sternglanz
pBluescript	Cloning vector	Fermentas
pBluescriptAMA1	Cloning intermediate	This study
pBTM116AMA1	LexA-Ama1p$^{231-593}$	This study
mTn-3XHA/GFP Library	Transposon library containing genomic fragments representative of the entire *S. cerevisiae* genome	M. Snyder
pUV1 Library	Library of *S. cerevisiae* 1-2Kb genomic inserts	N. M. Hollingsworth
pACTII Library	Library of *S. cerevisiae* 1-2Kb genomic inserts	N. M. Hollingsworth
pRS304SSP2[1]	*SSP2*	This study
pRS314SSP2[2]	*SSP2*	This study
pRS314SSP2F307A[3]	*SSP2F307A*	This study
pRS314SSP2F327A[4]	*SSP2F327A*	This study
pRS314SSP2C368A[5]	*SSP2C368A*	This study
pRS314SSP2F307A/F327A[6]	*SSP2F307A/F327A*	This study
pRS424SSP2MYC[7]	*SSP2MYC*	This study
pRS424SSP2HA[8]	*SSP2HA*	This study
pRS424Pspo20ProteinASSP2[9]	*SPO20pr-ProteinASSP2*	This study
pRS314Pspo20ProteinASSP2[10]	*SPO20pr-ProteinASSP2*	This study
pRS314PMPC54YFPSSP2[11]	*MPC54pr-YFPSSP2*	This study
pRS424PMPC54-YFPSSP2C368A[12]	*MPC54pr-YFPSSP2*	This study
pRS304SPO3-1[13]	*SPO3-1* (ts)	This study
pRS314SPO3-1[14]	*SPO3-1* (ts)	This study
pRS424SPO3-1[15]	*SPO3-1* (ts)	This study
pRS304SSP1[16]	*SSP1*	This study
pRS314SSP1	*SSP1*	This study
pRS424SSP1	*SSP1*	This study
pRS314SSP1HA[17]	*SSP1HA*	This study
pRS424SSP1HA[18]	*SSP1HA*	This study
pRS304SSP1KEN[19]	*SSP1KEN*	This study
pRS314SSP1KEN[20]	*SSP1KEN*	This study
pRS424SSP1KEN	*SSP1KEN*	This study
pRS314SSP1DBox[21]	*SSP1Dbox*	This study
pRS424SSP1DBox	*SSP1Dbox*	This study
pRS304SSP1DBoxKEN[22]	*SSP1DboxKEN*	This study
pRS424SSP1DBoxKEN	*SSP1DboxKEN*	This study
pKL187	Vector for making *CUP1* temperature sensitive *GAL1* regulated by *UBR1* map available	Euroscarf
pKL187ΔNotI[23]	Same as pKL187 but NotI site is deleted	This study
pKL187SSP1pr[24]	Same as pKL187 but *CUP1pr* replaced with *SSP1pr*	This study
p926	Integrative plasmid containing *GAL4.ER* fusion under the control of the *GPD1* promoter Linearize with Nde1	A. Amon
pKL142	Integrating plasmid *GAL1pr-UBR1* linearize with PmeI	Euroscarf
pUB221	*CUP1pr-UBI(HIS-MYC) TRP1/URA3 2μ*	W. Tansey
pUB223	*CUP1pr-UBI(HIS-MYC-R48/A76) TRP1 2μ*	W. Tansey

p413UB	Positive control for a ubiquitylated protein	W. Tansey
pRS426CUP1pr-HISUBG76A	*CUP1pr-HISUBG76A*	W. Tansey
pRS424SPO20pr-6HISMYCUB[25]	*SPO20pr-6HISMYCUB*	This study
pRS424SPO20pr-6HISMYCUBG76A[26]	*SPO20pr-6HISMYCG76A*	This study
pRS424AMA1	*AMA1*	K. Cooper
pRS424Ub[27]	*UB*	This study
pRS424SPO20pr-HA-UB[28]	*SPO20pr-HA-UB*	This study
pRS314Clb1[29]	*CLB1*	This study
pRS424Clb1	*CLB1*	This study
pRS314Clb4[30]	*CLB4*	This study
pRS424Clb4	*CLB4*	This study
pETTEV#3	TEV protease	K. Marcu
pRD53TEVProtease	TEV protease (PCR from pETTEV#3)	This study
p4428	Contains TEV protease cleavage site (SSMVSDTS)	K. Nasmyth
p402	Strategy for making *STE5pr-URA3*	A. Amon
pRS425Pste5-URA3	*STE5pr-URA3*	This study
pRS426Pste5-URA3	*STE5pr-URA3*	This study
pNFUSBiotinLYPT1	Long Biotin fused to N-terminus of *YPT1*	This study
pNFUSBiotinMYPT1	Medium Biotin fused to N-terminus of *YPT1*	This study
pNFUSBiotinSYPT1	Peptide of Biotin fused to N-terminus of *YPT1*	This study
pRD53SSP1HA	*GALpr-SSP1HA*	This study
pRS304GALpr-AMA1	*GALpr-AMA1*	This study
pRS314GALpr-AMA1	*GALpr-AMA1*	This study
pRS424GALpr-AMA1	*GALpr-AMA1*	This study
pRS306AMA1pr	*AMA1pr*	This study
pRS306AMA1	*AMA1*	This study
pRS306AMA1pr-AMA1	*AMA1pr-AMA1*	This study
pRS316AMA1pr-AMA1	*AMA1pr-AMA1*	This study
pRS426AMA1pr-AMA1	*AMA1pr-AMA1*	This study
pRS306CDC20pr	*CDC20pr*	This study
pRS306CDC20	*CDC20*	This study
pRS306CDC20pr-CDC20	*CDC20pr-CDC20*	This study
pRS306AMA1pr-CDC20	*AMA1pr-CDC20*	This study
pRS306CDC20pr-AMA1	*CDC20pr-AMA1*	This study
pRS306AMA1pr-A1	*AMA1pr-* N-Ama1P246-Cdc20 P249-C	This study
pRS306AMA1pr-A3	*AMA1pr-* N-Ama1I328-Cdc20I347-C	This study
pRS306AMA1pr-A5	*AMA1pr-* N-Ama1I475-Cdc20 I468-C	This study
pRS306AMA1pr-ACbox	*AMA1pr* NAma1P38-Cdc20P148-C	This study
pRS306AMA1pr-CACbox	*AMA1pr* N-Cdc20P148-Ama1P38-C	This study
pRS306AMA1pr-C1	*AMA1pr* N-Cdc20P249-Ama1P246-C	This study
pRS306AMA1pr-C3	*AMA1pr* N-Cdc20I347-Ama1328-C	This study
pRS306AMA1pr-C5	*AMA1pr* N-Cdc20I468-Ama1I475	This study

pRS306CDC20pr-A1	*CDC20pr* N-Ama1P246-Cdc20 P249-C	This study
pRS306CDC20pr-A3	*CDC20pr* N-Ama1I328-Cdc20I347-C	This study
pRS306CDC20pr-A5	*CDC20pr* N-Ama1I475-Cdc20 I468-C	This study
pRS306CDC20pr-C1	*CDC20pr* N-Cdc20P249-Ama1P246-C	This study
pRS306CDC20pr-C3	*CDC20pr* N-Cdc20I347-Ama1328-C	This study
pRS306CDC20pr-C5	*CDC20pr* N-Cdc20I468-Ama1I475	This study
pRS304AMA1pr-AMA1	*AMA1*	This study
pRS304AMA1pr-AMA1-IA	$AMA1^{R593A}$	This study
pRS314AMA1pr-AMA1-IA	$AMA1^{R593A}$	This study
pRS424AMA1pr-AMA1-IA	$AMA1^{R593A}$	This study
pRS306AMA1pr-AMA1-IA	$AMA1^{R593A}$	This study
pRS316AMA1pr-AMA1-IA	$AMA1^{R593A}$	This study
pRS426AMA1pr-AMA1-IA	$AMA1^{R593A}$	This study
pRS304AMA1pr-AMA1-ΔIR	$AMA1^{IR\Delta}$	This study
pRS314AMA1pr-AMA1-ΔIR	$AMA1^{IR\Delta}$	This study
pRS424AMA1pr-AMA1-ΔIR	$AMA1^{IR\Delta}$	This study
pRS306AMA1pr-AMA1-ΔIR	$AMA1^{IR\Delta}$	This study
pRS316AMA1pr-AMA1-ΔIR	$AMA1^{IR\Delta}$	This study
pRS426AMA1pr-AMA1-ΔIR	$AMA1^{IR\Delta}$	This study
pRS314MPC54DsRED		

(a) Plasmid construction details not discussed in thesis chapters are briefly designated by a superscript and summarized.

(1) pRS304SSP2 is constructed by a PCR amplification of *SSP2* with SSP2FKpn1 (ADO150) and SSP2RSpe1 (ADO149) to yield a ~2.2Kb fragment. PCR product digested with Kpn1 and Spe1and ligated into similarly digested pRS304.

(2) pRS314SSP2 is constructed by a PCR amplification of *SSP2* with SSP2FKpn1 (ADO150) and SSP2RSpe1 (ADO149) to yield a ~2.2Kb fragment. PCR product digested with Kpn1 and Spe1and ligated into similarly digested pRS314.

(3) pRS314SSP2F307A is constructed by a overlap PCR amplification of *SSP2* (template is pRS314SSP2) with primer pairs SSP2F307A (ADO131) and SSP2R307A (ADO132) and SSP2FKpn1 (ADO150) and SSP2RSpe1 (ADO149) . The PCR product was digested with Dpn1 and transformed into supercompetent bacterial cells. DNA sequencing used to verify correct site-directed mutagenesis alteration.

(4) pRS314SSP2F327A is constructed by a PCR amplification of *SSP2* (template is pRS314SSP2) with primer pairs SSP2F327A (ADO133) and SSP2R327A (ADO134) SSP2FKpn1 (ADO150) and SSP2RSpe1 (ADO149). PCR product digested with Dpn1 and transformed into supercompetent bacterial cells. DNA sequencing used to verify correct site-directed mutagenesis alteration.

(5) pRS314SSP2C368A is constructed by a PCR amplification of *SSP2* (template is pRS314SSP2) with primer pairs SSP2C368A (ADO135) and SSP2C468A (ADO136) SSP2FKpn1 (ADO150) and SSP2RSpe1 (ADO149). PCR product digested with Dpn1 and transformed into supercompetent bacterial cells. DNA sequencing used to verify correct site-directed mutagenesis alteration.

(6) pRS314SSP2F307A327A is constructed by a PCR amplification of *SSP2* (template is pRS314SSP2F307A) with primer pairs SSP2F327A (ADO133) and SSP2R327A (ADO134) and SSP2FKpn1 (ADO150) and SSP2RSpe1 (ADO149). PCR product digested with Dpn1 and transformed into supercompetent bacterial cells. DNA sequencing used to verify correct site-directed mutagenesis alteration.

(7) pRS424SSP2MYC is constructed by a PCR amplification of *SSP2MYC* using primers SSP2KpnIF (ADO150) and HT66SpeI (ADO94) and ADY174 as genomic template. PCR product digested with Kpn1 and Spe1 and ligated into similarly digested vector pRS424. PCR verification of C-terminal tag with primers SP2SQ3 (ADO140) and SSP2SpeI (ADO149).

(8) pRS424SSP2HA is constructed by a PCR amplification of *SSP2HA* using primers SSP2KpnIF (ADO150) and HT66SpeI (ADO94) and ADY171 as genomic template. PCR product digested with Kpn1 and Spe1 and ligated into similarly digested vector pRS424. PCR verification of C-terminal tag with primers SP2SQ3 (ADO140) and SSP2SpeI (ADO149).

(9) pRS424Pspo20ProteinASSP2 is constructed by a PCR amplification of *Pspo20ProteinASSP2* with primers ANO130 Kpn1and SSP2RSpeI (ADO149) and ADY162 as genomic template. PCR product digested with Kpn1 and Spe1 and ligated into similarly digested vector pRS424. PCR verification of N-terminal tag with primers ANO189 and SSP2RSpeI (ADO149).

(10) pRS314Pspo20ProteinASSP2 is constructed by a vector swap from pRS424PSPO20ProteinASSP2 digested with Kpn1 and Spe1 and ligated into similarly digested vector pRS314.

(11) pRS314PMPC54YFPSSP2 is constructed by a PCR amplification of *Pmpc54YFPSSP2* with primers MNO228 and SSP2RSpe1 and ADY165 as genomic template. PCR product digested with Bgl11 and SpeI and ligated into similarly digested vector pRS314.

(12) pRS424PMPC54YFPSSP2C368A is constructed by a PCR amplification of *PMPC54YFPSSP2* (template is pRS314PMPC54YFPSSP2) with primers SSP2C368A (ADO135) and SSP2C468A (ADO136). PCR product digested with Dpn1 and transformed into supercompetent bacterial cells. DNA sequencing used to verify correct site-directed mutagenesis alteration.

(13) *SSP1* temperature sensitive allele, *SPO3-1*, was sequenced with primers HT88, SSP1SQ511 and SSP1SQ1291 revealing a single amino acid change S225L (TCA to TTA). pRS304SPO3-1 is constructed by a PCR amplification of *SPO3-1* with primers MNO112 (420bp upstream of start and adds a NotI site) sense and MNO113 (downstream of stop and adds a XhoI site) and SH531 as genomic template. PCR product digested with NotI and XhoI and ligated into similarly digested vector pRS304.

(14) pRS314SPO3-1 is constructed by a vector swap from pRS304SPO3-1 digested with NotI and XhoI and ligated into similarly digested vector pRS314.

(15) pRS424SPO3-1 is constructed by a vector swap from pRS304SPO3-1 digested with NotI and XhoI and ligated into similarly digested vector pRS424.

(16) pRS304SSP1 is constructed the same way as pRS304SPO3-1 but uses AN120 as genomic template.

(17) pRS314SSP1HA is constructed by a PCR amplification of *SSP1HA* with primers MNO112 and HT66SpeI (ADO94) using TC529 as genomic template. PCR product digested with NotI and SpeI and ligated into similarly digested vector pRS314.

(18) pRS424SSP1HA is constructed by a vector swap from pRS314SSP1HA digested with NotI and XhoI and ligated into similarly digested vector pRS424.

(19) pRS304SSP1mKENbox is constructed by a overlap PCR amplification of *SSP1* (template is pRS304SSP1) with primer pairs FKENSSP1A (ADO124) and RKENSSP1A (ADO125) and MNO112 and

MNO113. The PCR product was digested with Dpn1 and transformed into supercompetent bacterial cells. DNA sequencing used to verify correct site-directed mutagenesis alteration.

(20) pRS314SSP1mKENbox is constructed by a vector swap from pRS304SSP1mKENbox digested with NotI and XhoI and ligated into similarly digested vector pRS314.

(21) pRS304SSP1mDbox is constructed the same way as pRS304SSP1mKENbox but uses primers FDboxSSP1A (ADO122) and RDboxSSP1A (ADO123).

(22) pRS304SSP1mDboxmKENbox is constructed the same was as pRS304SSP1mKENbox but uses pRS304SSP1mDbox as template and primers FKENSSP1A (ADO124) and RKENSSP1A (ADO125).

(23) pKL187ΔNot1 is constructed by digesting pKL187 with SacII and Sal1 (sites within multiple cloning site flanking Not1 site) to generate blunt end and fill in with dNTPs and T4 DNA polymerase. Confirmed with Not1 digest (new plasmid pKL187ΔNot1 has only one site and pKL187 has two Not1 sites).

(24) pKL187Pssp1 is constructed by replacing the *CUP1* promoter with the *SSP1* promoter in pKL187. *SSP1* promoter PCR amplified with primers SSP1FPromoterMfe1 (ADO117) and SSP1RpromoterEcoR1 (ADO118) with pRS314SSP1HA as template. PCR product (700bp) was digested with Mfe1 and EcoR1 and ligated into similarly digested pKL187 (*CUP1* promoter drops out).

(25) pRS424Pspo20-6HISMYCUB was constructed by PCR amplification of *HIS-UBI1* using primers pUBFBamH1 (ADO85) and pUBRPst1 (ADO87) and pUB221 as template. PCR product digested with BamHI and PstI and ligated into similarly digested vector pRS424Pspo20+term (H. Nakanishi).

(26) pRS424Pspo20-6HISMYCUBG76A is constructed the same as pRS424Pspo20-6HISMYCUB but uses pUB223 as PCR template.

(27) pRS424UB is constructed by a PCR amplification of Ubiqutin using AN117-4B as genomic template and primers UBUSEcoR1 (ADO51) and UBDSSpeI (ADO52). PCR product digested with EcoR1 and Spe1 and ligated into similarly digested vector pRS424.

(28) pRS424Pspo20HAUB is constructed by a PCR amplification *PSPO20HA* (~700 bp) using primers ANO110 and R3EcoR (ADO56) and pFa6AHIS5Pspo20HA as template to generate a XhoI site on the 3' end and an EcoRI site on the 5' end. PCR product digested with XhoI and EcoRI and ligated into similarly digested pRS424UB.

(29) pRS314CLB1 is constructed by a PCR amplification of *CLB1* (~2Kb) using primers USBHIpClb1 (ADO50) and DSNotIpClb1 (ADO51) and AN117-B as genomic template. PCR product was digested with BamHI and NotI and ligated into similarly digested vector pRS314.

(30) pRS314CLB4 is constructed by a PCR amplification of *CLB4* (~2Kb) using primers USBHI-PCLB4 (ADO47) and DSNOT1PCLB4 (ADO48) and AN117-4B as genomic template. PCR product was digested with BamHI and NotI and ligated into similarly digested vector pRS314.